Estudio del ensamblaje ribosómico en *Saccharomyces cerevisiae*

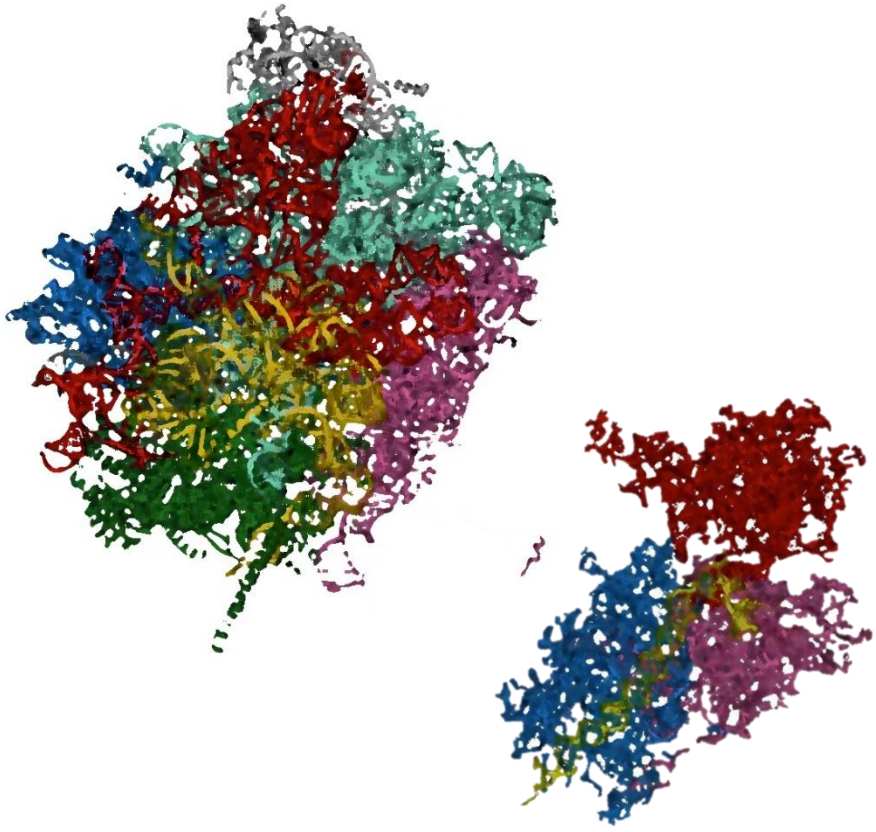

Francisco José Espinar Marchena

Tesis doctoral
2017

Departamento de Genética
Universidad de Sevilla

Estudio del ensamblaje ribosómico en *Saccharomyces cerevisiae*

Memoria presentada para aspirar al grado de
Doctor en Biología

Vº Bº: El director de la Tesis **El doctorando**

Jesús de la Cruz Díaz **Francisco José Espinar Marchena**

ÍNDICE

INTRODUCCIÓN

El Ribosoma. Estructura, función y evolución.

En todas las células, uno de los procesos más importantes que existen es el de expresión génica, de ahí que la mayor parte de la demanda energética celular se destine a la regulación y el mantenimiento de la correcta expresión de los genes. En el contexto de la expresión génica se establecen diversas rutas celulares entre las que se encuentra la síntesis de proteínas o traducción.

La traducción se entiende como el proceso por el cual las proteínas se construyen a partir de la información contenida en un RNA mensajero (mRNA) utilizado como molde. Entre la maquinaria que lleva a cabo este importante proceso destaca el ribosoma [1].

El ribosoma es aparentemente una ribozima compuesta por varios RNA ribosómicos (rRNAs) y proteínas ribosómicas distintas. Este complejo ribonucleoproteico se encuentra presente en todos los organismos y es esencial para la vida. Los virus parasitan los ribosomas de las células huésped para sintetizar sus propias proteínas víricas.

En todos los organismos, los ribosomas están compuestos por dos subunidades, una subunidad grande (50S en organismos procariotas y 60S en organismos eucariotas) y una subunidad pequeña (30S en organismos procariotas y 40S en organismos eucariotas). Además, existen ribosomas en las mitocondrias y cloroplastos.

La levadura de gemación *Saccharomyces cerevisiae*, organismo modelo eucariota utilizado en esta tesis, presenta una subunidad grande (60S) formada por 3 rRNAs (5S, 5.8S y 25S) y 46 proteínas ribosómicas [2]. Esta subunidad es la encargada de catalizar la formación del enlace peptídico que ocurre entre un aminoacil- y un peptidil-tRNA en una región universalmente conservada del ribosoma llamada centro peptidil-transferasa [3].

La subunidad pequeña está formada por un rRNA 18S y 33 proteínas ribosómicas [2]. Esta subunidad es la encargada de asegurar el correcto emparejamiento de bases codón-anticodón del mRNA y los tRNAs en el denominado centro descodificador [4].

Ambas subunidades (60S y 40S) forman el ribosoma 80S en *S. cerevisiae* mostrado en la **Figura 1**. En la última década, los estudios cristalográficos y de crio-microscopía electrónica han resuelto con gran detalle la estructura de los ribosomas tanto en organismos procariotas como en eucariotas, así como el de orgánulos, permitiendo determinar cómo han evolucionado los ribosomas [5-14].

La subunidad pequeña presenta una estructura marcada por la estructura secundaria del rRNA 18S donde las proteínas ribosómicas se distribuyen mayoritariamente en la periferia [15]. En la subunidad pequeña, se distinguen varios dominios estructurales

denominados cabeza, pico, hombro, pie, cuerpo y plataforma (**Figura 1**). El mRNA entra por un surco formado entre la cabeza y el hombro, y sale por otro surco formado entre la cabeza y la plataforma.

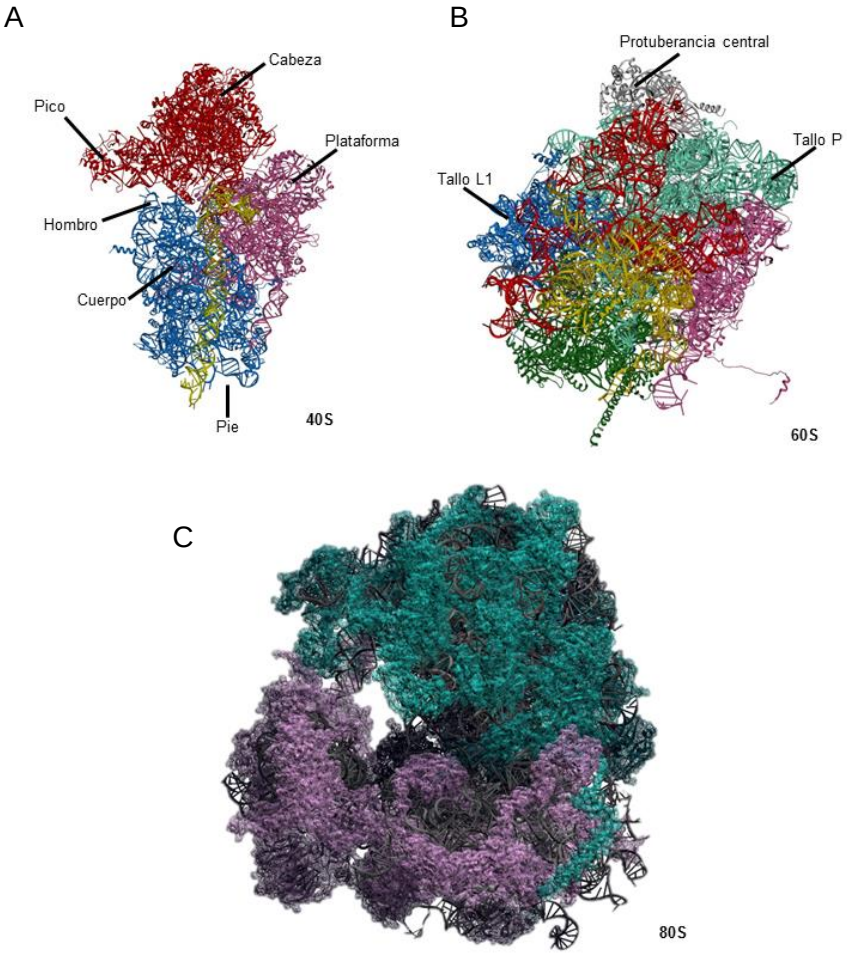

FIGURA 1. Estructura del ribosoma de *Saccharomyces cerevisiae*. (A) Representación (vista de la superficie de interacción entre subunidades) de las distintas regiones de la subunidad pequeña. **(B)** Representación (vista de la superficie de interacción entre subunidades) de las distintas regiones de la subunidad grande. **(C)** La asociación de ambas subunidades a través de puentes intermoleculares forma el ribosoma completo 80S (vista desde la entrada de los mRNAs); en gris se muestran los rRNAs de ambas subunidades, en color púrpura se muestran las proteínas ribosómicas de la subunidad 40S y en color azul las proteínas ribosómicas de la subunidad 60S. Los modelos se realizaron con el programa Chimera v.1.11.2 a partir del archivo pdb 4V88.

La subunidad grande presenta una estructura compacta parecida en eucariotas y procariotas, una región central conservada donde se encuentra la protuberancia central formada por el rRNA 5S y las proteínas L5 (uL18) y L11 (uL15), el tallo L1 formado por la proteína L1 (uL1), el rRNA 5.8S y el tallo P formado por una extensión del rRNA 25S en la que se asocia la proteína L12 (uL11), una estructura pentamérica formada por la proteína P0 (uL10) y dos heterodímeros de las proteínas ácidas P1 y P2 [16] (**Figura 1**).

Los ribosomas mitocondriales son ribosomas especializados, se encuentran permanentemente asociados a la membrana interna de la mitocondria y su estructura diverge de sus homólogos bacterianos y eucarióticos. En *S. cerevisiae* el ribosoma mitocondrial se denomina 74S y está formado por dos subunidades. Hasta la fecha solo se ha resuelto la estructura tridimensional de la subunidad grande o 54S que está formado por un rRNA 21S y 46 proteínas ribosómicas, 13 de las cuales son únicas del ribosoma mitocondrial [17]. Por otro lado también se ha resuelto el ribosoma mitocondrial completo de humano (55S) , compuesto por una subunidad grande o 39S que está formado por un rRNA 16S y 50 proteínas ribosómicas, y una subunidad pequeña o 28S formada por un rRNA 12S y 29 proteínas ribosómicas [18, 19]; en el caso de la subunidad pequeña de *S. cerevisiae* o 37S no se ha resuelto aún la estructura tridimensional. La subunidad 37S está formado por un rRNA 15S y aproximadamente 37 proteínas ribosómicas [19, 20]. El DNA mitocondrial solo codifica 8 proteínas que constituyen la cadena transportadora de electrones encargada de la respiración celular y la proteína ribosómica mitocondrial Var1, el resto de proteínas ribosómicas mitocondriales se codifican en el genoma nuclear [19]. Los ribosomas mitocondriales presentan características propias entre las que se encuentran unas mayores extensiones que proporcionan un mayor número de interacciones proteína-proteína comparado con sus homólogos bacterianos y eucarióticos; esto parece ser debido a la gran reducción de rRNA que presentan, y que es reemplazado por extensiones proteicas [19]. Los rRNAs mitocondriales presentan una gran cantidad de segmentos de expansión y son más flexibles que sus homólogos bacterianos y eucarióticos. Por otro lado, los ribosomas mitocondriales presentan un túnel de salida del péptido naciente diferente al que presentan sus homólogos bacterianos y eucarióticos [17].

La traducción en todos los organismos comienza con la asociación de ambas subunidades en presencia de un mRNA [1]. Esta asociación da lugar a la formación de 3 sitios de unión para los tRNAs: sitios A, P y E en el ribosoma. El sitio A constituye el lugar de entrada de los aminoacil-tRNAs, el sitio P es el lugar donde se cataliza la formación del enlace peptídico y el sitio E constituye el lugar de salida de los tRNAs desacetilados [21]. En la **Figura 2** se representa un esquema del proceso de traducción.

Se han encontrado tanto similitudes como diferencias entre los ribosomas presentes en distintos organismos. Lo más destacable es que todos los ribosomas comparten un núcleo central común que se corresponde básicamente con el ribosoma bacteriano y que incluye los centros funcionales básicos, tanto el centro peptidil-transferasa como el centro descodificador. Unido a este núcleo se extienden formando capas externas extras los dominios de expansión de los rRNAs y las proteínas exclusivas o las extensiones exclusivas

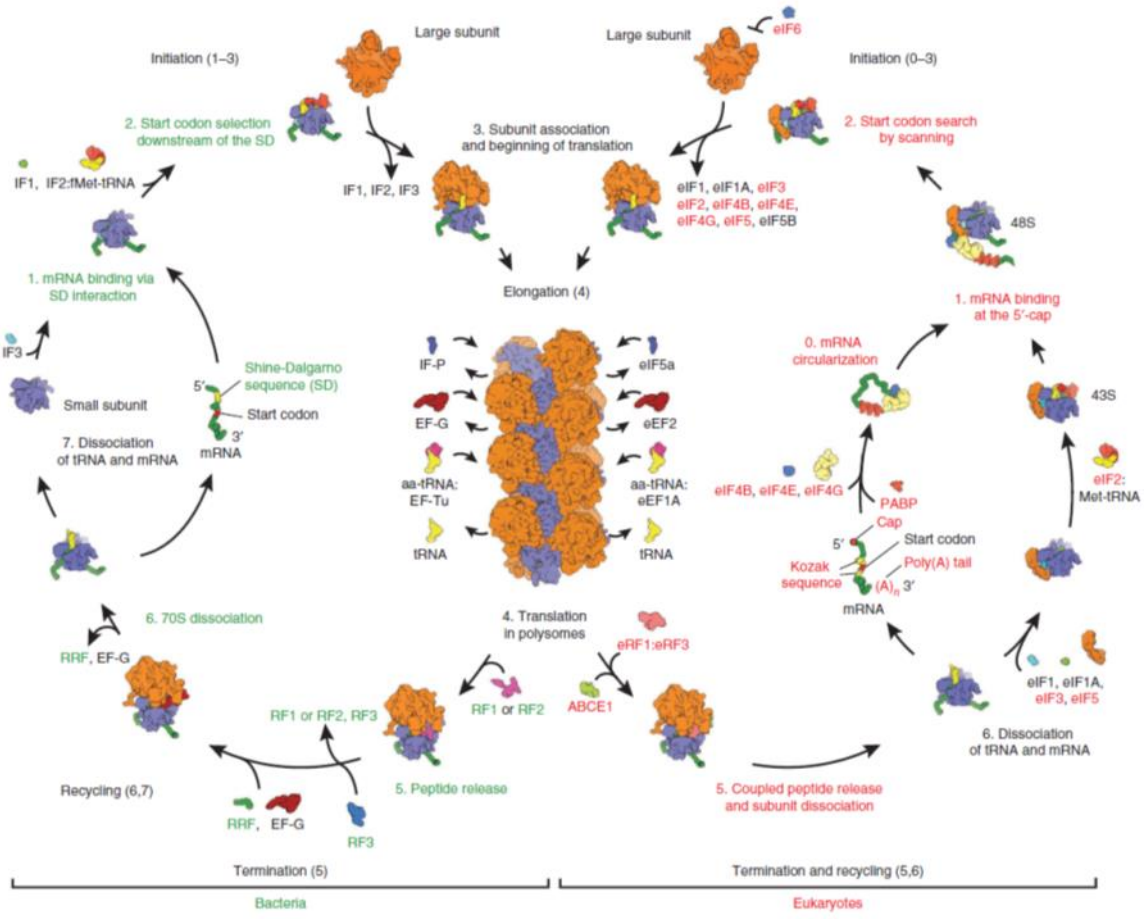

FIGURA 2. Proceso de traducción: iniciación, elongación y terminación. La principal diferencia en el proceso de traducción entre procariotas y eucariotas se encuentra en la iniciación. En procariotas, la unión de la subunidad pequeña al mRNA se realiza por la interacción entre una secuencia aguas arriba del codón de iniciación denominada secuencia Shine-Dalgarno y una secuencia complementaria en el extremo 3' del rRNA 16S. En el caso de los eucariotas, el mRNA se une a varios factores de iniciación que permiten la formación de un complejo de pre-iniciación (PIC). Este complejo escanea el mRNA hasta localizar el codón de iniciación, normalmente el primer codón AUG. Los procesos de elongación y terminación son muy parecidos en procariotas y eucariotas. Adaptado de [22].

de las proteínas ribosómicas en los ribosomas eucariotas [13]. A su vez, las mayores diferencias, encontradas en los ribosomas eucarióticos, se encuentran en la región expuesta al solvente donde aparecen diferentes expansiones de los rRNAs y extensiones de proteínas ribosómicas. Estos elementos proporcionan nuevas interacciones con elementos implicados en la traducción dando mayor robustez al proceso [22]. En la **Figura 3** se muestra la composición de ribosomas de diferentes organismos.

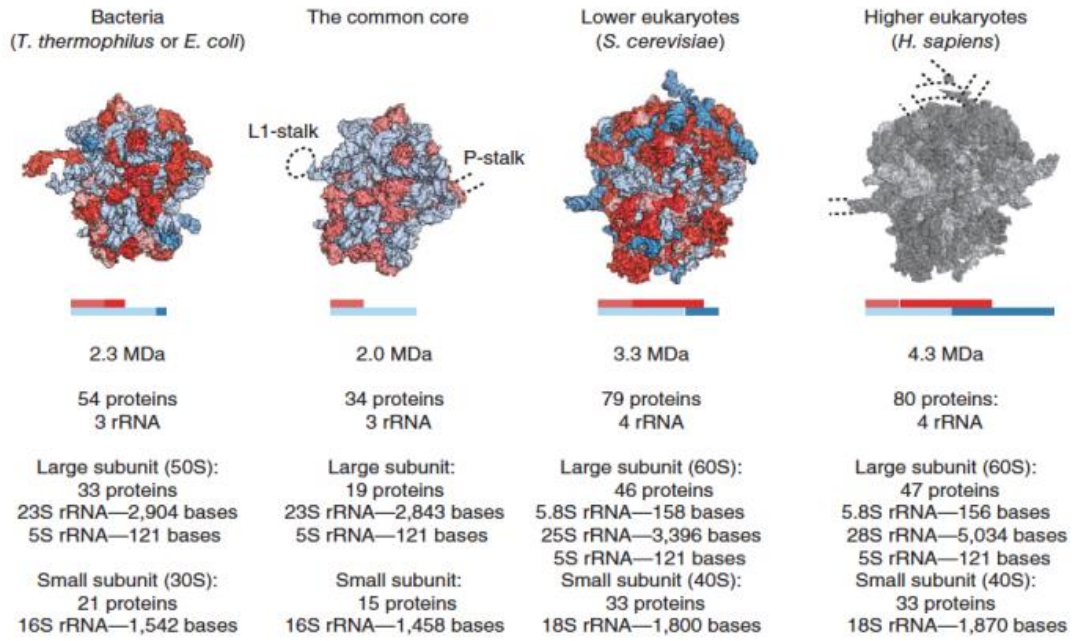

FIGURA 3. Composición del ribosoma procariota, eucariota y el núcleo central conservado. Se representa el núcleo central conservado donde se distinguen los rRNAs en color azul claro y las proteínas ribosómicas en color rojo claro. Las expansiones de los rRNAs específicos se muestran de color azul intenso y las proteínas ribosómicas específicas en color rojo intenso. Con líneas discontinuas, se indica la localización de los tallos L1 y P para los que los muchos estudios cristalográficos no han podido aun resolver sus estructuras. Adaptado de [22].

Síntesis de ribosomas en *S. cerevisiae*

La biogénesis del ribosoma es un proceso esencial para el crecimiento celular que requiere una gran demanda energética [23]; en fase exponencial, las células de *S. cerevisiae* producen alrededor de 2000 ribosomas por minuto [24], la transcripción de los rRNAs suponen el 60% del total de la actividad transcripcional [25], y el total de ribosomas corresponde al 15-20% de la masa celular [25]. Estos números son significativos de por qué el proceso de síntesis de ribosomas se encuentra rigurosamente regulado. En *S. cerevisiae*, la síntesis de ribosomas implica igualmente cerca de 80 RNAs pequeños nucleolares (snoRNAs) [26-28] y más 200 factores de proteicos [29, 30]. En humanos, las cifras aumentan hasta cerca de 300 snoRNAs y más de 600 proteínas [28]. Este importante proceso tiene su comienzo en el nucléolo continúa en el nucleoplasma y sus últimos pasos suceden en el citoplasma. La alta producción de ribosomas depende de los nutrientes disponibles en el medio. Tanto la transcripción de los rRNAs como la de las proteínas ribosómicas están interconectadas con el fin de evitar desbalances que puedan conllevar consecuencias perjudiciales para el correcto funcionamiento celular [31]. En todos los eucariotas se ha descrito que la ruta de señalización TOR (del inglés "**T**arget **O**f

Rapamycin") regula la biogénesis del ribosoma a varios niveles (**Figura 4**): participando tanto en la síntesis de pre-rRNAs a través de la regulación de la RNA polimerasa I (RNAPI) y la RNA polimerasa III (RNAPIII), como en la transcripción de los mRNAs de las proteínas ribosómicas, factores de ensamblaje y snoRNAs mediante la RNA polimerasa II (RNAPII), y finalmente en el procesamiento de los rRNAs y en el proceso de traducción [25, 31].

Procesamiento de los rRNAs

La etapa inicial de la biogénesis del ribosoma es la transcripción del DNA ribosómico (rDNA). En *S. cerevisiae*, el rDNA se localiza en el cromosoma XII y está formado por un alto número (aproximadamente 150) de repeticiones en tándem [32].

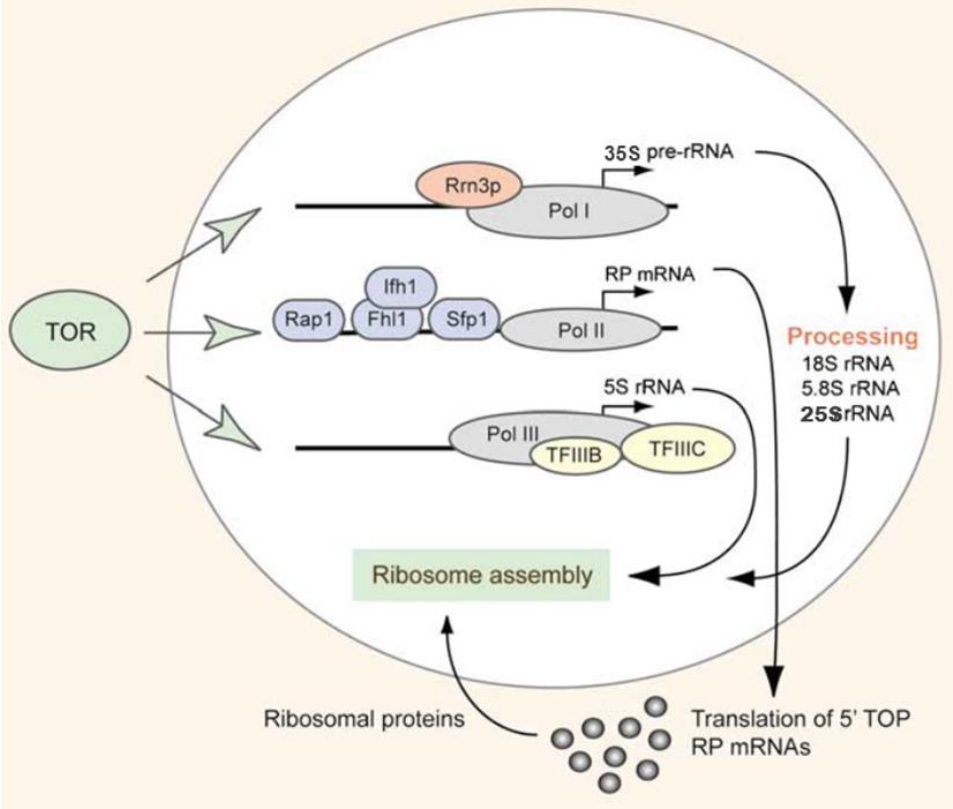

FIGURA 4. La ruta TOR regula la biogénesis del ribosoma a varios niveles. La ruta TOR controla la biogénesis del ribosoma: **(I)** a través de la RNAPI afectando a la transcripción del pre-rRNA 35S, **(II)** a través de la RNAPIII promoviendo la transcripción del precursor de 5S y algunos snoRNAs, **(III)** y a través de la RNAPII regulando la expresión de las proteínas ribosómicas y los factores de ensamblaje. Adaptado de [31].

Cada repetición consta de un gen que genera un transcrito primario de unas 9.1 kb que codifica el precursor 35S de los rRNAs 5.8S, 18S y 25S y que es transcrito por la RNAPI. En sentido contrario, presenta un gen que genera el precursor del rRNA 5S y que es transcrito por la RNAPIII (**Figura 5)**. No todas las repeticiones se encuentran activas simultáneamente, sino que el número de copias que se transcriben en cada momento depende de las necesidades celulares y el estado metabólico de las células [33].

Los pre-rRNAs nacientes sufren distintas modificaciones químicas [34] y son procesados mediante la participación de exo- y endonucleasas [35].

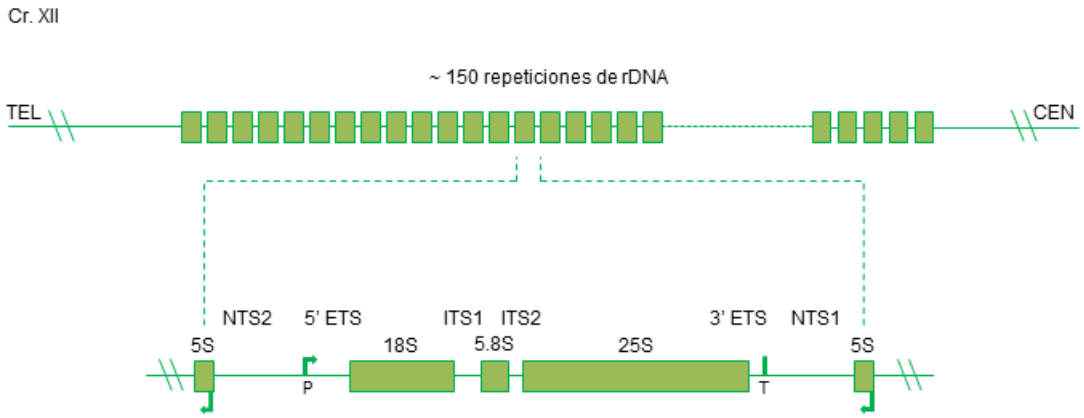

FIGURA 5. Organización del rDNA de *S. cerevisiae*. La levadura *S. cerevisiae* contiene múltiples copias de los genes ribosómicos, en el cromosoma XII, que se transcriben como un único precursor de unas 9.1 kb en repeticiones en tándem. En este precursor se encuentran el pre-rRNA 35S que tras procesarse da lugar a los rRNAs maduros 5.8S, 18S y 25S. Éstos están flanqueados por dos regiones espaciadoras externas (5'ETS y 3'ETS) y están separados por dos regiones espaciadoras internas (ITS1 separando 18S de 5.8S e ITS2 separando a 5.8S de 25S). El precursor rRNA 5S está separado de 35S por otras dos regiones espaciadora que no se transcriben (NTS). Con las letras P y T se indica la región promotora y terminadora del transcrito policistrónico.

El procesamiento de los rRNAs ocurre en el contexto de grandes complejos ribonucleoproteicos denominados partículas pre-ribosómicas [29]. Estas partículas además de los pre-rRNAs contienen multitud de factores no-ribosómicos (snoRNAs y proteínas), y distintos grupos de proteínas ribosómicas más o menos establemente ensambladas. En la mayoría de los casos, la perdida de función de alguno de estos factores origina defectos en el procesamiento de los pre-rRNAs. Hasta la fecha, sólo para unos pocos de estos factores, se ha descrito un mecanismo de acción molecular preciso. En el resto de los casos, la función exacta de los factores sigue siendo desconocida.

El procesamiento del precursor 35S comienza con los cortes endonucleolíticos consecutivos en los sitios A_0 y A_1, localizados en el 5'ETS, y posteriormente en el sitio A_2 localizado en la región interna ITS1; el corte en el sitio A_2 da lugar a los precursores 20S y $27SA_2$, que pertenecen a rutas de maduración aparentemente independientes de las partículas pre-40S y pre-60S [36, 37] (**Figura 6**).

Numerosas evidencias experimentales indican que la eliminación del 5'ETS del pre-rRNA 35S podría ocurrir antes de que éste último sea transcripto por completo [38], es decir, ocurrir de manera co-transcripcional. Estudios cinéticos de la maduración de los pre-rRNAs y la visualización mediante microscopia electrónica (EM) del transcrito naciente del pre-rRNA apoyan el hecho de que el corte en el sitio A_2 pueda ocurrir co-transcripcionalmente. En *S. cerevisiae* se estima que aproximadamente un 70% de los pre-rRNAs se procesan co-transcripcionalmente en fase exponencial de crecimiento [39, 40].

En cualquier caso, como se ha mencionado anteriormente, el corte en el sitio A_2 separa las rutas de maduración de partículas pre-40S y pre-60S, originando los precursores 20S y $27SA_2$ los cuales se procesan de manera aparentemente independiente. En el caso de la formación de la partícula pre-40S, el pre-rRNA 20S se procesa en su extremo 3' en el sitio D por la endonucleasa Nob1 en el contexto de una partícula ribosómica denominada "80S_like" en el citoplasma [41]. En el caso del pre-rRNA $27SA_2$ el procesamiento es más complejo. El $27SA_2$ puede seguir dos rutas alternativas de maduración, cuya principal diferencia es la forma de procesar la región interna ITS1. En la ruta principal, aproximadamente, el 85% de todo el pre-rRNA $27SA_2$ se procesa en el sitio A_3 por la endonucleasa RNasa MRP [42], resultando en el pre-rRNA $27SA_3$ que es digerido posteriormente 5'-3' exonucleoliticamente hasta el sitio B_{1S} para dar lugar al precursor $27SB_S$, que posee el extremo 5' maduro del rRNA $5.8S_S$ [43, 44]. En la ruta minoritaria, aproximadamente, el 15% de todo el pre-rRNA $27SA_2$ es procesado directamente en el sitio B_{1L}, mediante un corte endonucleolítico por una nucleasa aún desconocida. Este corte origina el pre-rRNA $27SB_L$ que presenta el extremo 5' maduro del rRNA $5.8S_L$ [45]. Al mismo tiempo que se completa el procesamiento del sitio B_1, ocurre el procesamiento del extremo 3' del rRNA 25S mediante la digestión 3'-5' exonucleolítica desde el sitio B_0 hasta el sitio B_2 presente en el pre-rRNA 27SA [46, 47].

Parece ser que los pre-rRNAs $27SB_S$ y $27SB_L$ se procesan siguiendo las mismas reacciones de maduración. La primera reacción consiste en el corte en el sitio C_2, que separa los pre-rRNAs 7S y 25.5S (26S) que darán lugar a los rRNAs maduros 5.8S y 25S, respectivamente [46]. Recientemente se ha demostrado *in vitro* que el "complejo Las1"

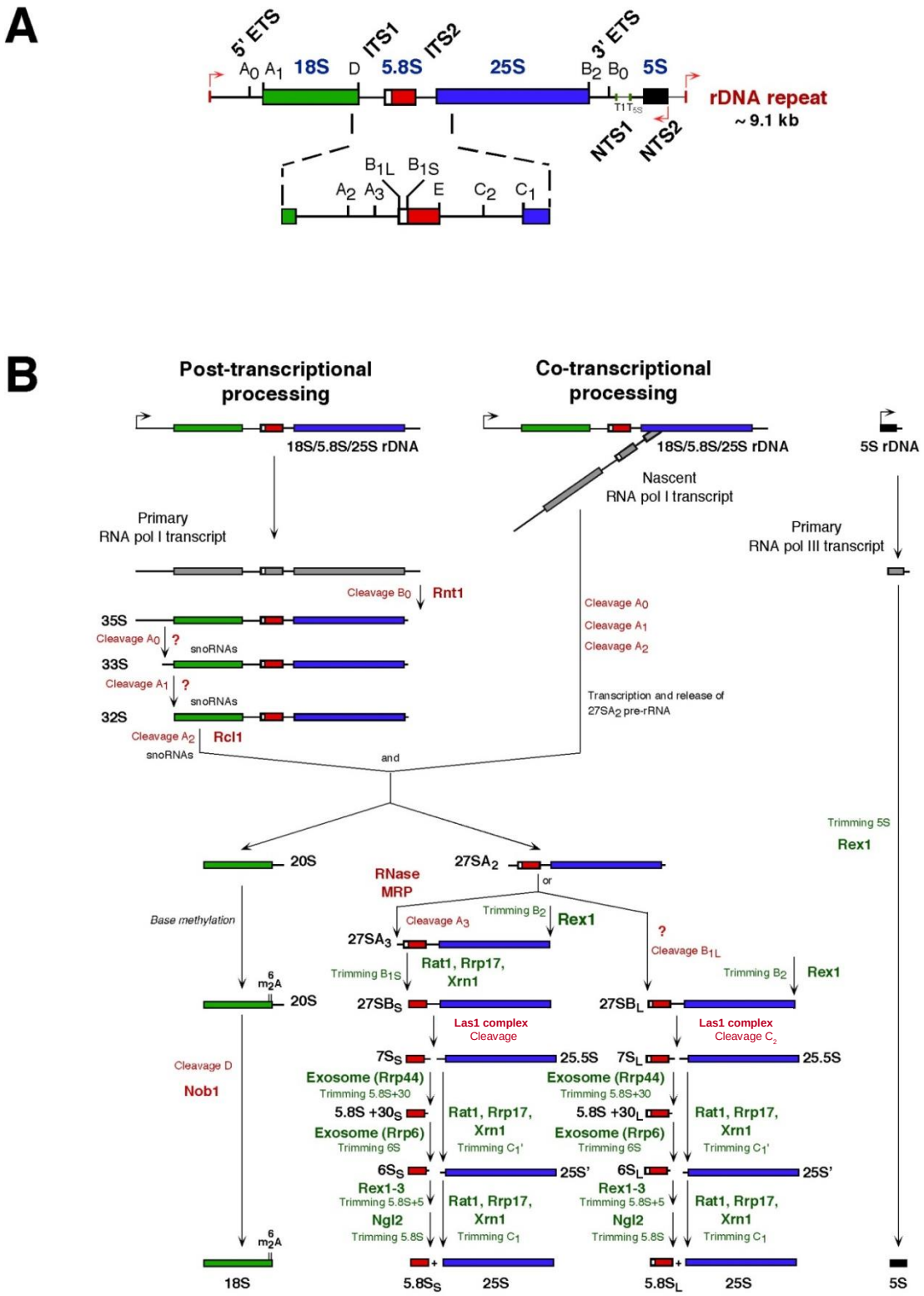

FIGURA 6. Esquema del procesamiento de los rRNAs en *S. cerevisiae*. (A) Organización de una repetición del rDNA donde se indica la localización de los sitios de corte. **(B)** Esquema de la ruta de maduración de los pre-rRNAs. En rojo se muestran las enzimas endonucleolíticas y en verde las enzimas exonucleolíticas. Las nucleasas aún no identificadas se han marcado con un símbolo de interrogación. Adaptado de [48].

compuesto por cuatro subunidades: Las1, una endonucleasa; Grc3, una 5' polinucleótido kinasa; Rat1, una 5'-3' exonucleasa y su cofactor Rai1, una 5' pirofosfatasa, es el responsable del corte en el sitio C_2 [49]. Este corte genera un pre-rRNA 7S con un extremo 3' con un 2',3' fosfato cíclico, y un pre-rRNA 26S con un extremo 5' con un grupo OH. El grupo fosfato cíclico que presenta el pre-rRNA 7S en su extremo 3' podría ser el responsable de la estabilidad de este intermediario y protegerlo del procesamiento a 5.8S [49]. El pre-rRNA 7S se procesa en el extremo 3' por una serie de 3'-5'exonucleasas [50-53] que da lugar al menos a dos intermediarios estables, los pre-rRNAs 5.8S+30 generado por la subunidad Rrp44 del exosoma, y el pre-rRNA 6S generado por la subunidad Rrp6.

Recientemente, se ha demostrado que la maduración del extremo 3' del precursor 6S ocurre en el citoplasma [54] mediante una serie de reacciones consecutivas llevadas a cabo por las nucleasas Rex1, Rex2, Rex3 [52] y Ngl2 [53]. Esto da lugar a las dos especies de rRNA 5.8S denominadas $5.8S_L$ y $5.8S_S$. El pre-rRNA 26S generado tras el corte en C_2 es fosforilado por Grc3 permitiendo que Rat1-Rai1 se procese a un intermediario 25S'; posteriormente, las enzimas Rat1/Rrp17 maduran este intermediario hasta la especie madura del rRNA 25S [44, 49, 55].

Por otra parte de manera independiente, el rRNA 5S se transcribe por la RNAPIII como un precursor que presenta su extremo 5' maduro, pero cuyo extremo 3' se extiende varios nucleótidos del extremo 3' maduro. La maduración del pre-rRNA 5S consiste en la digestión 3'-5' exonucleolítica de estos nucleótidos llevada a cabo por la exonucleasa Rex1 [52, 56].

Las proteínas ribosómicas en *S. cerevisiae*

Las 79 proteínas ribosómicas de *S. cerevisiae* (**Figura 7A y 7B**), se codifican por 138 genes; en la mayoría de los casos, los genes están duplicados dando lugar a proteínas parálogas. Los mRNAs de las proteínas ribosómicas representan el 50% de toda la transcripción realizada por la RNAPII. Los genes de estas proteínas constituyen un agrupamiento funcional conocido como regulón RP [57]; la característica que presentan la mayoría de estos genes es la presencia en sus promotores de un sitio de unión del factor de transcripción Rap1 [58]. Además, algunos genes de proteínas ribosómicas presentan un sitio de unión para el factor Abf1 [25]. Se ha demostrado que la unión defectiva de Rap1 a los promotores de las proteínas ribosómicas provoca una disminución del 75% de la transcripción de estos genes [59]. En la regulación de la transcripción del regulón RP intervienen diversos factores de transcripción y señales intra- y extracelulares que están

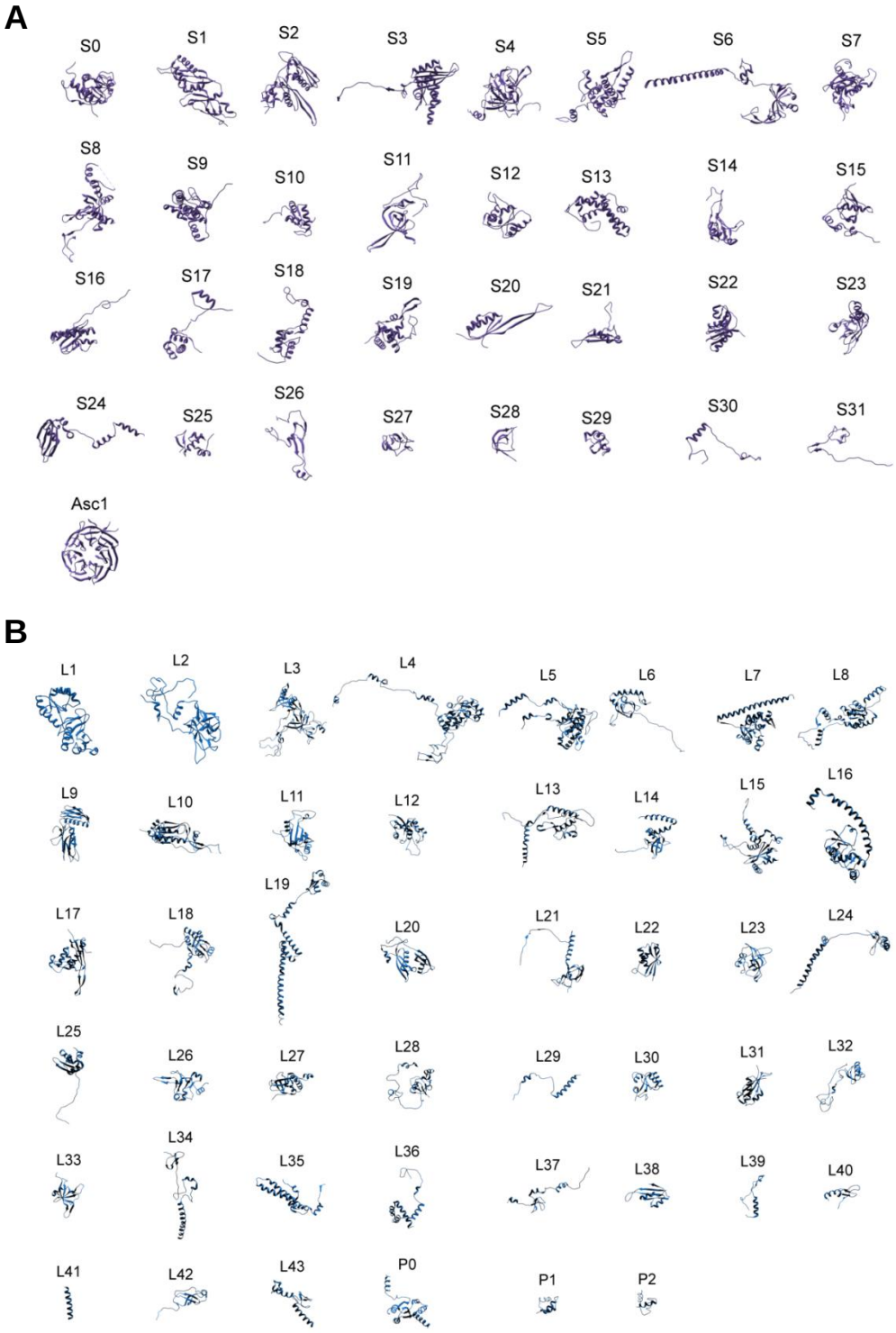

FIGURA 7. Estructura tridimensional de las proteínas ribosómicas de la subunidad pequeña y grande del ribosoma de *S. cerevisiae*. (A) Estructura tridimensional de las 33 proteinas ribosómicas que conforman la subunidad pequeña del ribosoma de *S. cerevisiae*. **(B)** Estructura tridimensional de las 46 proteínas ribosómicas que conforman la subunidad grande del ribosoma de *S. cerevisiae*. Las proteínas ribosómicas aunque bien conservadas, presentan extensiones específicas en eucariotas, que juegan papeles importantes en diferentes puntos del proceso de ensamblaje de la propia proteína o interactuando con otras proteínas vecinas. La representación fue generada con el programa Chimera v.1.11.2 a partir del archivo pdb: 4V88.

integradas en la ruta TOR (**Figura 8**), la cual como se ha mencionado anteriormente, mantiene el correcto balance en la producción de los rRNAs y las proteínas ribosómicas [25, 31].

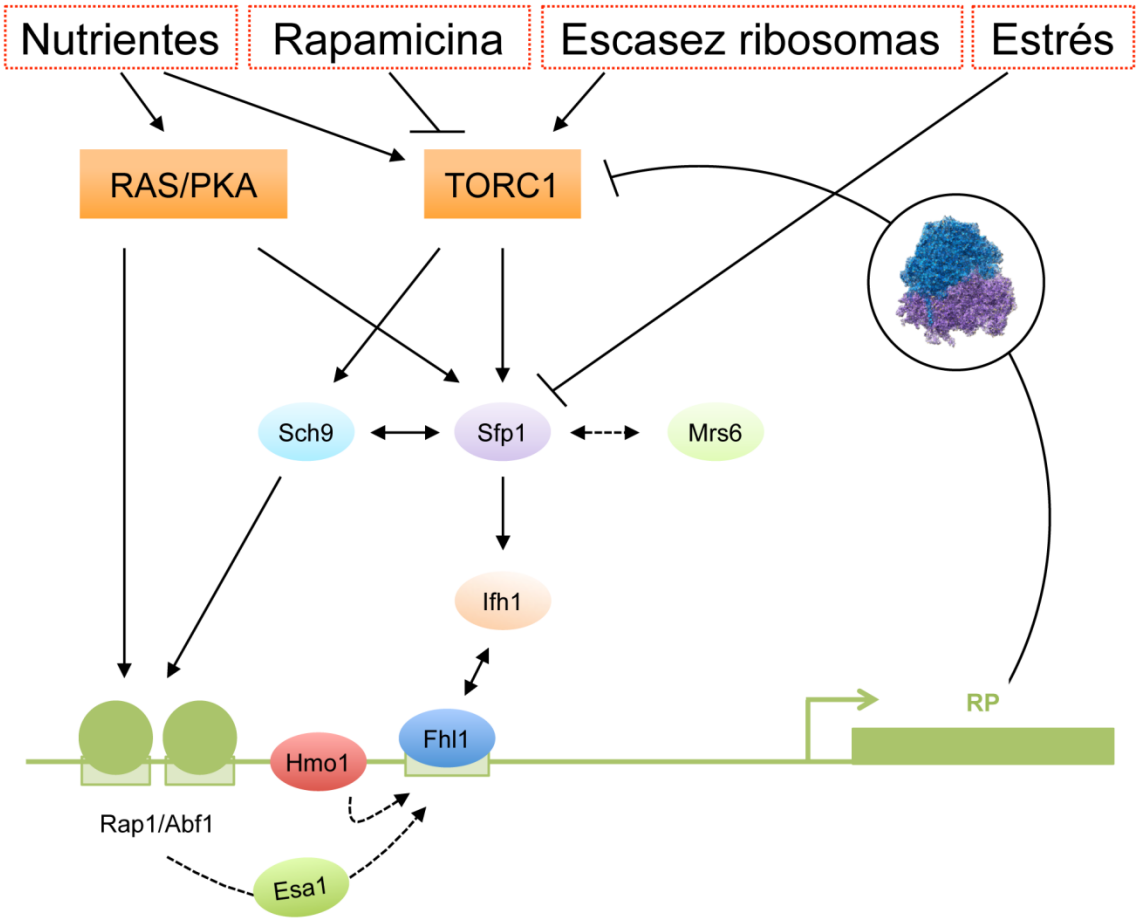

FIGURA 8. Regulación de la transcripción de los genes de proteínas ribosómicas (RP). Determinadas señales tanto extracelulares como intracelulares inducen o reprimen la ruta TOR y RAS/PKA como se indica en la figura. Estas señales se canalizan mediante una cascada de señalización que implica factores integradores como Sfp1 y Sch9. El factor activador clave de los genes RP es Ifh1, el cual se une a los promotores gracias a su interacción con el factor Fhl1 [60]. Mrs6 es un factor importante implicado en la regulación de la localización subcelular de Sfp1, y éste a su vez, regula la localización de los factores Ifh1 y Fhl1 en el núcleo. Por otro lado la actividad quinasa del factor Sch9 es esencial; se especula que fosforila al factor Rap1 [61, 62]. Rap1 y Hmo1 son factores de transcripción que cooperan para regular positivamente la transcripción de los genes de las proteínas ribosómicas. Esa1 es una acetil-transferasa de histonas que elimina la acción represora de los nucleosomas. Hay dos sitios de unión para Rap1 en el promotor de la mayoría de los genes de proteínas ribosómicas. Cuando la proteína Rap1 se une, se activa la transcripción. Se ha observado que algunos genes de proteínas ribosómicas presentan un sitio de unión al factor Abf1 en sus promotores. Adaptada de la Tesis Doctoral de Fernando Gómez Herrero.

Las proteínas ribosómicas son normalmente de pequeño tamaño y de carácter básico, con la excepción de las proteínas del tallo P (P1 y P2) que aunque pequeñas presentan un carácter ácido; el carácter básico proporciona un entorno en el cual se neutraliza las cargas negativas de los residuos fosfatos de los rRNAs [63]. Muchas de las proteínas ribosómicas presentan una estructura diferenciada en dos dominios: una región globular fuertemente estructurada que en la mayoría de los casos se localiza en la superficie del ribosoma, y una región formada por una o varias extensiones normalmente intrínsecamente desordenadas que es frecuente que se introduzcan hacia el interior del ribosoma (**Figura 9**).

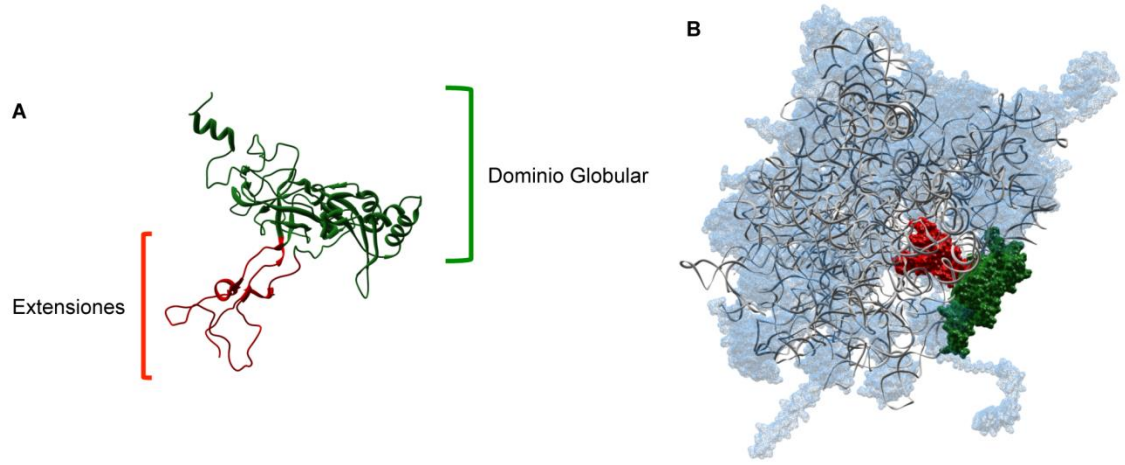

FIGURA 9. Estructura tridimensional de la proteína ribosómica L3 (uL3) de *S. cerevisiae*. (A) Estructura tridimensional de L3 (uL3) donde se muestra una región coloreada en verde que forma los dominios globulares de la proteína y una región en rojo que corresponde con las extensiones de la misma, una amino-terminal y otra como un lazo central. **(B)** Localización de la proteína L3 (uL3) en el contexto de la subunidad 60S del ribosoma. Se observa que el dominio globular de la proteína se sitúa en la superficie del ribosoma en contacto con el exterior mientras que las extensiones de la proteína se introducen en el interior del ribosoma. Realizado con el programa Chimera v.1.11.2 a partir de los archivos pdb: 3u5i y 3u5h.

Muchos genes de proteínas ribosómicas se encuentran duplicados, las proteínas parálogas pueden ser idénticas pero en numerosos ejemplos no lo son totalmente. Se ha llegado a especular que el ensamblaje de uno u otro parálogo afecta al funcionamiento del ribosoma. Desde un punto de vista general, tomando la posibilidad de diferentes especies de rRNA (el caso de $5.8S_S$ o $5.8S_L$) y proteínas ribosómicas, podemos imaginar un escenario de ribosomas con distinta composición, que podría reflejarse en distinta funcionalidad, es decir, un escenario de ribosomas especializados. Esta idea se ha confirmado para ribosomas de distintos tejidos de organismos eucariotas superiores pero

hasta el momento no se ha podido demostrar selectividad real de estos ribosomas hacia ciertos mRNAs para que se traduzcan diferencialmente [64].

Durante mucho tiempo se ha pensado que la función ribosómica residía exclusivamente en las proteínas ribosómicas y que los rRNAs servían de esqueleto estructural. Con la aparición del concepto de RNA catalítico y la obtención de datos que relacionaban de manera casi exclusiva a los rRNAs con la función ribosómica, se estableció la hipótesis no probada de que el ribosoma es una ribozima, dónde la actividad catalítica del centro peptidil-transferasa es llevada a cabo por el rRNA 25S (o 23S) [65, 66]. En las últimas dos décadas, la resolución de estructuras de ribosomas de distintos organismos a nivel atómico [67] ha confirmado que las proteínas ribosómicas se encuentran relativamente lejos de los centros funcionales como para ser responsables de la acción catalítica, aunque son esenciales para el funcionamiento general del ribosoma [66].

En las últimas décadas casi todo el esfuerzo investigador se había enfocado en el análisis del papel de los factores de ensamblaje en la biogénesis del ribosoma. Poco se conocía sobre la importancia de las proteínas ribosómicas en este proceso [68-77]. Se han encontrado principios generales entre el ensamblaje de ribosomas procariotas y eucariotas, aunque debido a la mayor complejidad del ribosoma eucariota los procesos no son del todo equivalentes ni están aun completamente resueltos [78].

La nomenclatura de las proteínas ribosómicas ha sufrido cambios drásticos no deseables a lo largo de los últimos años, dando lugar a confusiones debido a que proteínas ortólogas procariotas y eucariotas tenían nombres distintos; así la proteína L5 bacteriana se corresponde con la proteína L11 de *S. cerevisiae*, a su vez la proteína L5 de levadura es la proteína L18 en bacterias. Esto parece haber sido solucionado con el establecimiento de una nomenclatura que evidentemente necesita un periodo de adaptación para su correcta asimilación por parte de la comunidad científica que estudia el ribosoma [79] (**Tabla 1**).

Maduración de la partícula pre-ribosómica temprana 90S

Como he mencionado anteriormente, el procesamiento de los rRNAs ocurre en el contexto de grandes complejos ribonucleoproteicos formados por distintos pre-rRNAs, algunas proteínas ribosómicas y numerosos factores de ensamblaje. La composición de las partículas pre-ribosómicas es distinta dependiendo del estado de maduración de las mismas. La primera partícula pre-ribosómica detectada es la partícula 90S o también conocida como procesoma SSU (del inglés ***S****mall-****SU****bunit processome*) [80, 81]. La partícula 90S es un complejo macromolecular de aproximadamente 2.2 MDa que contiene al

Nueva nomenclatura para las proteínas de la subunidad pequeña del ribosoma.

Nombre nuevo[a]	Rango taxonómico[b]	Nombre en bacteria	Nombre en levadura	Nombre en humano
bS1	B	S1	–	–
eS1	A E	–	S1	S3A
uS2	B A E	S2	S0	SA
uS3	B A E	S3	S3	S3
uS4	B A E	S4	S9	S9
eS4	A E	–	S4	S4
uS5	B A E	S5	S2	S2
bS6	B	S6	–	–
eS6	A E	–	S6	S6
uS7	B A E	S7	S5	S5
eS7	E	–	S7	S7
uS8	B A E	S8	S22	S15A
eS8	A E	–	S8	S8
uS9	B A E	S9	S16	S16
uS10	B A E	S10	S20	S20
eS10	E	–	S10	S10
uS11	B A E	S11	S14	S14
uS12	B A E	S12	S23	S23
eS12	E	–	S12	S12
uS13	B A E	S13	S18	S18
uS14	B A E	S14	S29	S29
uS15	B A E	S15	S13	S13
bS16	B	S16	–	–
uS17	B A E	S17	S11	S11
eS17	A E	–	S17	S17
bS18	B	S18	–	–
uS19	B A E	S19	S15	S15
eS19	A E	–	S19	S19
bS20	B	S20	–	–
bS21	B	S21	–	–
bTHX	B	THX	–	–
eS21	E	–	S21	S21
eS24	A E	–	S24	S24
eS25	A E	–	S25	S25
eS26	E	–	S26	S26
eS27	A E	–	S27	S27
eS28	A E	–	S28	S28
eS30	A E	–	S30	S30
eS31	A E	–	S31	S27A
RACK1	E	–	Asc1	RACK1

[a] b: bacteriano, e: eucariótico, u: universal
[b] B: bacteria, A: arquea, E: eucariota

Nomenclatura para las proteínas de la subunidad grande del ribosoma.

Nombre nuevo[a]	Rango taxonómico[b]	Nombre en bacteria	Nombre en levadura	Nombre en humano
uL1	B A E	L1	L1	L10A
uL2	B A E	L2	L2	L8
uL3	B A E	L3	L3	L3
uL4	B A E	L4	L4	L4
uL5	B A E	L5	L11	L11
uL6	B A E	L6	L9	L9
eL6	E	–	L6	L6
eL8	A E	–	L8	L7A
bL9	B	L9	–	–
uL10	B A E	L10	P0	P0
uL11	B A E	L11	L12	L12
bL12	B	L7/L12	–	–
uL13	B A E	L13	L16	L13A
eL13	A E	–	L13	L13
uL14	B A E	L14	L23	L23
eL14	A E	–	L14	L14
uL15	B A E	L15	L28	L27A
eL15	A E	–	L15	L15
uL16	B A E	L16	L10	L10
bL17	B	L17	–	–
uL18	B A E	L18	L5	L5
eL18	A E	–	L18	L18
bL19	B	L19	–	–
eL19	A E	–	L19	L19
bL20	B	L20	–	–
eL20	E	–	L20	L18A
bL21	B	L21	–	–
eL21	A E	–	L21	L21
uL22	B A E	L22	L17	L17
eL22	E	–	L22	L22
uL23	B A E	L23	L25	L23A
uL24	B A E	L24	L26	L26
eL24	A E	–	L24	L24
bL25	B	L25	–	–
bL27	B	L27	–	–
eL27	E	–	L27	L27
bL28	B	L28	–	–
eL28	E	–	–	L28
uL29	B A E	L29	L35	L35
eL29	E	–	L29	L29
uL30	B A E	L30	L7	L7
eL30	A E	–	L30	L30
bL31	B	L31	–	–
eL31	A E	–	L31	L31
bL32	B	L32	–	–
eL32	A E	–	L32	L32
bL33	B	L33	–	–
eL33	A E	–	L33	L35A
bL34	B	L34	–	–
eL34	A E	–	L34	L34
bL35	B	L35	–	–
bL36	B	L36	–	–
eL36	E	–	L36	L36
eL37	A E	–	L37	L37
eL38	A E	–	L38	L38
eL39	A E	–	L39	L39
eL40	A E	–	L40	L40
eL41	A E	–	L41	L41
eL42	A E	–	L42	L36A
eL43	A E	–	L43	L37A
P1/P2	A E	–	P1/P2 (AB)	P1/P2 (αβ)

[a] b: bacteriano, e: eucariótico, u: universal
[b] B: bacteria, A: arquea, E: eucariota

TABLA 1. Nomenclatura unificada de las proteínas ribosómicas. Se muestra la nueva nomenclatura adaptada por el área de trabajo del ribosoma de todas las proteínas ribosómicas de las subunidad pequeña (izquierda) y de la subunidad grande (derecha). Se señalan cuales son exclusivas de bacterias (B), cuáles de arqueas (A), y cuáles de eucariotas (E). Adaptado de [79].

pre-rRNA 35S, unos 70 factores de ensamblaje y numerosos snoRNAs. Muy recientemente, los grupos de Ed Hurt y Sebastian Klinge han conseguido determinar la estructura tridimensional de la partícula 90S a 7.3 Å de resolución del ascomiceto extremófilo *Chaetomium thermophilum* [82] (**Figura 10**) y a 5.1 Å de *S. cerevisiae* [83], respectivamente. *C. thermophilum*, está estrechamente relacionado con *S. cerevisiae*, compartiendo hasta un 73% de homología entre sus proteínas [84]. Varios estudios han determinado que la formación de esta partícula sucede mediante el ensamblaje modular de 6 sub-complejos: U3 snoRNP, el sub-complejo Mpp10-Imp3-Imp4, UTP-A (formado por las proteínas Utp4, Utp5, Utp8, Utp9, Utp10, Utp15 y Utp17), UTP-B (formado por las proteínas Utp1, Utp6, Utp12, Utp13, Utp18 y Utp21), UTP-C (formado por las proteínas Rrp7, Utp22, Ckb1, Cka1, Ckb2 y Cka2) y el subcomplejo Bms1-Rcl1, otras enzimas como Emg1 y Kre33, y factores estructurales como Utp20, Noc4 y Nop14, que se asocian de manera secuencial sobre el pre-rRNA naciente [82, 83, 85-88] (**Figura 11**). El completo ensamblaje del procesoma SSU permite que la endonucleasa Utp24 realice el corte en los sitios A_1 y A_2 [89], separando el rRNA 18S del 5' ETS y parte del ITS1. Muchos de estos factores son necesarios para la correcta maduración del rRNA 18S, sin embargo muy pocos de ellos son necesarios para la correcta maduración de los rRNAs de la subunidad grande [80, 81].

El corte en el sitio A_2 separa las rutas de maduración de las partículas que formarán parte de las dos subunidades, las tempranas pre-40S (43S) y pre-60S (66S), las cuales maduran de manera aparentemente independientes (**Figura 12**). Las partículas pre-40S tempranas contienen el pre-rRNA 20S y 12 factores fuertemente asociados, de los cuales Rrp12, Nop14, Enp1, Hrr25, Dim1, Asc1 y Pno1 se encuentran también en la partícula 90S y Tsr1, Ltv1, Nob1, Rio2 y Bub23 sólo se encuentran en las partículas pre-40S [90, 91]; las partículas pre-60S contienen el pre-rRNA $27SA_2$ y a diferencia de la simplicidad que conlleva la maduración de las partículas 40S, la maduración de las partículas pre-60S es más compleja, encontrándose diferentes factores dependiendo de la etapa de maduración. Entre estos factores se encuentran: Nop7, Nog1, Noc2, Nsa2, Nsa3, Nug1 y Tif6. Por otro lado, algunos de los factores que son específicos de la ruta de maduración de partículas pre-60S son: Ssf1, Noc1, Noc3, Nsa1, Rsa4, Rix1 o Arx1 [92-96]. Las células sintetizan cantidades equimolares de ambas subunidades ribosómicas, por lo que deben existir mecanismos de regulación que mantenga esta relación, a pesar de la separación en la maduración de ambas subunidades. Estos mecanismos se basan, al menos, en la transcripción de un único transcrito común para ambas subunidades, y la presencia de factores de ensamblaje comunes para ambas rutas de maduración que actúan a distintos tiempos entre otros [97-100].

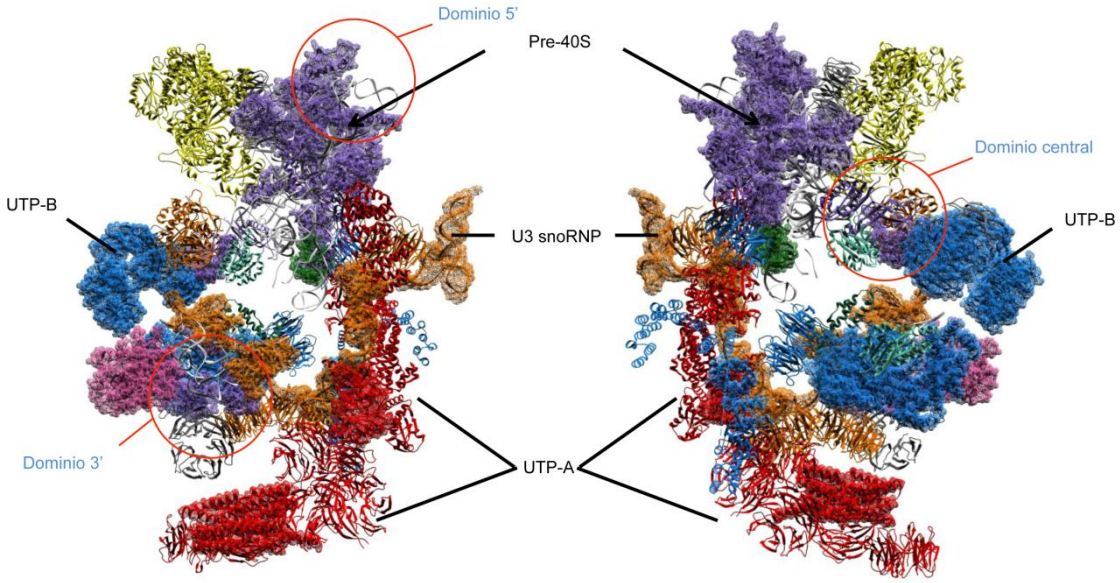

FIGURA 10. Estructura tridimensional de la partícula 90S de *Chaetomium thermophilum* obtenida mediante crio-microscopía electrónica. Se muestra la estructura de la partícula pre-ribosómica 90S de este hongo. Se observa la localización de los distintos sub-complejos necesarios para la maduración de la subunidad 40S (morado), entre los que se destacan: U3 snoRNP (naranja), UTP-A (rojo) y UTP-B (azul). Adaptada de [82].

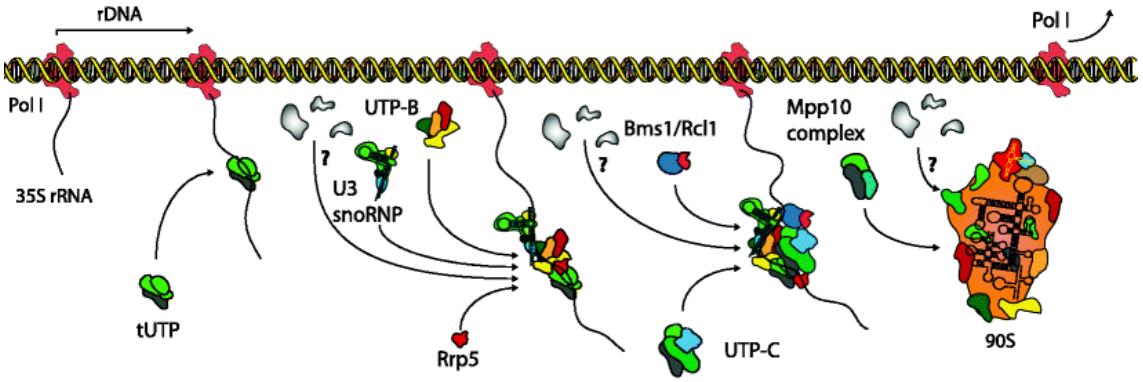

FIGURA 11. Modelo para la formación de la partícula pre-ribosómica 90S. La asociación jerárquica de sub-complejos al pre-RNA 35S comienza con la asociación del complejo tUTP o UTP-A. Esta asociación inicial permite las subsiguientes incorporaciones de los demás sub-complejos. Las etapas de ensamblaje de U3 snoRNP y UTP-B, que ocurre de manera independiente, guían la formación de 90S; estas dos etapas son necesarias para el ensamblaje posterior de varios componentes [101-104]. El ensamblaje de la GTPasa Bms1 es necesario para la incorporación de otros factores y del sub-complejo Mpp10. La incorporación de Rrp5 es crucial para el reclutamiento del sub-complejo UTP-C pero no para los sub-complejos tUTP/UTP-A, U3 snoRNP o UTP-B [85, 105]. Adaptado de [106].

El ensamblaje de la subunidad 40S

Tanto el procesamiento del pre-rRNA como la unión de las proteínas ribosómicas al pre-rRNA 20S ocurre en gran parte de forma co-transcripcional y en el nucléolo. Aunque solo se ha descrito una partícula pre-40S estable, nuclear, es posible que existan hasta al menos cuatro partículas intermedias [48], cada una definida por los cortes que requiere el pre-rRNA naciente hasta formar el pre-rRNA 20S.

Análisis globales han demostrado que el ensamblaje de las proteínas ribosómicas de la subunidad pequeña sigue un patrón jerárquico [76, 77] (**Figura 13**). Generalmente, las primeras proteínas ribosómicas se ensamblan en la zona de la subunidad denominada cuerpo, de manera temprana durante la transcripción. A continuación, se ensamblan las proteínas que dan lugar a la zona denominada cabeza; estas proteínas suponen hasta el 70% de todas las proteínas ribosómicas que conforman la subunidad pequeña. Por último, las proteínas que se unen en un estadio más tardío de maduración ocupan su lugar en distintas zonas. El hecho de que el proceso de ensamblaje ocurra de forma co-transcripcional es consistente con la observación de que hasta 21 proteínas ribosómicas de la subunidad pequeña co-precipitan el pre-rRNA 20S. Sólo las proteínas S11 (uS17) y S13 (uS15), que se unen a la plataforma, co-precipitan cantidades significativas del pre-rRNA 35S [77].

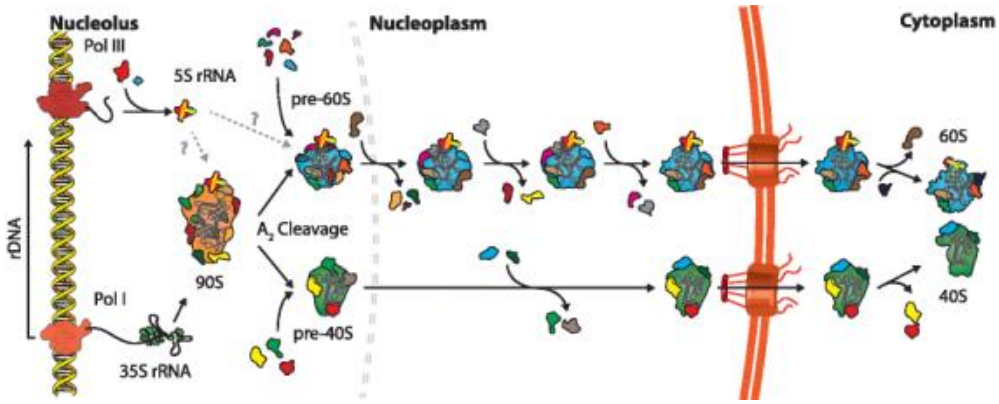

FIGURA 12. Ruta de ensamblaje del ribosoma eucariota. El primer precursor ribosómico en formarse es 90S (naranja) compuesto por factores y proteínas ribosómicas de la subunidad pequeña que son reclutados sobre el pre-rRNA 35S. Tras ocurrir el corte en el sitio A_2, la subsiguiente maduración ocurre en dos rutas independientes: el precursor de 40S (verde) y el precursor de 60S (azul). A lo largo de ambas rutas, ocurren asociaciones de distintos factores que dirigen unidireccionalmente la maduración a través del nucleoplasma hacia el complejo de poro nuclear. Los últimos pasos de maduración ocurren en el citoplasma. Adaptado de [106].

A pesar de la aceptación de este modelo de ensamblaje de las proteínas de la subunidad pequeña, se han descrito casos en los que se ha asumido un ensamblaje tardío,

y posteriormente, se ha comprobado que estas proteínas están presentes en partículas tempranas como 90S o pre-40S, con las que presentan asociaciones no estables, un ejemplo de ello es la proteína S31 (eS31) [107]. Estos resultados indican que las proteínas ribosómicas de la subunidad pequeña se ensamblan de manera laxa a las partículas pre-40S tempranas y sólo a lo largo de la maduración, la interacción con el rRNA se va haciendo más fuerte y estable [77].

Curiosamente el orden en el que se ensamblan las proteínas ribosómicas de la subunidad pequeña en *S. cerevisiae in vivo* presenta gran paralelismo al ensamblaje *in vitro* estudiado para las proteínas ribosómicas bacterianas [12, 108-110] y probablemente al de las proteínas humanas [111]. Por tanto, el proceso de ensamblaje refleja las características biofísicas de las interacciones RNA-proteína estables de la subunidad pequeña del ribosoma [78].

Varios factores de ensamblaje retrasan la incorporación de ciertas proteínas ribosómicas por competición de su sitio de unión a las partículas pre-ribosómicas. Ejemplo de ello son las proteínas S10 (eS10) y S26 (eS26); la unión prematura de S10 en la estructura del pico de la subunidad pequeña se bloquea por la presencia del factor Ltv1, y la unión de S26 a la plataforma es bloqueada por las proteínas Pno1/Dim2 [112]. Para que el factor Ltv1 se libere de la partícula pre-40S es necesario que sea fosforilado por la quinasa Hrr25 [113]. En el caso de Pno1 se desconoce su mecanismo de reciclaje. Interesantemente, se ha observado que las proteínas S10 y S26 se encuentran en la entrada y salida del canal donde se une el mRNA. Esta situación sugiere un mecanismo de control por el que la liberación de un factor de ensamblaje controla la maduración de la subunidad 40S impidiendo su función previniendo el reclutamiento del mRNA a las partículas pre-40S inmaduras. Este comportamiento en el que los factores de ensamblaje ocupan el lugar de la proteína ribosómica hasta el momento oportuno de su unión al ribosoma se conoce con el nombre genérico de la “hipótesis de los *placeholders*” [114, 115].

Las últimas etapas de maduración de la subunidad pequeña ocurren en el citoplasma, lugar donde se ensamblan las últimas proteínas ribosómicas, se genera el extremo 3’ maduro del rRNA 18S y se disocian los factores de ensamblajes que aún permanecen unidos. Se ha descrito la existencia de un ciclo similar a uno de traducción que actúa como punto de control en la correcta maduración de subunidades ribosómicas funcionales [41, 116]. Parece ser que el pico es la estructura que madura más tarde, y en este estadio de maduración se han descrito hasta siete factores de ensamblaje (Enp1, Ltv1, Rio2, Tsr1, Dim1, Nob1 y Pno1) unidos a distintas regiones de la partícula pre-40S en el pico, la plataforma y la interfase entre ambas subunidades [112]. Recientemente, se ha

demostrado que los últimos pasos de maduración comienzan con el ensamblaje de la proteína ribosómica S3 (uS3). De forma co-traduccional, la proteína S3 se asocia con una proteína chaperona denominada Yar1 formando un complejo [117, 118]. La proteína S3 se encuentra en este complejo con su extremo amino-terminal rotado, y mientras que su extremo carboxílico permite su dimerización. El complejo $(S3)_2$-Yar1 es transportado al núcleo, y una vez allí, el factor Ltv1 reemplaza a la chaperona Yar1 formándose de este modo un complejo S3-Ltv1-Enp1. La asociación inicial de este complejo con la partícula pre-40S se realiza mediante el extremo carboxilo terminal de S3 [119, 120]. Ltv1 impide que la proteína S3 interaccione con la proteína S20 a la vez que impide que el extremo amino de S3 consiga su estructura final; de este modo, el factor Ltv1 previene que el ensamblaje de S3 ocurra de manera prematura. La fosforilación de Ltv1 por la quinasa Hrr25 [113], junto a la rotación del extremo amino terminal de la proteína S3, promueve la liberación del factor Ltv1, permitiendo que la proteína S3 ocupe su lugar definitivo en la partícula pre-40S [118]. El ensamblaje de S3 permite el ensamblaje posterior de la proteína S10 [112]. También, se ha observado que la liberación de Ltv1 es necesaria para que la subunidad pequeña pueda unirse con la subunidad grande, en la que está involucrada la GTPasa eIF5B [113]. Esta GTPasa cumple un papel importante en la maduración citoplasmática de la partícula pre-40S ayudando en la interacción de la subunidad pequeña y la subunidad grande en el intermediario denominado “80S-like” [41, 116] (**Figura 14**). En esta partícula pre-40S tardía, además de una serie de intercambios entre factores de ensamblaje y proteínas ribosómicas, sucede el corte en el extremo 3’ del pre-rRNA 20S. La endonucleasa Nob1, es estimulada tanto por GTP como por ATP, este proceso es dependiente de la GTPasa eIF5B [41]. La liberación de la partícula 40S que contiene el rRNA 18S maduro es llevada a cabo por el factor de terminación Rli1 y su cofactor Dom34; ambas proteínas también participan en la disociación del ribosoma 80S maduro durante la terminación de la traducción. En este punto la subunidad 40S ha madurado completamente salvo por la ausencia de S26 (eS26) [77, 116]. El ensamblaje preciso de S26 no está aclarado dado que otros estudios indican que S26 se une en el núcleo a complejos 90S [121].

Por otro lado, se ha descrito una ruta alternativa del último paso de maduración del pre-rRNA 20S a 18S, el cual es dependiente de la ATPasa Rio1, que favorece la disociación del factor Pno1, que ocupa una posición solapante con la posición que posteriormente ocupará la endonucleasa Nob1. Además, como anteriormente he mencionado, la actividad ATPasa favorece la reacción de Nob1 [122]. De igual manera, la ATPasa Rio1 podría promover la formación de la partícula “80S-like”.

A)

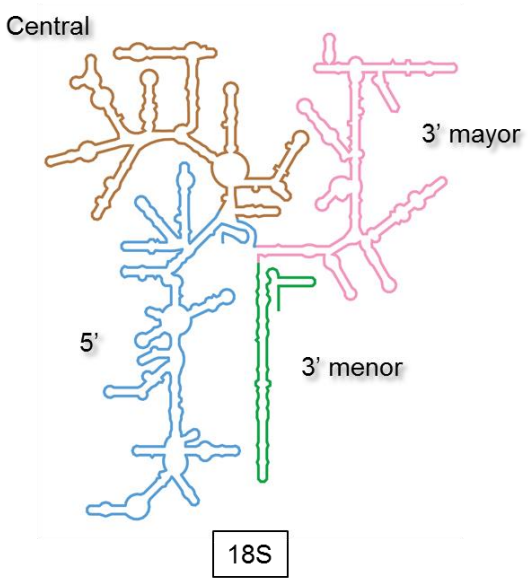

B)

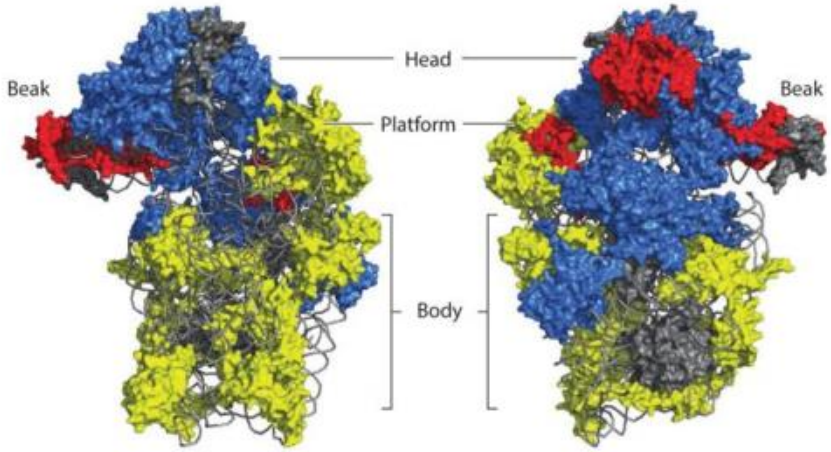

FIGURA 13. Esquema de ensamblaje de las proteínas de la subunidad pequeña. A) Representación de la estructura secundaria del rRNA 18S. B) Representación tridimensional del rRNA 18S. En amarillo, se muestran las proteínas que se ensamblan de forma temprana, muchas de ellas situadas en la región del cuerpo. En azul, se muestran las proteínas que se ensamblan posteriormente formando la región de la cabeza. Por último, en rojo se muestran las proteínas ribosómicas que se ensamblan de forma tardía. En gris, se muestran proteínas para las que aún se desconoce la posición y el tiempo de ensamblaje en la subunidad pequeña. Adaptada de [78].

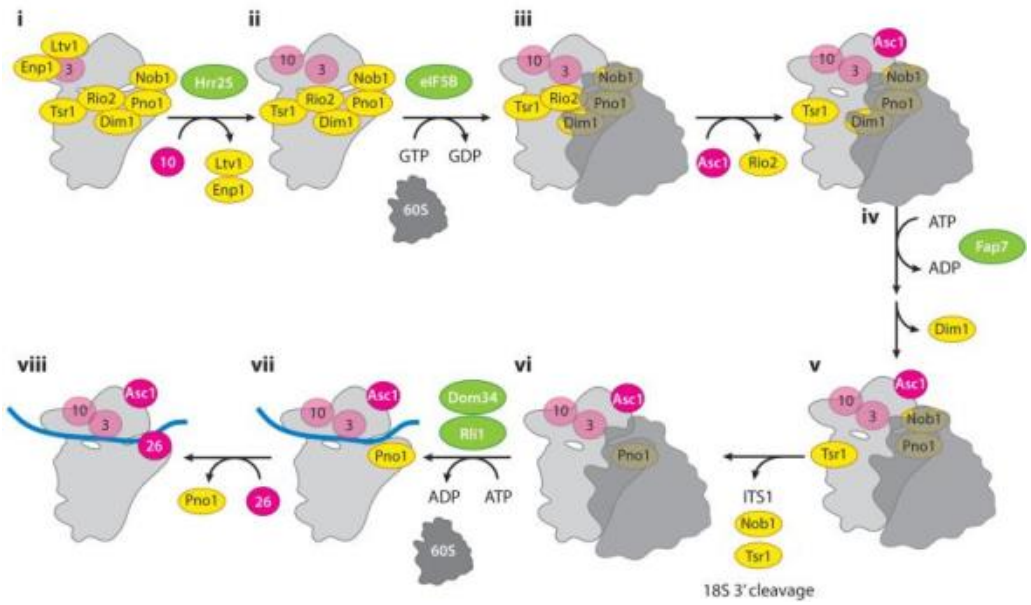

FIGURA 14. Últimas reacciones de maduración de la subunidad 40S. Modelo de los eventos de maduración citoplasmática de la subunidad pequeña. En amarillo, se muestran los factores que se unen de forma estable a partículas pre-40S; en magenta, se muestran las proteínas ribosómicas, y en color verde, los factores que se unen de forma más débil. La partícula pre-40S se muestra en color gris claro y la subunidad 60S en gris oscuro; el mRNA se muestra en color azul. Los distintos pasos se describen previamente en el texto. Adaptado de [78].

Recientemente se ha cristalizado el factor Tsr1, una proteína estructuralmente parecida a una GTPasa traduccional pero que no presenta ni sitio de unión a GTP ni actividad hidrolítica. Se ha observado que Tsr1 ocupa una posición que solapa con la de la GTPasa eIF5B y la ATPasa Rio1. La asociación de Tsr1 a las partículas pre-40S bloquea el canal de unión de los mRNAs, previene la asociación de la misma con la subunidad 60S y bloquea la unión de los factores eIF5B y Rio1. El mecanismo por el que se libera el factor Tsr1 de la partícula pre-40S aún se desconoce [123].

El ensamblaje de la subunidad 60S

El ensamblaje de la subunidad 60S presenta mayor complejidad que el de su análoga pequeña. A diferencia del ensamblaje de la subunidad pequeña que ocurre en su mayor parte de forma co-transcripcional, sólo las primeras etapas de la formación de las partículas pre-60S más tempranas ocurren de esta forma. Como he mencionado anteriormente, la maduración de la subunidad 60S se inicia con el corte en el sitio A_2 del pre-rRNA 35S [39, 40, 124]. Una vez finalizada la transcripción se forma el primer precursor detectable de pre-rRNA denominado pre-rRNA 27SA_2. El factor Rrp5 se localiza asociado en

el ITS1 adyacente a los sitios A_2 y A_3, y se ha demostrado que favorece los cortes en A_0, A_2 para producir el rRNA 18S y en el sitio A_3 por la RNasa MRP para dar lugar a los rRNAs 5.8S y 25S [100]. Muchas de las proteínas ribosómicas de esta subunidad y numerosos factores de ensamblaje están involucrados específicamente en el proceso de maduración [95]. Las proteínas ribosómicas en esta etapa aún presentan interacciones débiles con los pre-rRNAs que en muchos casos no son las interacciones definitivas que tienen con los rRNAs maduros. A medida que transcurre el proceso de maduración, estas interacciones se van haciendo más robustas y las proteínas ribosómicas van ocupando sus posiciones definitivas [125].

En un principio, los estudios para comprobar el papel de las proteínas ribosómicas durante el ensamblaje de las subunidades 60S se enfocaban en provocar únicamente la represión transcripcional de unas pocas proteínas individuales, y la constatación fenotípica de los efectos tras esta represión en el crecimiento celular, en los niveles de subunidades totales, polirribosomas, procesamiento de los pre-rRNAs y el transporte núcleo-citoplasmático de partículas pre-ribosómicas [126-137]. Actualmente, el estudio del papel de las proteínas ribosómicas también incluye análisis sistemáticos en los que se estudia la composición de partículas pre-ribosómicas purificadas y cómo éstas cambian tras la pérdida de función o eliminación de aquellas proteínas ribosómicas en estudio [125, 138-140]. Gracias a estos estudios, se ha descubierto qué conjunto de proteínas ribosómicas afectan específicamente a las etapas tempranas de la maduración de la subunidad 60S, cuales afectan a las etapas intermedias y cuales a las etapas tardías y citoplasmáticas. Curiosamente, los conjuntos de proteínas que afectan principalmente a etapas tempranas o tardías en la maduración de las partículas ribosómicas tienen una correlación con su localización en el ribosoma. Así, las proteínas necesarias para las etapas tempranas del procesamiento del pre-rRNA $27SA_2$ se localizan en la superficie soluble de la subunidad 60S unidas a los dominios I y II del rRNA 25S. El siguiente grupo de proteínas, que son necesarias para las etapas intermedias de maduración se encuentran localizadas en los alrededores de la salida del túnel de salida de los polipéptidos nacientes (PET, en inglés), unidas a los dominios I y III del rRNA 25S y al rRNA 5.8S. Por otro lado, las proteínas que se necesitan para el procesamiento del pre-rRNA 7S se localizan en la superficie de contacto entre subunidades. Por último, las proteínas necesarias para los últimos estadíos nucleares y citoplasmáticos de maduración se localizan alrededor de la protuberancia central, donde se sitúa el rRNA 5S, entre los dominios II y V del rRNA 25S (**Figura 15**). Este proceso jerárquico recuerda vagamente al proceso que sigue el ensamblaje *in vitro* de la subunidad grande bacteriana [141], sugiriendo que muchos de los principios que gobiernan el ensamblaje de la subunidad grande están como sucede para la subunidad pequeña

conservados evolutivamente, a pesar de la mayor complejidad de la biogénesis del ribosoma en eucariotas.

Si desgranamos más específicamente las etapas de maduración de la subunidad 60S, llama la atención que durante las etapas tempranas de su ensamblaje es necesaria la estabilización de los extremos 3' y 5' del pre-rRNA $27SA_2$ la cual se lleva a cabo mediante la participación de una serie de factores entre ellos Rrp5 [100]. Se ha observado que la proteína ribosómica L3 (uL3) se une a los dominios del pre-rRNA $27SA_2$ donde se sitúan sus extremos. La proteína L3 (uL3) en el ribosoma maduro ocupa una posición cercana al extremo 5' del rRNA 5.8S y al extremo 3' del rRNA 25S [142]. Además de la proteína L3 (uL3), se ha observado que un conjunto de factores de ensamblaje relacionados genéticamente con L3 (uL3) participa en esta estabilización inicial y compactación de la partícula pre-60S más temprana. Estos factores incluyen, además de Rrp5, las proteínas nucleolares Npa1/Urb1, Npa2/Urb2, Rsa3, Nop8 y las helicasas de RNA Dbp6, Dbp7, Dbp9 [100, 143].

Transcurridos estos primeros pasos de maduración, en los pasos intermedios se engloban los procesos de eliminación de la región interna ITS1 para lo cual es necesario la formación de una estructura a modo de pseudonudo en la estructura del rRNA 5.8S y el plegamiento del ITS2. Posteriormente ocurre el plegamiento de los dominios I y II creando una plataforma que ayuda a la formación de la estructura terciaria de los rRNAs [144].

El siguiente paso en el ensamblaje es la asociación de proteínas ribosómicas con los dominios I y III, permitiendo el corte en el sitio C_2 en la región interna ITS2. Los factores necesarios para el corte en el sitio C_2 (Nsa2 y Nog2/Nug2) se reclutan gracias al ensamblaje de algunas proteínas ribosómicas (L9 (uL6), L17 (uL22), L19 (eL19), L23 (uL14), L25 (uL23), L26 (uL24), L27 (eL27), L31 (eL31), L34 (eL34), L35 (uL29), L37 (eL37) [145, 146]. Por otro lado estas proteínas ribosómicas asociadas en estos pasos intermedios son necesarias para el correcto ensamblaje posterior de las proteínas ribosómicas L2 (uL2), L39 (eL39) y L43 (eL43) localizadas en la superficie inter-subunidad adyacentes al centro peptidil-transferasa (PTC, en inglés) [125]. A su vez las proteínas L2 (uL2) y L43 (eL43) junto con Nog2 son necesarias para el procesamiento del pre-rRNA 7S [125]. Mencionar que no se conoce el mecanismo por el cual se acopla el ensamblaje de estas proteínas con el procesamiento de este pre-rRNA. Recientemente se ha purificado un intermediario de pre-60S utilizando el factor Nog2 etiquetado con TAP, donde se ha observado que la GTPasa Nog2 está presente durante tres procesos importantes de la maduración de subunidades 60S: la rotación del complejo 5S-RNP, la construcción del PTC y la eliminación de ITS2. En este intermediario

A)

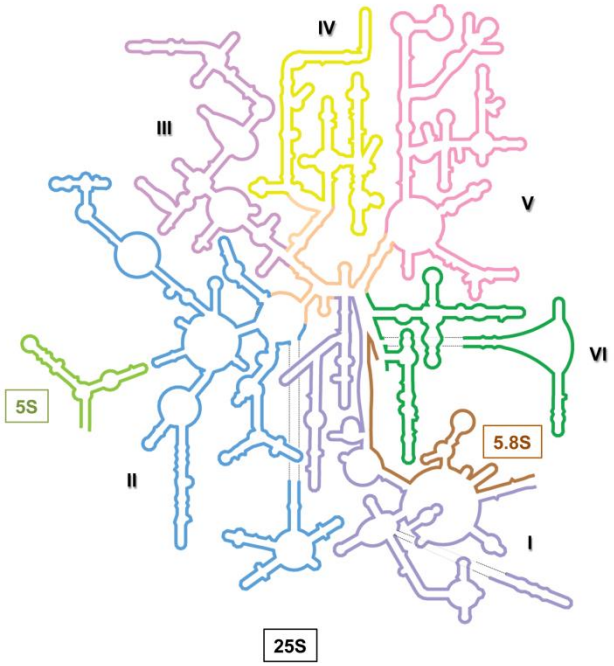

B)

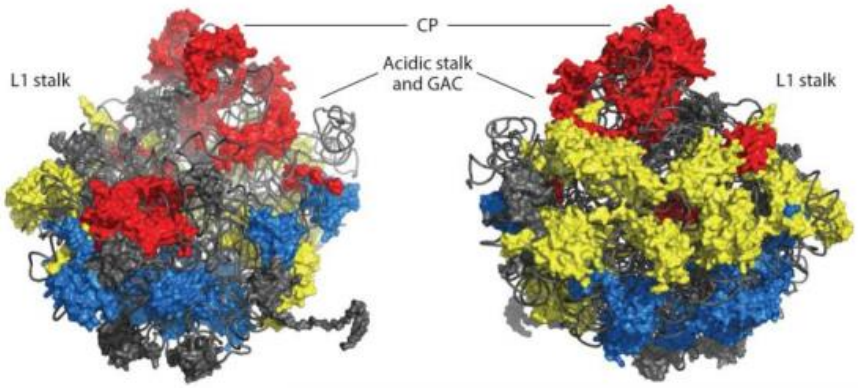

FIGURA 15. Ensamblaje de las proteínas ribosómicas de la subunidad grande del ribosoma. A) Representación de la estructura secundaria de los rRNAs de la subunidad 60S. B) Representación tridimensional del rRNAs de la subunidad 60S; en amarillo, se muestran las proteínas que se ensamblan de forma temprana las cuales se localizan en la superficie de la subunidad 60S. En azul, aquellas proteínas que se ensamblan de manera intermedia y que se localizan alrededor de la salida del túnel de salida del polipéptido naciente. Por último, en rojo, se muestran las proteínas ribosómicas que se ensamblan de forma tardía y que se encuentran formando parte de la protuberancia central. Adaptada de [78].

se han observado catorce factores asociados a una región que han denominado región "*arc*" que se localiza en la superficie de interacción con la subunidad pequeña, entre la protuberancia central y el túnel de salida del polipéptido. Estos factores son Rsa4, Nsa2,

Mtr4, Nog1, Tif6, Rlp24, Bud20, Arx1, Nog2, Rpf2 y Rrs1 y cinco factores adyacentes a la zona de ITS2, Nop53, Nop7, Rlp7, Cic1, Nop15 [147]. La actividad de la ATPasa Rea1 provoca cambios conformacionales en las partículas pre-60S nucleoplásmicas tardías que estimulan la actividad GTPasa de Nog2, cuyas actividades son necesarias para el transporte de éstas al citoplasma [148]. La liberación de Nog2 permite la asociación del factor de transporte núcleo-citoplasmático Nmd3 cuyo sitio de unión solapa con el de Nog2 [148, 149]. Por otro lado, la GTPasa Nog1 presenta una función dual, su dominio amino terminal interacciona con los factores Nog2 y Nsa2 mientras que su dominio carboxilo terminal interacciona con los factores Tif6, Rlp24, Arx1 y las proteínas ribosómicas L3 (uL3), L31 (eL31), L22 (eL22), L19 (eL19) y L35 (uL29). Se sugiere que mientras el extremo amino de Nog1 actúa en el remodelado del centro, el extremo carboxilo terminal aparentemente actúa como un “andamio molecular” para la asociación de numerosos factores de ensamblaje y el ensamblaje de algunas proteínas ribosómicas además de participar en un control de calidad de la construcción del túnel de salida del polipéptido [147, 150]. Como se mencionó anteriormente en este intermediario se observó que Nop53 se localiza cerca del sitio ITS2, lo cual tiene sentido porque Nop53 recluta el factor Mtr4, el cual participa en la eliminación de ITS2 mediante el exosoma [151].

El último paso antes de la salida de partículas pre-60S del núcleo es la formación de la protuberancia central que contiene el rRNA 5S unido a las proteínas L5 (uL18) y L11 (uL5). Recientemente, ha sido demostrado que las proteínas L5 (uL18) y L11 (uL5) se importan al núcleo juntas a través de un complejo formado por la carioferina Kap104 y la importina Syo1. Los extremos aminos de las proteínas L5 (uL18) y L11 (uL5) interaccionan con Syo1, cuya secuencia de señalización nuclear NLS es reconocida por Kap104. Tras el transporte al núcleo, la proteína Ran unida a GTP libera a Kap104 y el complejo Syo1-L5-L11 se asocia con el rRNA 5S. Syo1 se libera probablemente durante el ensamblaje del 5S-RNP al pre-60S [152] (**Figura 16**). El complejo 5S-RNP se ensambla en la partícula pre-ribosómica 60S mediante los factores de ensamblajes Rpf2 y Rrs1 [130]. En este paso, actúan los factores Rsa4 y Nog1 que contribuyen en la estabilización de la protuberancia central prematura y el remodelado del 5S-RNP que inicialmente presenta una conformación rotada 180º de su posición final, ocasionando a su vez, la rotación de algunas hélices del rRNA 25S [153]. Aparentemente esta conformación alterada proporciona los sitios de unión de factores de ensamblaje durante momentos específicos del proceso de maduración y establece un control temporal de la formación de la protuberancia central.

La proteína ribosómica L21 (eL21) se localiza en la protuberancia central cerca del complejo 5S-RNP. Esta proteína se ha demostrado que es necesaria para la interacción de factores implicados en el remodelado de la protuberancia central como son Rsa4 y Nog1

mencionados anteriormente. Por otro lado, el ensamblaje de la proteína L21 (eL21) parece ser un pre-requisito para que la ATPasa Rea1 pueda liberar de manera eficiente a los factores Rsa4 y Ipi1 [125, 154]. La liberación de los factores Rpf2 y Rrs1 unidos con el 5S-RNP, y del factor Rsa4 son necesarios para la correcta rotación del 5S-RNP a su posición final. La reorganización del 5S-RNP y la liberación del factor Nog2 parecen estar acoplados al transporte de la partícula pre-60S al citoplasma, la liberación del factor Nog2 permite que el factor de transporte núcleo-citoplasmático Nmd3 se asocie a las partículas pre-60S, puesto que ocupan posiciones solapantes [148]. Por otro lado parece ser que la reorientación de la protuberancia central favorece la asociación del factor Mex67 para llevar a cabo el transporte al citoplasma [155].

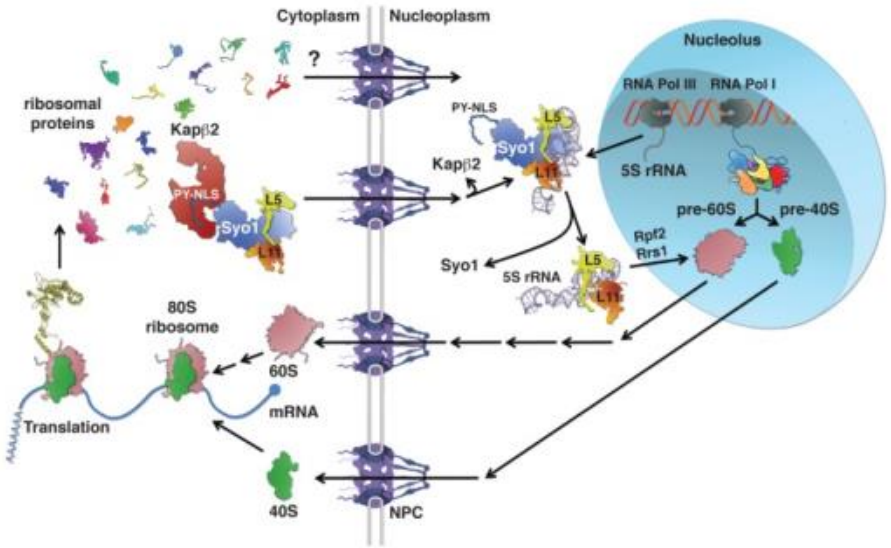

FIGURA 16. Ensamblaje del complejo 5S-RNP. El complejo Syo1-L5-L11 que se forma en el citoplasma, se importa al núcleo con la ayuda de la carioferina Kap104. En el núcleo, el complejo Syo1-L5-L11 se unen al rRNA 5S. La actividad de RanGTP unida a Kap104 promueve la liberación de Syo1. En este punto, el complejo 5S-RNP se incorpora a la partícula pre-ribosómica 60S. Los factores Rpf2 y Rrs1 ayudan en el reclutamiento de 5S-RNP a la partícula pre-60S generando la protuberancia central prematura. Adaptada de [156].

Una vez en el citoplasma, las partículas pre-60S se someten a los últimos pasos de maduración, entre ellos el procesamiento del pre-rRNA 6S a 5.8S, la asociación de las últimas proteínas ribosómicas y la liberación de los factores de ensamblaje que aún quedan unidos (**Figura 17**). Las proteínas ribosómicas de ensamblaje citoplasmático se localizan en la superficie de la subunidad que interacciona con la subunidad pequeña, adyacentes a la protuberancia central, al centro peptidil-transferasa y al centro activador de GTPasa. Se

piensa que los últimos pasos de maduración están precisamente destinados a completar los sitios activos. Se ha demostrado que la ausencia de las proteínas ribosómicas que se ensamblan en estos últimos pasos citoplasmáticos, como las proteínas L29 (eL29) y L40 (eL40), o la represión transcripcional de la proteína L10 (uL16), dan lugar a defectos en la unión de la subunidad grande con la subunidad pequeña durante el proceso de traducción [134, 157, 158].

El ensamblaje prematuro de proteínas como L10 (uL16), L24 (eL24) o P0 (uL10) en partículas pre-60S está bloqueado estéricamente por factores de ensamblajes que ocupan sus sitios de unión, constatando nuevamente la presencia de factores tipo "*placeholders*". Es durante los últimos pasos de maduración citoplasmática cuando las subunidades 60S nacientes se someten a un nuevo chequeo para comprobar el ensamblaje correcto del sitio P en los centros peptidil-transferasa y activador de GTPasa. El primer factor en actuar parece ser que es la ATPasa AAA Drg1, la cual es reclutada y activada por el factor Rlp24; a su vez Drg1 promueve la liberación de Rlp24, permitiendo el ensamblaje posterior de la proteína ribosómica L24 (eL24) que es paráloga al factor [159, 160]. Esta etapa permite la unión del factor Rei1 que junto con la ATPasa Ssa1 y su cofactor Jjj1 liberan los factores Arx1 y Alb1 [161-163]. Por otro lado, la proteína ribosómica L12 (uL11) recluta al factor de ensamblaje Yvh1 que interviene en la liberación de Mtr4 permitiendo que la proteína ribosómica P0 se ensamble de forma irreversible a la partícula pre-60S citoplasmática [161, 164-166]. Muy recientemente, se ha demostrado que la liberación de Mtr4 favorecida por el factor Yvh1 permite la asociación de los factores de transporte Mex67-Mtr2 en el núcleo en el sitio que ocupaba Mtr4, permitiendo su transporte al citoplasma. Allí, los factores Yvh1 y Mex67-Mtr2 se liberan y favorecen el ensamblaje de la proteína ribosómica P0 [167]. Sin embargo, en ausencia de la proteína ribosómica L12 (uL11), que no es esencial, no se ha observado que haya diferencias en la eficiencia de reciclaje del factor Mtr4 al núcleo [168]. La proteína ribosómica L10 (uL16) presenta un lazo flexible en su estructura que, debido a su proximidad al sitio P, es responsable de detectar si el ensamblaje del centro peptidil-transferasa es correcto. En ese caso, se activan los factores Efl1 y Sdo1, que favorecen la liberación del factor Tif6 [169]. A su vez, este proceso favorece la liberación del factor Nmd3 llevada a cabo por la GTPasa Lsg1. Es el correcto ensamblaje del tallo P el que activa y une el factor Efl1, el cual podría acoplar este punto de control con la liberación de factores que previenen la interacción de la subunidad grande con la subunidad pequeña de forma prematura.

Mecanismos de vigilancia en la biogénesis del ribosoma

Como he estado mencionando en secciones anteriores, los puntos de verificación estructural y funcional de las partículas pre-ribosómicas son frecuentes a lo largo de la ruta de maduración de las subunidades ribosómicas. Éstos aseguran el correcto ensamblaje del ribosoma. Muchos de estos controles ocurren en el nucléolo. Entre ellos destacan las distintas verificaciones realizadas por el complejo TRAMP asociado al exosoma [170]. Esta ruta parece actuar en los casos en los que ciertos factores de ensamblaje no son capaces de unirse o llevar a cabo su función, lo que podría provocar el bloqueo de las partículas pre-ribosómicas que no pueden progresar en su maduración, simplemente por falta de reciclado de los factores asociados.

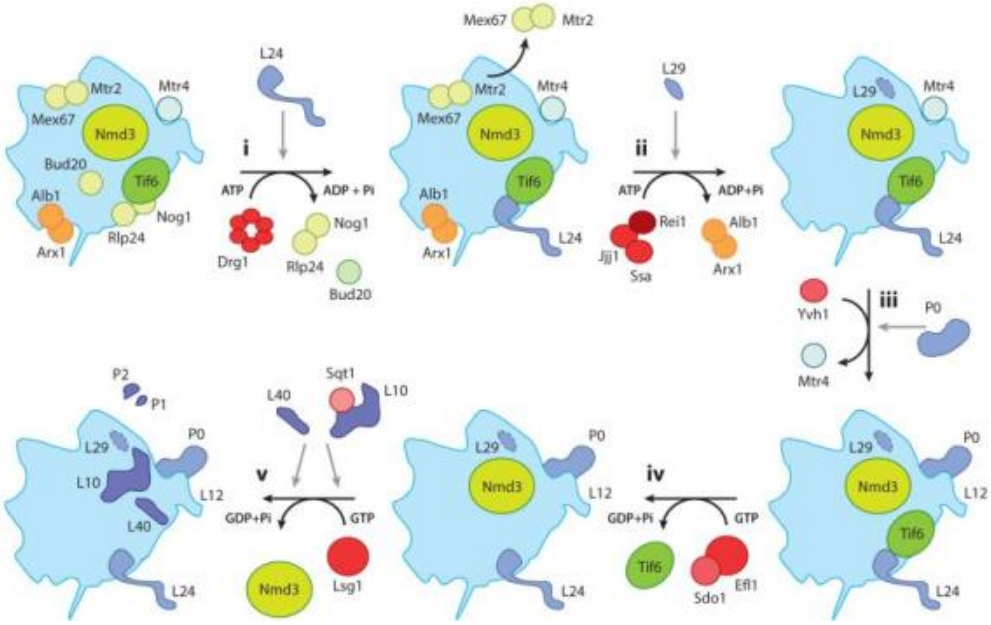

FIGURA 17. Últimas etapas de la maduración de la subunidad 60S. Las partículas pre-60S citoplasmáticas contienen solo unos pocos factores de ensamblaje que se liberan tras las últimas reacciones de remodelado citoplasmático. La incorporación de L29 (eL29) en el citoplasma requiere evidencia experimental. Es de destacar la liberación del factor Tif6 que provoca la activación de la GTPasa Lsg1, que a su vez promueve la liberación del factor de exportación Nmd3. Por otro lado, el ensamblaje de la proteína L10 (uL16) requiere de la participación de la chaperona Sqt1, la cual es también necesaria para la liberación del factor Nmd3. Las proteínas acídicas P1 y P2, que pueden existir en su forma libre, se asocian aparentemente de manera co-traduccional a las subunidades 60S durante la fase de iniciación de la traducción. Adaptada de [78].

El complejo TRAMP está compuesto por una polimerasa de poli-adenina (Tfr4 ó Tfr5), una helicasa de RNA (Mtr4) y una proteína con dedos de zinc (Air1 ó Air2). Este complejo se encarga de añadir pequeñas colas de poli-$(A)_n$ en el extremo 3' de los RNAs aberrantes, incluyendo aquellos que provienen de los rRNAs. Posteriormente, el exosoma

detecta la cola de poli-$(A)_n$ y realiza la degradación en sentido 3'-5'. Se ha sugerido que la mayoría de los complejos TRAMP-exosoma se concentran en unos compartimentos nucleolares denominados "No-body" [170].

En el citoplasma, las partículas pre-ribosómicas y los ribosomas aberrantes son degradados mediante la ruta denominada "*Non-functional rRNA Decay*" (NRD). Según se trate de una subunidad pequeña o una grande aberrante, esta ruta utiliza distintos factores. Así, el NRD de la subunidad pequeña comparte componentes con una ruta de degradación de mRNAs denominada "*No-Go Decay*" (NGD) [171], mientras que el NRD de la subunidad grande utiliza la ubicuitinación [172]. Mientras que la degradación de la subunidad pequeña parece ser dependiente de traducción [171], la degradación de la subunidad grande se lleva a cabo por el proteasoma citoplasmático (*UPS* en inglés) y es dependiente de ubicuitinación [172]. Los sustratos de degradación de la subunidad pequeña al igual que la de los mRNAs se localizan en los gránulos citoplasmáticos, conocidos como "*P-bodies*", donde se encuentran las enzimas encargadas de la degradación, tales como la exonucleasa 5'-3' Xrn1, y las GTPasas Ski7 y Hbs1. En cambio, los sustratos de degradación de la subunidad grande se acumulan en compartimentos peri-nucleares [172].

Finalmente, mencionar que dependiendo del estado fisiológico (condiciones de estrés, inanición, o fase estacionaria, etc), las células activan mecanismos de reciclaje del exceso de ribosomas y partículas pre-ribosómicas tales como la ribofagia, un tipo de macro-autofagia selectiva de subunidades 60S maduras. Esta ruta implica la proteasa de ubicuitina Ubp3, su activador Bre5 des-ubicuitinando y la ubicuitin-ligasa Rsp5 ubicuitinando ciertas proteínas asociadas a ribosomas [170, 173]. Se desconocen los mecanismos de ribofagia de subunidades pequeñas.

La ruta ribofágica especifica de partículas pre-ribosómicas se denomina "*Piecemeal Microautofagia of the Nucleus*" (PMN), es un tipo de micro-autofagia selectiva donde se encuentra implicada la vacuola y la envuelta nuclear [174] (**Figura 18**).

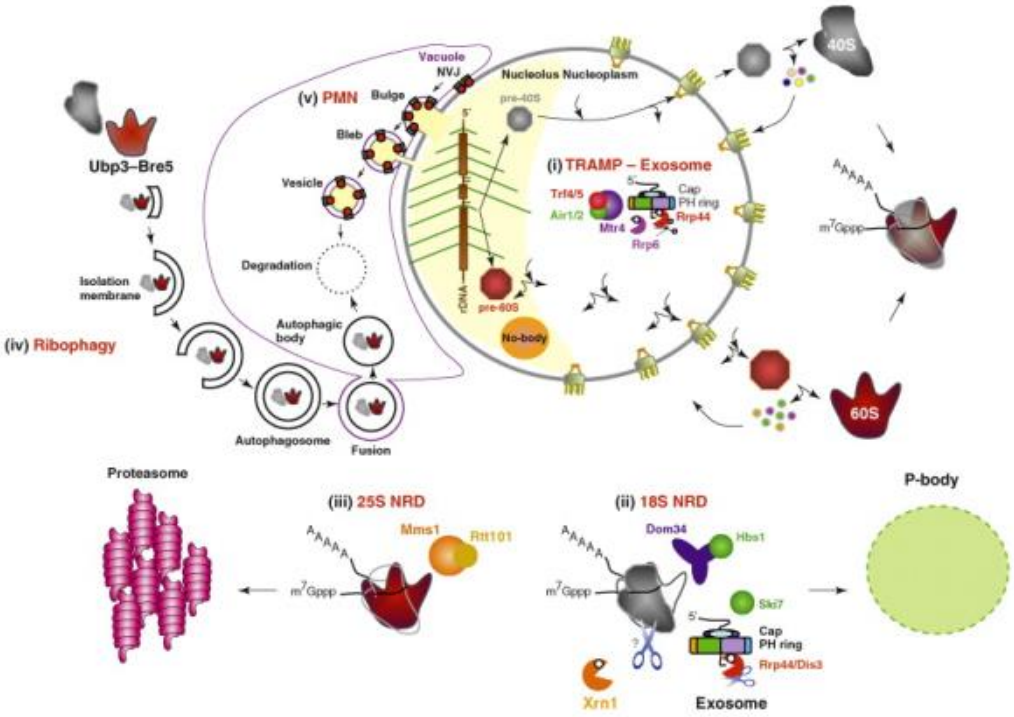

FIGURA 18. Rutas principales de degradación del RNA ribosómico. (i) Mecanismo de degradación de los pre-rRNAs defectuosos por el complejo TRAMP-exosoma en el núcleo y nucléolo. **(ii)** Mecanismo de degradación de subunidades 40S maduras (18S NRD) llevaba a cabo por la maquinaria del NGD. **(iii)** Mecanismo de degradación de la subunidad 60S madura (25S NRD), en la que participa el proteasoma. **(iv)** Ribofagia de la subunidad 60S madura. **(v)** Micro-autofagia selectiva de componentes nucleolares (PMN). Adaptada de [170].

OBJETIVOS

El objetivo final de esta tesis ha sido profundizar en el conocimiento del proceso de biogénesis de la subunidad grande del ribosoma eucariota, usando como modelo la levadura *Saccharomyces cerevisiae*. Para ello, hemos estudiado el efecto que provoca la eliminación de dos proteínas ribosómicas en dicho proceso, las cuales aún no habían sido analizadas ni caracterizadas en este contexto. En concreto, se ha pretendido:

1.- Caracterizar funcionalmente el papel de la proteína ribosómica L16 (uL13) durante el ensamblaje de la subunidad 60S.

2.- Caracterizar funcionalmente el papel de la proteína ribosómica L14 (eL14) en la biogénesis de la subunidad 60S.

CAPÍTULO 0

Las proteínas ribosómicas L14 y L16 del ribosoma de *Saccharomyces cerevisiae*

Nuestro laboratorio tiene como objetivo principal el estudio del proceso de biogénesis del ribosoma eucariota y trabaja principalmente con *Saccharomyces cerevisiae* como organismo modelo. Entre otros proyectos, nuestro laboratorio intenta comprender la función precisa de las proteínas ribosómicas durante el ensamblaje de las subunidades ribosómicas. Así, en el mismo, se ha abordado la caracterización funcional de distintas proteínas ribosómicas tales como L3 [129], L35 [131], L26 [133], L37 [136], L40 [134] o P0 [166] de la subunidad grande y S31 [107], S18, S10 y S12 (en progreso) de la subunidad pequeña. Entre otras cosas por su proximidad con la proteína L3 en la subunidad ribosómica 60S madura, se planteó como objetivo de esta Tesis Doctoral la caracterización funcional de las proteínas ribosómicas L14 y L16, que como se explica a continuación son vecinas próximas entre sí en la subunidad 60S madura. Ambas proteínas presentan un tamaño pequeño y carácter básico, características generales de las proteínas ribosómicas. En la **Figura 1** de este capítulo se muestra la localización de estas dos proteínas en el contexto ribosómico.

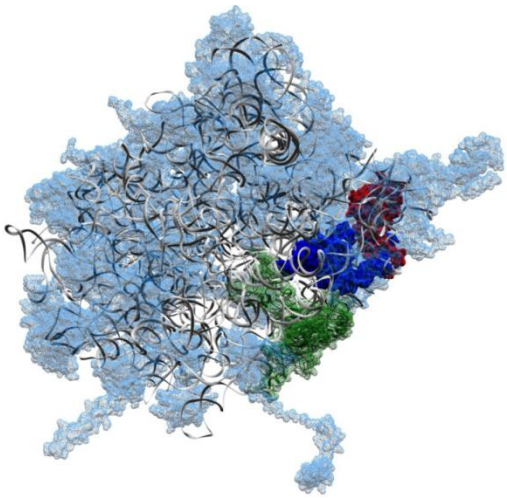

FIGURA 1. Localización de L3, L14 y L16 en la subunidad grande del ribosoma de *S. cerevisiae*. Estructura tridimensional de la subunidad 60S (superficie de interacción entre subunidades). En verde, se muestra la proteína ribosómica L3, en azul la proteína L16 y en rojo la proteína L14. En celeste se muestran las restantes proteínas ribosómicas que componen la subunidad grande del ribosoma y en gris los rRNAs. Realizado con el programa Chimera v.1.11.2 a partir de los archivos pdb: 3u5h y 3u5i.

A su vez, las proteínas L14 y L16 se encuentran cercanas a las proteínas L6 (eL6), L9 (uL16), L20 (eL20) y L33 (eL33) localizadas en la zona expuesta al solvente del ribosoma. Ambas muestran interacciones con los dominios II y VI del rRNA 25S (Ver Figura 15 de la introducción, pagina 32). Además L16 interacciona con el rRNA 5.8S (**Figura 2**).

La proteína L14 está codificada por dos genes parálogos, *RPL14A* y *RPL14B*. Estos dos genes muestran una similitud de secuencia muy alta que origina proteínas muy similares de 138 aminoácidos cada una; la única diferencia existente entre L14A y L14B consiste en un cambio del aminoácido alanina (A) en *RPL14A*, por una glicina (G) en *RPL14B*, en la posición 89. Las diferencias más llamativas se observan en regiones no codificantes tales como las presentes en el único intrón que ambos genes poseen. Este hecho sugiere que a diferencia de las regiones codificantes no ha habido restricción por presión selectiva en los intrones y abre la posibilidad de que puedan existir procesos de regulación específicos para cada parálogo.

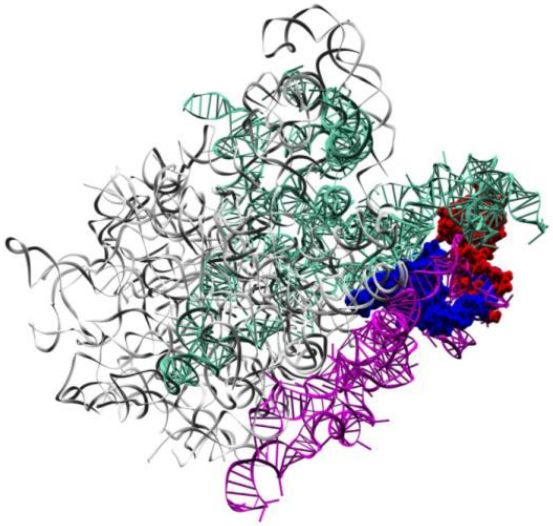

FIGURA 2. Interacción de las proteínas L14 y L16 con los rRNAs en el contexto de la subunidad 60S madura. Estructura tridimensional de la subunidad 60S del ribosoma de *S. cerevisiae*. Se muestran únicamente los rRNAs y las proteínas L14 (rojo) y L16 (azul). En color turquesa, se muestra el dominio II del rRNA 25S, y en color fucsia el dominio VI. En gris se muestra el resto de dominios del rRNA 25S, 5S y 5.8S. Realizado con el programa Chimera v.1.11.2 a partir de los archivos pdb: 3u5h y 3u5i.

A su vez, la proteína L16 está también codificada por dos genes parálogos *RPL16A* y *RPL16B*. Ambos genes presentan una similitud de secuencia muy alta, sintetizando cada uno, una proteína de 198 aminoácidos. Las proteínas L16A y L16B presentan una similitud del 92% a nivel de aminoácidos. La mayoría de las diferencias de secuencias se encuentran nuevamente en el intrón que presentan ambos genes.

Respecto a sus estructuras proteicas, L14 presenta un dominio globular y 2 extensiones, una mayor que corresponde con el extremo carboxilo terminal y una pequeña que corresponde con el dominio amino terminal (**Figura 3**). En el caso de la proteína L16,

ésta presenta un dominio globular y una extensión carboxilo terminal que se muestra en la **Figura 3**.

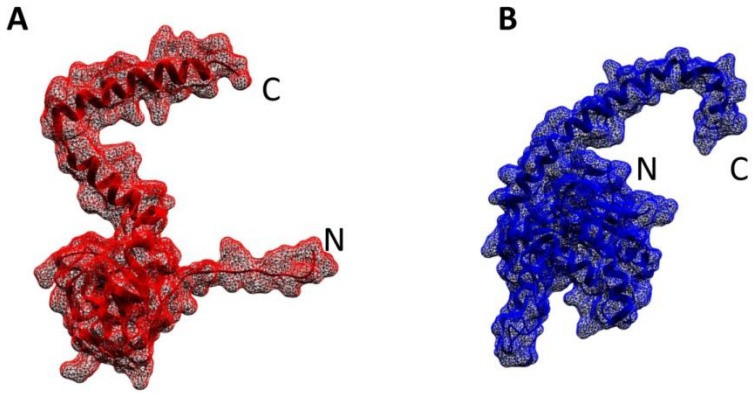

FIGURA 3. Morfología de las proteínas L14 y L16. (A) Estructura tridimensional de la proteína ribosómica L14. Se marca con N y C sus extremos amino y carboxilo, respectivamente. **(B)** Estructura tridimensional de la proteína ribosómica L16. Se marca con N y C sus extremos amino y carboxilo, respectivamente. Realizado con el programa Chimera v.1.11.2 a partir del archivo pdb 3u5i.

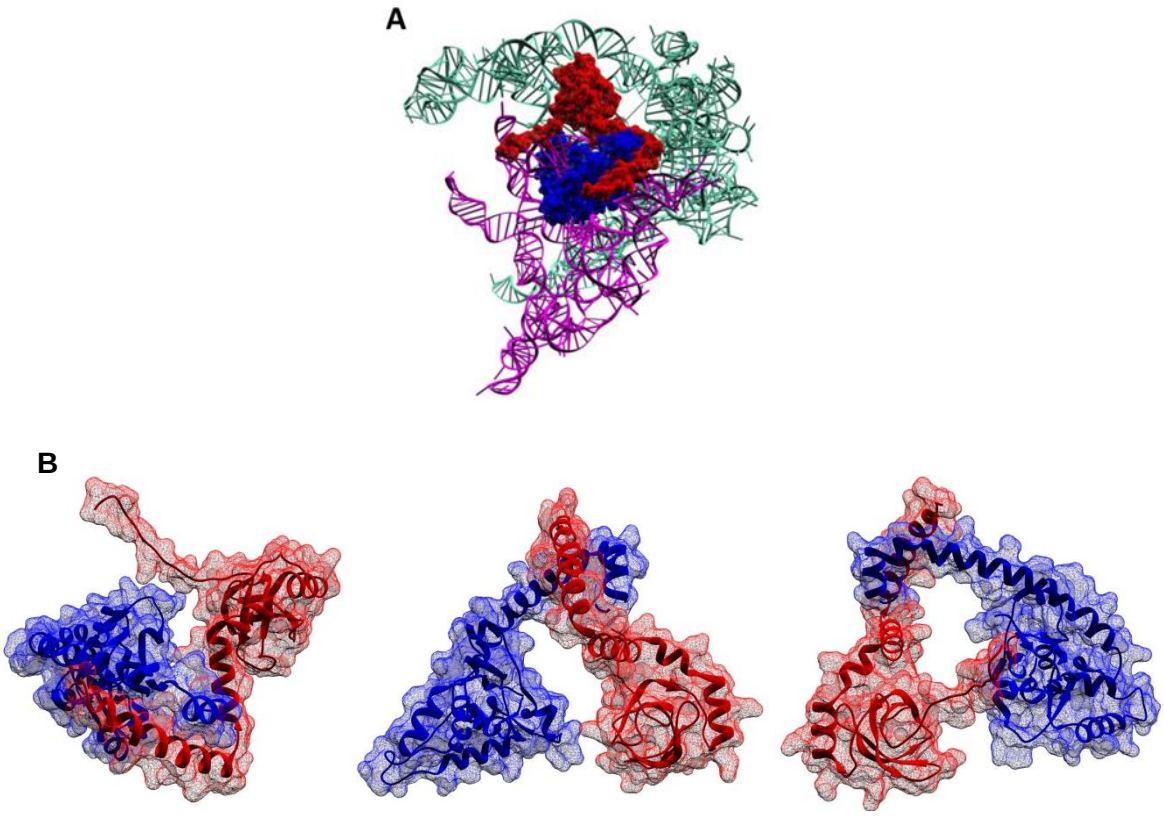

FIGURA 4. Interacción física entre L14 y L16. (A) Se muestra en turquesa y fucsia los dominios II y VI del rRNA 25S respectivamente, que conforman el entorno molecular de las proteínas L14 (rojo) y L16 (azul) interaccionando entre sí. **(B)** Detalle de la interacción de las proteínas L14 (rojo) y L16 (azul) en distintas orientaciones. Realizado con el programa Chimera v.1.11.2 a partir de los archivos pdb: 3u5h y 3u5i.

Ambas proteínas interaccionan íntimamente entre sí por las α-hélices de sus extensiones C-terminales. Los aminoácidos implicados de la proteína L14 son los últimos 30 y de la proteína L16, los últimos 25. Ambas proteínas interaccionan principalmente mediante interacciones apolares entre residuos, exceptuando dos puentes salinos encontrados, uno entre el grupo carboxilo de la última alanina de la proteína L14 y el grupo ε-amino de la lisina 177 de L16, y el otro entre el grupo carboxilo de la última tirosina de L16 y el grupo guanidina de la arginina 109 de L14, según se deduce de la disposición de ambas proteínas en el cristal resuelto de la subunidad 60S madura (**Figura 4**).

Como se ha mencionado anteriormente, uno de los objetivos de esta Tesis ha consistido en el estudio de las consecuencias funcionales de la disrupción de estas interacciones sobre el proceso de ensamblaje de las subunidades 60S.

Al comienzo de este trabajo, la única información disponible sobre la proteína L16 era un estudio sistemático realizado por el grupo del profesor Philipp Milkereit. En este estudio, se reprimía la transcripción de algunos genes de proteínas ribosómicas y a continuación se estudiaba los efectos que éstos causaban sobre el procesamiento de los pre-rRNAs y el transporte nucleo-citoplásmatico de partículas pre-60S [175]. Dependiendo del parecido en los defectos observados tras la represión, las proteínas ribosómicas se clasificaron en distintos grupos funcionales. La proteína L16 junto a las proteínas ribosómicas L3, L4, L7, L8, L18, L20, L32 y L33 fue incluida en el grupo de proteínas cuya represión causaba una acumulación en el precursor 35S, no presentaban el precursor $27SA_2$ y afectaban al procesamiento del extremo 5' del rRNA 5.8S. En esta Tesis quisimos profundizar en la caracterización funcional de la proteína L16 y su extremo carboxilo terminal en la síntesis del ribosoma. Respecto a la proteína L14, al comienzo de esta Tesis, no se disponía de ninguna información al respecto. En esta Tesis hemos iniciado el estudio funcional de la misma tras su represión transcripcional. También hemos estudiado la composición de partículas tempranas pre-60S tras la represión transcripcional de L14. Cuando este trabajo estaba en progreso, se publicó un artículo donde descubrían la interacción genética de la helicasa de RNA Mak5 y el factor de biogénesis Ebp2 con la proteína L14A. En este estudio, se propuso que posiblemente lo que ellos denominaron "grupo Mak5" (compuesto por Ebp2, Nop16 y Rpf1) podría estar implicado en dirigir los cambios conformacionales necesarios para el ensamblaje de un módulo preformado compuesto por las proteínas ribosómicas L6, L14 y L16 en el contexto de los segmentos de expansión ES7L y ES39L del rRNA 25S [176].

CAPÍTULO 1

Role of the yeast ribosomal protein L16 in ribosome biogenesis

INTRODUCTION

Ribosomes are highly complex ubiquitous macromolecular assemblies that are responsible for the synthesis of all cellular proteins from mRNA templates. In all cells, ribosomes are composed of two ribosomal subunits (r-subunits), the large one about twice the size of the small one. The recent determination of the atomic structures of the r-subunits has confirmed that the majority of the ribosomal RNA (rRNA) and ribosomal proteins (r-proteins) from prokaryotic ribosomes is conserved in eukaryotes, although additional rRNA sequences, referred to as expansion-segments, extra extensions within conserved r-proteins and eukaryote-specific r-proteins have increased significantly the mass and complexity of cytoplasmic eukaryotic ribosomes [22, 142, 177].

Synthesis of eukaryotic ribosomes is a highly complex process that takes successively place in the nucleolus, nucleoplasm and cytoplasm [30, 178, 179]. The speed, directionality and accuracy of this process depend on a myriad of small nucleolar RNAs and protein *trans*-acting factors [29, 106]. Within the nucleolus, the mature 18S, 5.8S and 25S rRNAs are first co-transcribed as a single large precursor by RNA polymerase I, whereas the pre-5S pre-rRNA is independently transcribed by RNA polymerase III [32, 180]. Pre-rRNAs are processed via well-known pathways that require a series of sequential endo- and exonucleolytic reactions [35, 48, 181]. Pre-rRNA processing takes place inside pre-ribosomal particles, which are formed by the association of many *trans*-acting factors with the pre-rRNAs and the assembled r-proteins; this process occurs concomitantly to most pre-rRNA modification and folding reactions [178]. Cleavage at processing site A_2 leads to the formation of 43S and 66S pre-ribosomal particle intermediates of the small and large r-subunits, respectively, which then follow independent maturation pathways [179, 182]. While 43S pre-ribosomal particles are rapidly exported to the cytoplasm [183], early 66S pre-ribosomal particles undergo hierarchical maturation involving pre-rRNA processing, association and release of *trans*-acting factors, structural remodelling of the particles, stable assembly of r-proteins and acquisition of export competence [29, 93, 179]. Upon appearance in the cytoplasm, the final maturation steps, which include dimethylation and cleavage of 20S pre-rRNA to yield mature 18S rRNA within the 40S r-subunit, 3'-end exonucleolytic processing of 6S pre-rRNA to mature 5.8S rRNA within the 60S r-subunit, and the dissociation of *trans*-acting factors and the assembly of the few remaining r-proteins in both r-subunits, enable r-subunits to acquire their competence in translation [179, 184].

Most of our current knowledge concerning ribosome biogenesis in eukaryotes comes from studies with the yeast *Saccharomyces cerevisiae* (hereafter named only yeast). More than 300 protein *trans*-acting factors have been identified and functionally characterized in yeast, although the precise functions by which these proteins operate are only beginning to

be unravelled [30, 178, 185]. As for *trans*-acting factors, functional analyses have demonstrated that many r-proteins act as active players in the maturation and nucleo-cytoplasmic transport of pre-ribosomal particles [144]. The principles governing the assembly of r-proteins start to be understood [76, 77, 125, 140, 144, 175], however, how r-proteins participate in driving formation or rearrangement of structures within pre-ribosomal particles remains in many cases yet to be unveiled. Finally, the functions of some r-proteins in ribosome biogenesis, especially those belonging to the large r-subunit, and their correct timing of assembly, are currently under intensive investigation.

We are interested in understanding the contribution of 60S r-proteins to ribosome biogenesis (e.g. [129, 133, 136, 144, 166, 186]). In this study, we have undertaken the functional characterization of yeast L16 (uL13 according to the recently proposed r-protein nomenclature [79]). Yeast L16, which is encoded by two paralogous genes, *RPL16A* and *RPL16B*, shares a notable sequence identity with bacterial L13, which is an essential protein required for early assembly of 50S r-subunits *in vivo* [187, 188] and in vitro [74]. L16 also shows substantial homology to mammalian L13a, which is an early assembling 60S r-protein with no apparent role in pre-rRNA processing and the assembly and function of ribosomes, but with an important role in global rRNA methylation and, as an extra-ribosomal free r-protein, in modulating the translation of a subset of proteins in different cell types of the immune system [189-191]. Eukaryotic L16/L13a contains a specific C-terminal extension of unclear role during mammalian ribosome biogenesis [190]. In contrast to mammalian L13a and as previously reported in a systematic study [192], we show in this study that L16 is required for the normal accumulation of 60S r-subunits in yeast. Depletion of L16 causes instability of early and intermediate pre-ribosomal particles, as shown by low steady-state levels and massive turnover of the 27S and 7S pre-rRNAs. As a consequence, depletion of L16 impairs nucleocytoplasmic export of pre-60S r-particles. Moreover, L16 stably assembles into 90S pre-ribosomal particles. Finally, we clearly show that deletion of the eukaryote-specific C-terminal extension of yeast L16 causes lethality and impairs ribosome biogenesis; however, presence of this extension is not strictly essential for pre-rRNA processing and L16 assembly. While the present work was in progress, Milkereit and co-workers have independently reported similar findings on the role of the C-terminal extension of yeast L16 r-protein [192].

RESULTS

Depletion of L16 leads to a strong 60S r-subunit shortage

The r-protein L16 protein is a constituent of the 60S r-subunit and it consists of an evolutionary conserved N-terminal globular body and a long eukaryote-specific C-terminal extension formed by two α-helices. L16 is located on the solvent-side of the 60S subunit in close proximity to L3, L14 and L33 **(Fig. 1A)**. The globular domain of L16 binds to rRNA nucleotides within domains II and VI of 25S/5.8S rRNAs while its extension binds only nucleotides within domain VI, most of them in the expansion segment ES39L [11]. At the protein level, L16 mediates interactions with distinct regions of other r-proteins such as L6, L9, L20, L33, and most notably the most distal α-helix of its C-terminal extension interacts with the most distal α-helix of the eukaryote-specific C-terminal extension of L14 **(Fig. 1B)**.

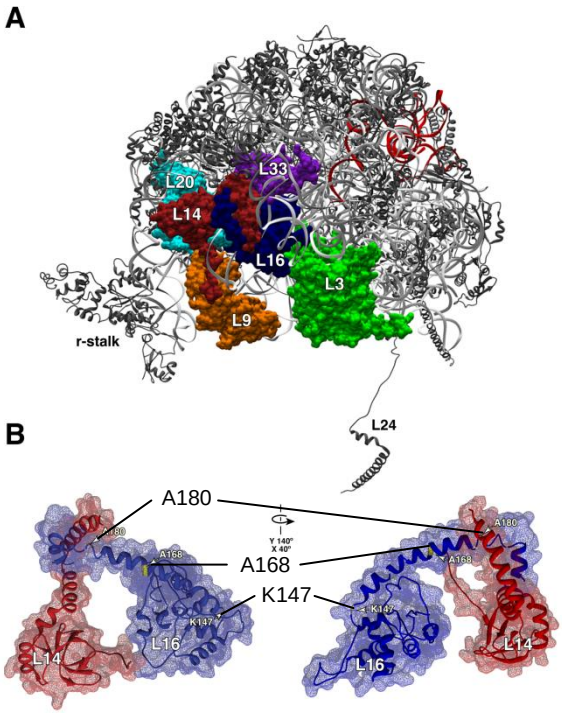

Fig. 1. Location of L16 in the yeast 60S r-subunit. (A) Position of L16 and its immediate nearby r-proteins, in the context of the 60S r-subunit. The remaining 60S r-proteins are coloured in black, 25S and 5S rRNAs in pale gray, and 5.8S rRNA in red. Note that the 5' end of 5.8S rRNA is in proximity of the above r-proteins. **(B)** Structure of the ribosome-bound L16 and L14 r-proteins showing the interaction between their eukaryote-specific C-terminal extensions. The amino acids used for the serial deletion mutants of RPL16B are indicated. The representations were rendered with UCSF Chimera [193], using the atomic model for the crystal structure of the yeast 80S ribosome (PDB files 3U5I and 3U5H, [10].

This latter interaction is mainly mediated by apolar patches, except for the presence of two salt bridges, the first one between the carboxylic group of the last alanine residue in L14 and the ε-amino group of lysine 177 in L16, and the second one between the carboxylic group of the last tyrosine residue in L16 and the guanidinium group of arginine 109 in L14.

A previous systematic functional study has revealed that depletion of yeast L16 results in a defect in early processing reactions on the pathway that converts 27SA pre-rRNAs into mature 25S and 5.8S rRNAs [175]. To further address the role of L16 in ribosome biogenesis, we first investigated the ribosome and polysome content upon *in vivo* depletion of L16 in a *rpl16a*Δ *rpl16b*Δ [pGAL1-RPL16B] strain (hereafter named *GAL::RPL16* strain) grown in rich medium containing galactose (YPGal) and shifted to rich medium containing glucose (YPD). This strain showed wild-type growth on YPGal plates but was unable to grow on YPD plates **(Fig. 2A)**.

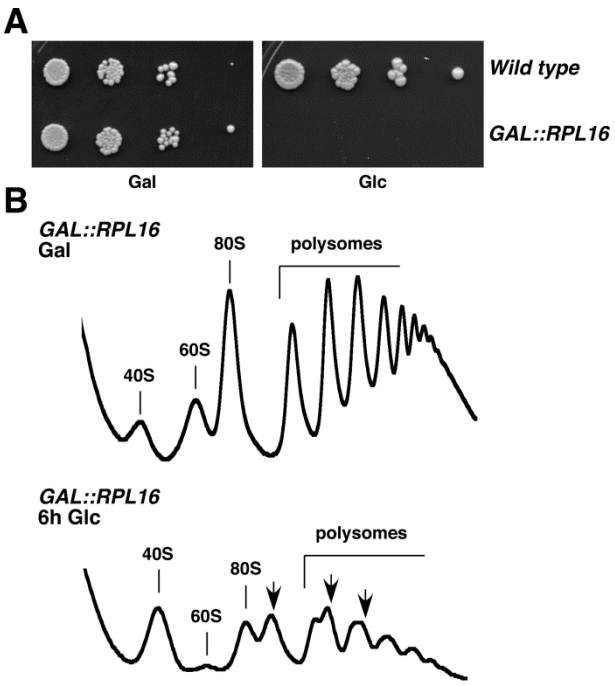

Fig. 2. Depletion of L16 results in a shortage of 60S r-subunits. (A) Growth comparison of the strains W303-1A (*Wild type*) and FEY251 [pAS24-RPL16B] (*GAL::RPL16*). These two strains were grown in liquid YPGal medium and diluted to an OD600 of 0.05. Serial 5-fold dilutions were spotted onto YPGal (Gal) and YPD (Glc) plates, which were incubated at 30 ºC for 3 days. **(B)** Polysome profile analysis of *GAL::RPL16* cells grown in YPGal (Gal) or shifted to YPD (Glc) for 6 h. Cells were collected at an OD600 of around 0.8. Whole cell extracts were prepared and 10 A_{260} units of each extract were resolved in 7-50% sucrose gradients. The A_{254} was continuously measured. Sedimentation is from left to right. The peaks of free 40S and 60S r-subunits, 80S vacant ribosomes/monosomes and polysomes are indicated. Half-mers are labelled by arrows.

Moreover, it showed a normal polysome profile when grown in liquid YPGal; however, when shifted to liquid YPD it already showed after 6 h an aberrant profile, consisting of a clear decrease in the levels of free 60S versus free 40S r-subunits, a strong decrease in the 80S peak and polysomes and the appearance of large half-mer polysomes **(Fig. 2B)**. These results demonstrate that, as expected, depletion of L16 leads to a strong deficit in 60S relative to 40S r-subunits.

Depletion of L16 impairs pre-rRNA processing and induces the turnover of 27S pre-rRNAs

To examine in more detail the pre-rRNA processing defects initially described for a *GAL::RPL16* strain after a 2-4 h shift to YPD [175], we assayed changes in steady-state levels of pre- and mature rRNAs during a time-course of L16 depletion. Northern blot analysis showed a significant accumulation of 35S pre-rRNA and the appearance of the aberrant 23S species at early time points of depletion **(Fig. 3A)**. Levels of $27SA_2$ pre-rRNAs also initially accumulated but mildly decreased at later time points of depletion. Almost no 27SB pre-rRNA was detected at any time point after the shift **(Fig. 3A)**. As a consequence, levels of 7S pre-rRNA, 25S rRNA, and to a lesser extent 5.8S rRNAs decreased **(Fig. 3A-B)**. No alterations in the ratio between the long and short forms of 5.8S rRNAs were detected. Formation of mature 18S and 5S rRNAs was also mildly reduced. Moreover, primer extension analysis confirmed that there was a slight increase in the stop at site A_2 at the early time points after the shift **(Fig. 3C)**. The $27SA_3$ pre-rRNA, which cannot be readily detected by northern blotting, clearly accumulated in the L16-depleted strain, as shown by the stop at site A_3. In agreement with the northern analysis, the intensity of the stop at site B_{1S} decreased substantially upon depletion of L16. However, that of the stop at site B_{1L} remained practically unaffected during the first time points and slightly increased at later time points of depletion **(Fig. 3C)**.

Pulse-chase RNA labelling experiments with [^{3}H]-uracil were also performed in wild-type and *GAL::RPL16* cells after a 8 h shift to minimal medium containing glucose and lacking uracil (SD-Ura). In wild-type cells, the 35S precursor was converted rapidly into 27S and 20S pre-rRNAs, which were efficiently processed to mature 25S and 18S rRNA, respectively **(Fig. 4)**. In contrast, in the *GAL::RPL16* strain, only some 35S and 20S pre-rRNAs and traces of 27S, and aberrant 23S pre-rRNAs were detected. In these conditions, mature 18S rRNA, although less than in the wild-type strain, was still formed but practically no mature 25S was produced at any time of chase.

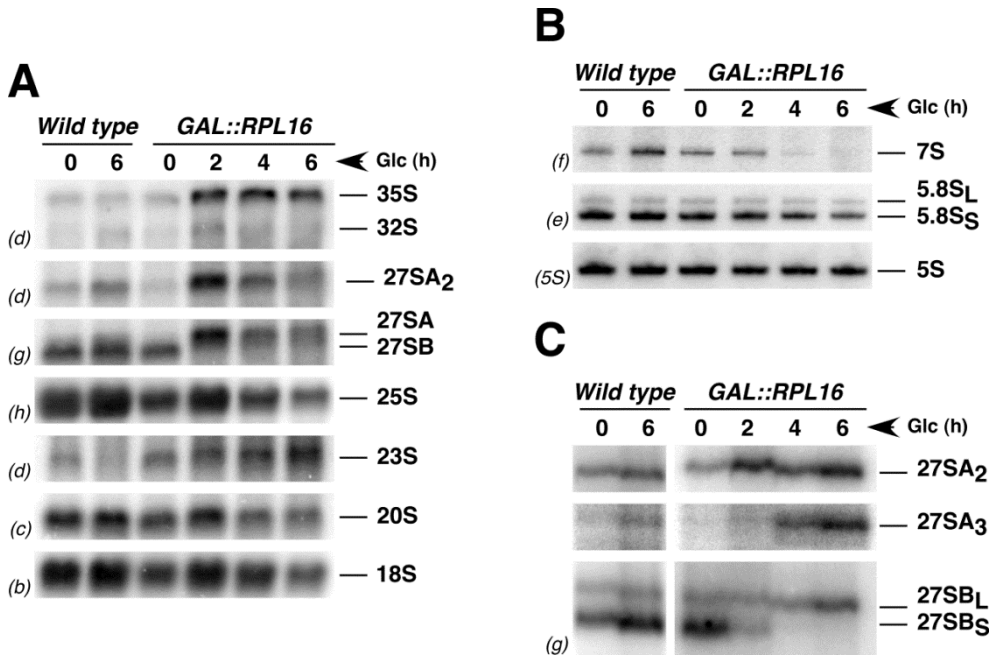

Fig. 3. Depletion of L16 negatively affects the steady-state levels of pre- and mature rRNAs. Strains W303-1A (Wild type) and FEY251 [pAS24-RPL16B] (*GAL::RPL16*) were grown in liquid YPGal medium, and shifted to liquid YPD medium. Cells were harvested at the indicated times, total RNA was extracted from each sample and equal amounts (5 µg) of RNA were subjected to northern hybridization or primer extension analysis. **(A)** Northern blot analysis of high-molecular-mass pre- and mature rRNAs. **(B)** Northern blot analysis of low-molecular-mass pre- and mature rRNAs. Probes, between parentheses, are described in the Experimental Procedures section. **(C)** Primer extension analysis with probe g within ITS2. This probe allows detection of $27SA_2$ (as the stop at site A_2), $27SA_3$ (as the stop at site A_3) and 27SB pre-rRNAs (as stops at sites B_{1L} and B_{1S}).

Taken together, these results indicate that L16 is required for conversion of 27S pre-rRNAs into mature 25S and 5.8S rRNAs, more specifically, for the processing of $27SA_2$ and $27SA_3$ pre-rRNAs to 27SB pre-rRNA species. In addition, L16 depletion affects negatively ITS2 processing since, although $27SB_S$ pre-rRNA underaccumulates, $27SB_L$ pre-rRNA continues to be produced but fails to be converted to $7S_L$ pre-rRNA.

Remarkably, our results suggest that there might be a considerable degradation of pre-rRNAs upon depletion of L16, most likely due to abortive formation of early pre-60S r-particles.

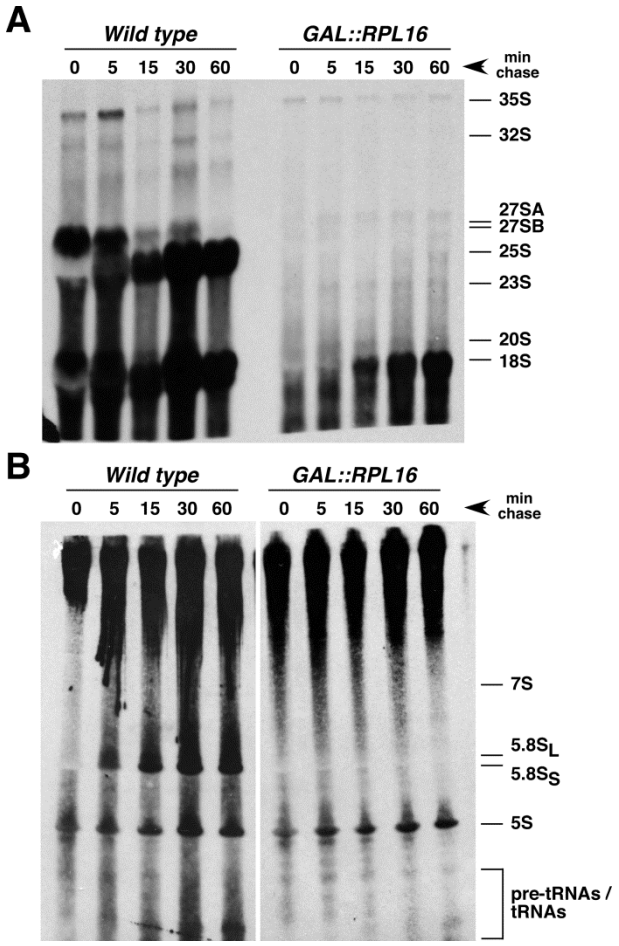

Fig. 4. Depletion of L16 induces turnover of 27S pre-rRNAs. Strains W303-1A (*Wild type*) and FEY251 [pAS24-RPL16B] (*GAL::RPL16*) were transformed with YCplac33 (*CEN URA3*), grown at 30 ºC in liquid SGal-Ura medium to mid log phase and then shifted to liquid SD-Ura medium for 8 h. Cells were pulse-labelled with [5,6-^{3}H]uracil for 2 min followed by a chase with a large excess of unlabelled uracil for the times indicated. Total RNA was extracted from each sample and 20,000 cpm was loaded and separated on **(A)** a 1.2% agarose-6% formaldehyde gel or **(B)** a 7% polyacrylamide-8M urea gel, transferred to nylon membranes and visualized by fluorography. The positions of the different pre- and mature rRNAs are indicated.

Depletion of L16 impairs export of pre-60S r-particles from the nucleus to the cytoplasm

Different reports have described that defective pre-60S r-subunits are retained in the nucle(ol)us and hence not exported to the cytoplasm when there is a failure during the nuclear phases of large r-subunit maturation (i.e. [131, 136, 175, 194]). Thus, to determine whether depletion of L16 impairs nuclear export of pre-60S r-particles, we analyzed the location of the 60S reporter L25-eGFP in the *GAL::RPL16* strain. As expected for an r-protein, L25-eGFP was found predominantly in the cytoplasm in the *GAL::RPL16* strain grown in selective SGal medium **(Fig. 5)**.

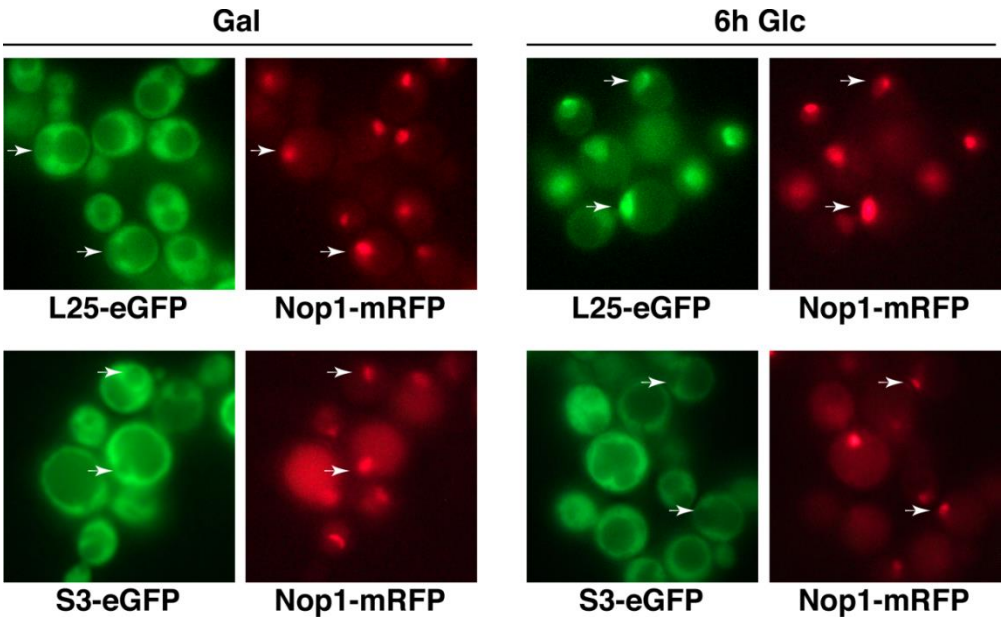

Fig. 5. Depletion of L16 leads to nuclear retention of pre-60S r-particles. FEY251 [pAS24-RPL16B] cells co-expressing Nop1-mRFP and either the 60S r-subunit reporter L25-eGFP or the 40S r-subunit reporter S3-eGFP were grown in SGal-Trp (Gal) or shifted to SD-Trp (Glc) up to 6 h. The subcellular localization of the GFP-tagged r-proteins and the Nop1-mRFP nucleolar marker was analyzed by fluorescence microscopy. Arrows point to nucleolar fluorescence. Approximately 200 cells were examined for each reporter, and practically all cells gave the results shown in the pictures.

However, following a shift to selective SD medium, L25-eGFP accumulated in the nucle(ol)us as denoted by its co-localization with the nucleolar Nop1-mRFP marker **(Fig. 5)**. We did not observe nuclear accumulation of L25-eGFP in the isogenic W303-1A wild-type control strain grown in identical conditions (data not shown). The nuclear retention was specific for the 60S r-subunit reporter, since no accumulation of nuclear fluorescence was observed when the location of the 40S r-subunit reporter S3-eGFP was studied in the *GAL::RPL16* strain under non-permissive conditions **(Fig. 5)**. We conclude that the nucleo-cytoplasmic and/or intranuclear transport of pre-60S r-particles is specifically impaired upon depletion of L16.

L16 assembles within early pre-ribosomal particles

Assembly of r-subunits occurs mainly in the nucle(ol)us, although a few r-proteins only associate with pre-ribosomal particles in the cytoplasm [144]. In the late 1970s, the Planta laboratory demonstrated that nuclear assembling r-proteins could associate with pre-ribosomal particles either at an early or a late stage of the r-subunit maturation process [195]. These experiments suggested that L16 (then named L21) assembled rather early. More

recently, the Milkereit group has shown by systematic analyses of the composition of early and late pre-60S r-particles that L16 clustered with a large group of r-proteins whose levels were similar in both classes of particles, suggesting that, indeed, L16 could be an early nuclear assembling r-protein [125]. To investigate in more detail the timing of L16 assembly, we assessed the presence of L16 within distinct pre-ribosomal particles upon purification of GFP-tagged proteins specific for 90S (Pwp2/Utp1, Nop58/Nop5) [42, 43], early (Ssf1, Nsa1, Nop7), intermediate (Nop7, Rix1), late (Arx1) and cytoplasmic (Arx1, Lsg1/Kre35) pre-60S r-particles [93, 94, 96, 196-198], and mature 60S r-subunits (P0) [199]. Purified particles were analyzed by SDS-PAGE and L16, two other r-proteins (L1 and L10) and selected *trans*-acting factors (Nop1, Has1, Mrt4) were detected by western blotting using specific antibodies. The distribution of the *trans*-acting factors indicated that the corresponding particles were specifically purified (see, [134]). Notably, L16 significantly co-enriched with all tested pre-ribosomal particles **(Fig. 6)**, as also did L1, which was used as a control of an early assembling r-protein [166]. In clear contrast, L10, which was used as a cytoplasmic assembling r-protein control [125, 200], was practically absent from early and intermediate pre-60S r-particles, very modestly represented in late and cytoplasmic pre-60S r-particles but significant enriched in P0-GFP containing particles **(Fig. 6)**. Together, these data reveal that L16 already associates at the stage of early nuclear pre-ribosomal particles.

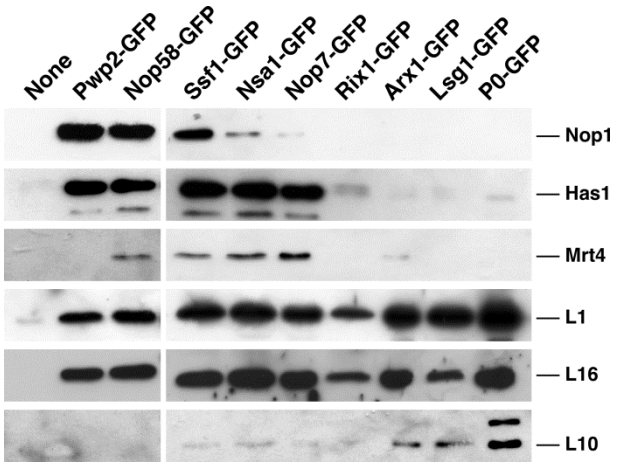

Fig. 6. L16 r-protein stably assembles into 90S pre-ribosomal particles. The indicated GFP-tagged proteins were used as baits to affinity purify 90S or distinct pre-60S r-particles. A non-tagged isogenic strain was used as a negative control. Equivalent amounts of the corresponding purified particles were separated by SDS-PAGE and subjected to western blot analysis. Note that the Rix1- and Lsg1-GFP containing complexes are slightly underloaded. Specific antibodies were used to detect the Nop1, Has1 and Mrt4 *trans*-acting factors and the L1, L10 and L16 r-proteins.

The eukaryote-specific C-terminal extension of L16 is required for growth

Extensions of eukaryotic r-proteins have not yet thoroughly studied (i.e. see, [176, 201, 202]). To study the role of the eukaryote-specific C-terminal extension of L16 in cell growth and ribosome biogenesis, we cloned full-length *RPL16B* and three serial *rpl16b* truncation alleles under the control of the cognate *RPL16B* promoter into the YCplac111 centromeric plasmid. Upon transformation of these constructs into the *rpl16a*Δ *rpl16b*Δ [YCplac33-RPL16B] strain (hereafter *RPL16* shuffle strain), cells were subjected to plasmid shuffling on 5-fluorootic acid (5-FOA) containing plates. Expression of wild-type L16B (full-length L16B consists of 198 amino acids) or the truncated L16B protein variant lacking the last 18 amino acids (L16B-N180 construct), as the sole sources of L16 in the cells, conferred a wild-type growth phenotype **(Fig. 7A)** and a normal polysome profile (data not shown). However, expression of the truncated protein variants lacking the last 30 (L16B-N168 construct) or the last 51 amino acids (L16B-N147 construct) did not support growth **(Fig. 7A)**.

To further analyze the role of the C-terminal extension of L16, we transformed the above plasmid-borne truncated alleles of *RPL16B* into a yeast strain conditionally expressing an N-terminally HA-tagged L16B fusion-protein from a *GAL1* promoter (*GAL::HA-RPL16* strain). None of the truncated L16 variants conferred a dominant-negative growth phenotype on selective SGal medium **(Fig. 7B)**. Upon depletion of wild-type HA-L16 on selective SD medium, only full-length L16B and the L16B-N180 variant supported growth, whereas the L16B-N168 and L16B-N147 proteins did not **(Fig. 7B)**. Moreover, on selective SD medium, polysome profiles were normal upon expression of full-length L16B and the L16B-N180 variant, but indistinguishable of those obtained upon L16-depletion upon expression of the L16B-N168 and L16B-N147 proteins (data not shown). Next, we studied the expression and stability of the truncated forms of L16 from extracts of *GAL::HA-RPL16* cells grown in selective SGal medium or shifted to selective SD medium for 12 h. As shown in **Fig. 7C**, all truncated forms of L16B were detected, although the L16B-N168 and L16B-N147 seemed to accumulate to a lesser extent; however, we cannot exclude the possibility that a substantial number of epitopes could have been removed with the truncations, and hence, that the recognition efficiency of the anti-L16 polyclonal antibodies have diminished resulting in weaker detection of the truncated L16B-N168 and L16B-N147 proteins. Taking into account that r-proteins unable to assemble into ribosomes are rapidly degraded (i.e. [203]), these results suggest that all the truncated forms of L16 could get incorporated into pre-60S r-particles (see below). It has been reported that the expression of certain r-protein gene mutants from plasmids leads to a much softer phenotype than their expression from their chromosomal loci (i.e. [204]). Indeed, for most duplicated r-protein genes, plasmidic

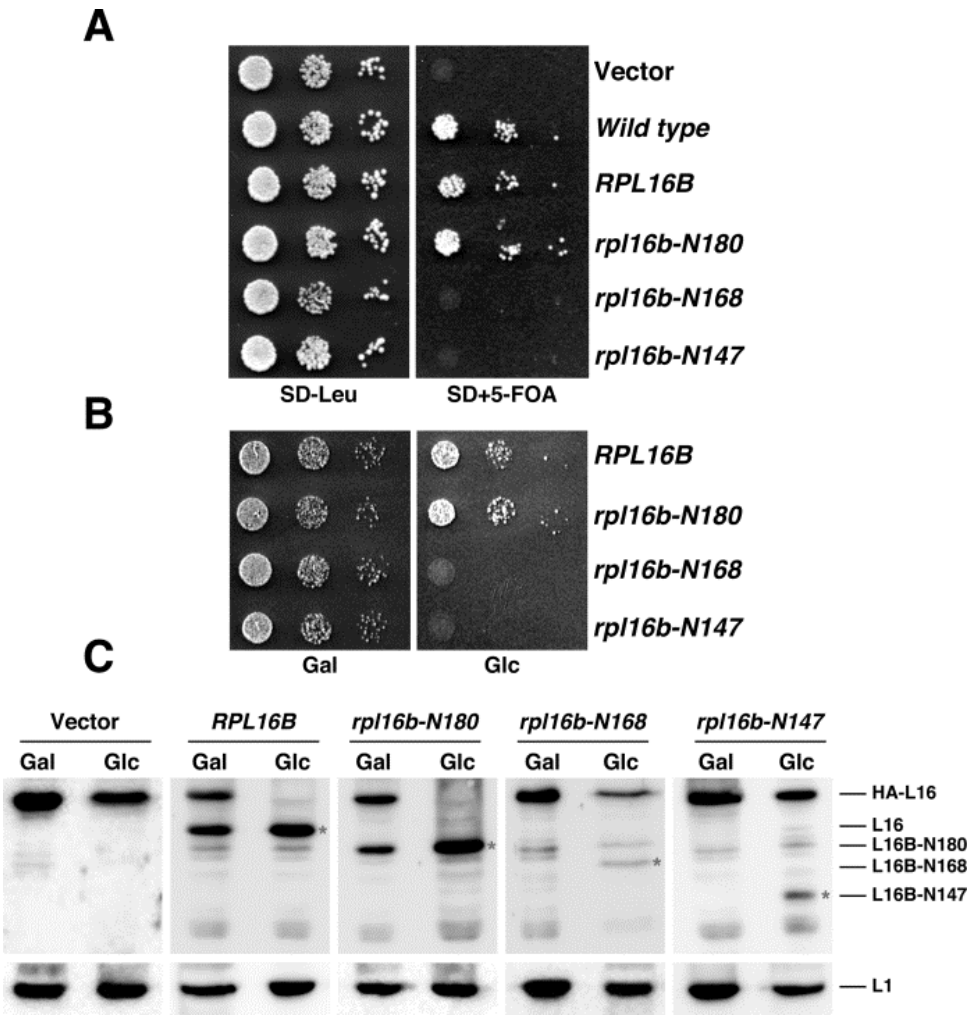

Fig. 7. Growth phenotype and expression levels of L16 in strains bearing wild-type or truncated variants of L16B. (A) *In vivo* phenotypes of the different C-terminal truncation mutants. Empty vector (YCplac111) and YCplac111-borne wild-type *RPL16B* or the indicated *rpl16b* alleles expressed from the *RPL16B* cognate promoter were transformed into the *RPL16* shuffle strain, FEY251 [YCplac33-RPL16B]. Transformants were serially diluted 5-fold on SD-Leu and SD+5-FOA plates, which were incubated for 3 days at 30 ºC. The W303-1A strain (*Wild type*) was used as a control. **(B)** The strain FEY251 [pAS25-RPL16B], which expressed a 2xHA-tagged L16 fusion protein from the *GAL1* promoter, was transformed with YCplac111-borne wild-type *RPL16B* or the indicated *rpl16b* alleles. Transformants were serially diluted 5-fold on SGal-Leu and SD-Leu plates, which were incubated for 3 days at 30 ºC. **(C)** Expression levels of YCplac111-borne wild-type *RPL16B* and the indicated *rpl16b* mutant alleles in the FEY251 [pAS25-RPL16B] strain. Whole cell extracts were prepared from cells grown in SGal-Leu (Gal) or shifted to SD-Leu (Glc) for 24 h. Equivalent amounts of cell extracts were separated by SDS-PAGE and levels of the L16 r-protein variants (indicated by asterisks) were determined by western blot analysis using anti-L16 antibodies.

expression of only one of the two r-protein paralogues normally rescues the growth and ribosome biogenesis defects of the strain lacking both paralogues (discussed in [205]). Thus, to check whether multiple copies of *rpl16b-N180* suppressed the absence of L16, we constructed a strain containing a single *rpl16b-N180* allele at its natural chromosomal locus.

As shown in **Fig. 8A**, this strain grew as well as a wild-type strain when present in an *RPL16A* background and similarly as an *rpl16a* null mutant when present in an *rpl16a*Δ background. Western blot analysis showed that the truncated L16B-N168 protein was fairly well expressed **(Fig. 8B)**. Moreover, polysome profile analysis showed that the *rpl16a*Δ *rpl16b-N180* strain displayed a mild reduction in the amount of free 60S r-subunits as well as an accumulation of half-mer polysomes **(Fig. 8C)**. This profile was identical to that obtained for an isogenic *rpl16a*Δ single mutant (data not shown), indicating that when expressed from a plasmid, the rpl16b-N180 construct was in fact suppressing the defects of both *rpl16a* and *rpl16b* null alleles. Thus, we conclude that, at least, the last 18 amino acids of yeast L16 protein are fully dispensable for growth and ribosome production under laboratory conditions.

Importance of the C-terminal extensión of L16 in 60S r-subunit biogénesis

We next wanted to examine in more detail the consequences of assembly of the truncated L16 proteins. First, we studied whether the truncated mutants lead to defects in pre-rRNA processing. To do so, the *GAL::HA-RPL16* strain harbouring an empty YCplac111 vector, or YCplac111-borne copy of either wild-type or the truncated versions of L16B were grown in selective SGal medium, and shifted to selective SD medium for different times. RNA was extracted at the different time points and the levels of pre-rRNA intermediates assayed by northern blotting. As shown in **Fig. 9**, and in agreement with the absence of apparent defects in growth and ribosome production, expression of L16B-N180 led to wild-type levels of pre-rRNAs and mature rRNAs. Therefore, the last 18 amino acids of L16B are also dispensable for pre-rRNA processing under laboratory conditions. However, expression of L16B-N168 and L16B-N147 resulted in pre-rRNA processing defects similar to those found in the L16-depleted strain, including low levels of 27SB and 7S pre-rRNAs and mature 25S rRNAs. Strikingly, the levels of these pre-rRNAs were reduced to a lesser extent in the truncation mutants than in the L16-depleted strain **(Fig. 9)**. Residual levels of full-length L16 in the truncated mutants might have not accounted for the slight increase in these pre-rRNAs since a similar increase did not occur in the *GAL-HA-RPL16* strain transformed with a empty vector, which also presented substantial levels of full-length L16 even 24 h after the shift to selective SD medium (see **Fig. 7C**).

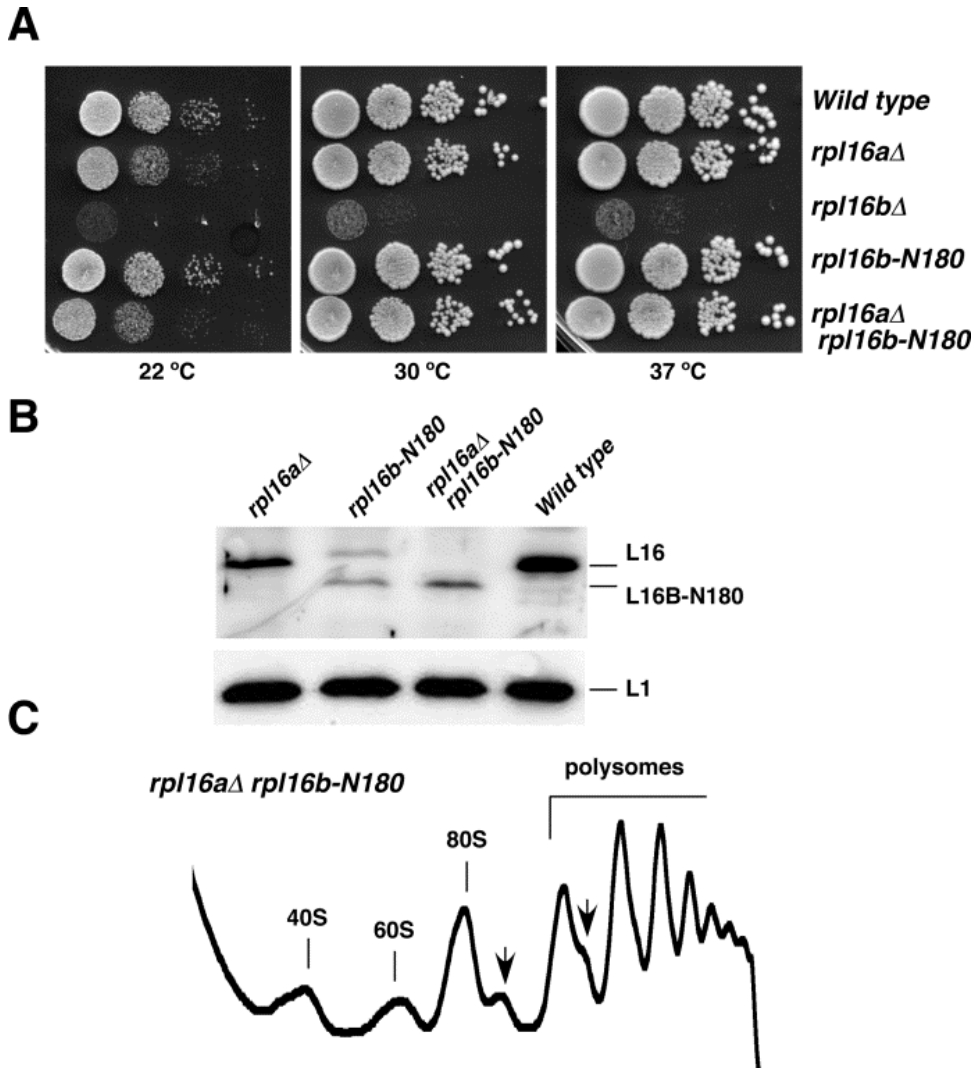

Fig. 8. The genomically integrated *rpl16b-N180* allele confers a wild-type phenotype. (A) Growth analysis of the indicated strains compared to their isogenic wild-type control. Cells of strains FEY206 (*rpl16a*Δ), FEY209 (*rpl16b*Δ), JFY01 (*rpl16b-N180*), JFY02 (*rpl16a*Δ *rpl16b-N180*) and W303-1A (*Wild type*) were serially diluted 5-fold and spotted on YPD plates, which were incubated at 30 ºC for 3 days. **(B)** The indicated strains were grown in liquid YPD medium and harvested at an OD_{600} of 0.8, whole cell extracts were prepared and equivalent amounts of the cell extracts subjected to western blot analysis with antibodies against the r-proteins L16 and L1. **(C)** Polysome profile of the double *rpl16a*Δ *rpl16b-N180* mutant. Ten A_{260} of the whole cell extract from the JFY02 strain were resolved in a 7-50% sucrose gradient. The A_{254} was continuously measured. Sedimentation is from left to right. The peaks of free 40S and 60S r-subunits, 80S free couples/monosomes and polysomes are indicated. Half-mers are labelled by arrows.

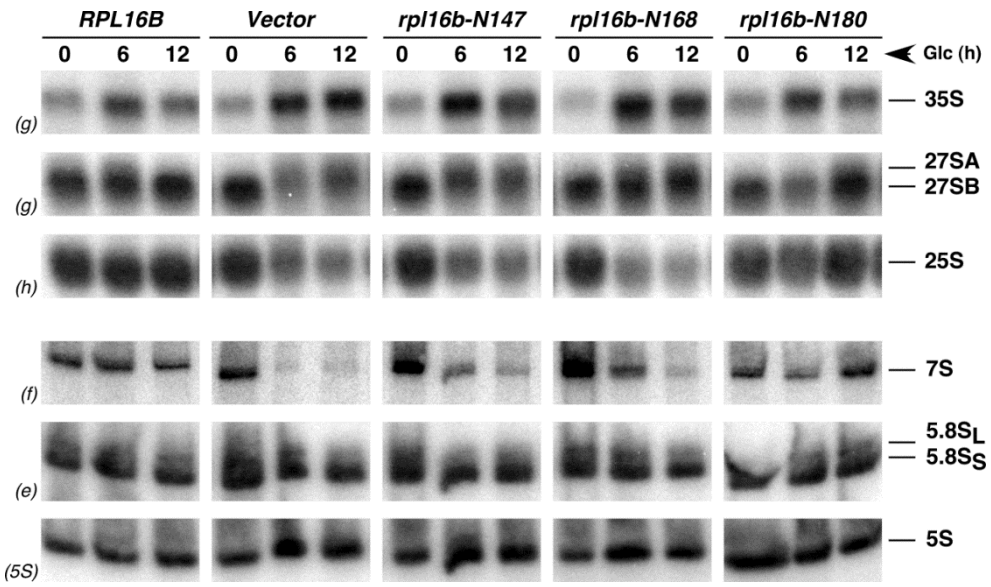

Fig. 9. Role of the C-terminal extension of L16 in pre-rRNA processing. The strain FEY251 [pAS25-RPL16B] harbouring the empty YCplac111 plasmid (Vector), or YCplac111-borne wild-type *RPL16B* or the indicated truncated *rpl16b* alleles were grown in liquid SGal-Leu and shifted to liquid SD-Leu for the indicated times. Cells were harvested and total RNA extracted. Equal amount (5 µg) of total RNA was separated on an agarose gel (first three upper panels) or on a polyacrylamide gel (lower panels), transferred onto nylon membranes, and hybridized with the indicated probes (between parentheses; probes are described in the Experimental Procedures section).

Together, these results strongly suggest that assembly of the non-viable truncated versions of L16B minimally but significantly stabilize early and medium pre-60S r-particles, hence, decreasing their rate of turnover.

To determine whether assembly of the truncated L16B variant proteins, similarly as L16 depletion does, impairs nuclear export of pre-60S r-particles, we analyzed the location of the 60S reporter L25-eGFP in the different strains expressing the truncated L16B proteins used in this study. In selective SGal medium, L25-eGFP was found predominantly in the cytoplasm.

However, following a shift to selective SD medium for 6 h, L25-eGFP accumulated in the nucle(ol)us in about 90 % of the ca. 200 examined cells expressing L16B-N168 or L16B-N147, this percentage is similar to that obtained upon depletion of L16. In contrast, no nuclear accumulation of L25-eGFP was observed in cells expressing either full-length or L16B-N180 protein (data not shown). We conclude that assembly of the truncated L16B-

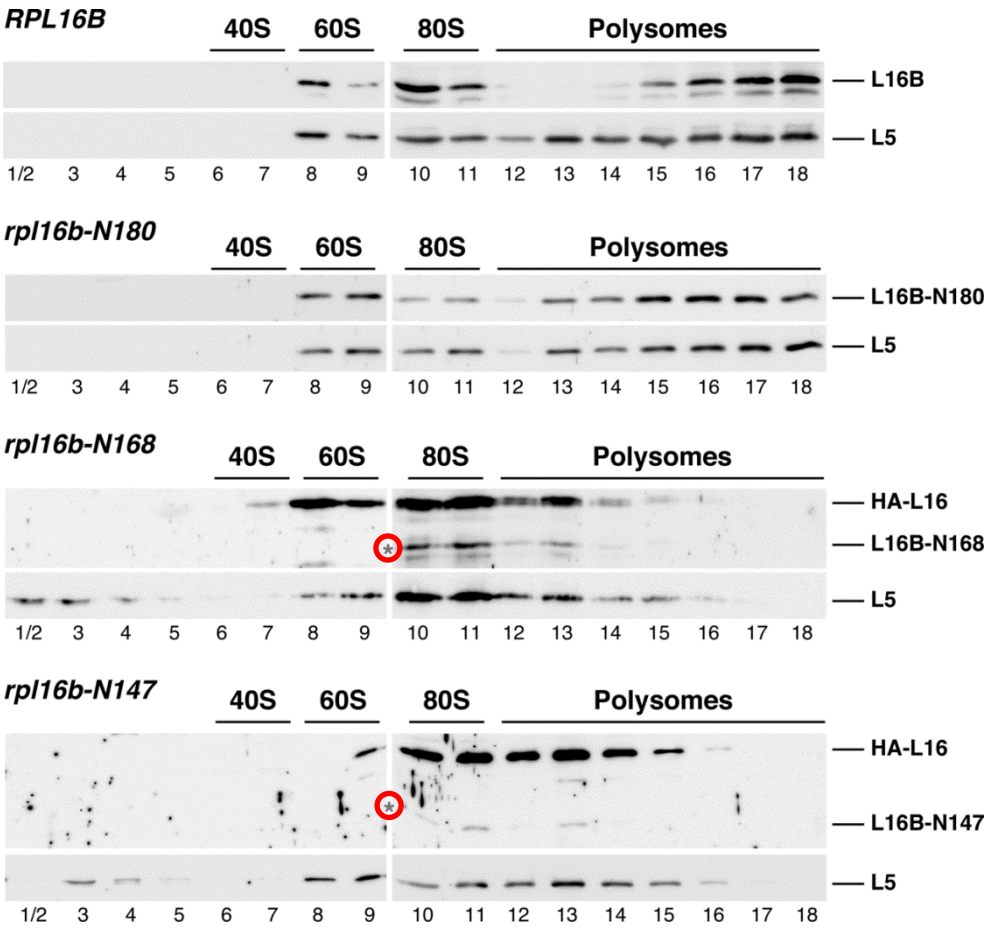

Fig. 10. Analysis of the incorporation of C-terminally truncated L16 variant proteins into pre-60S/60S r-subunits and translating ribosomes. The strain FEY251 [pAS25-RPL16B] harbouring YCplac111-borne wild-type *RPL16B* or the indicated truncated *rpl16b* alleles were grown in liquid SGal-Leu and shifted to liquid SD-Leu for 24 h. Cell extracts were prepared under polysome-preserving conditions and ten A_{260} units of each extract were resolved in 7–50% sucrose gradients and fractionated. Proteins were concentrated by TCA precipitation and subjected to western analysis using anti-L16 and anti-L5 antibodies. The position of free 40S and 60S r-subunits, 80S free couples/monosomes and polysomes have been obtained from the recorded A_{254} profile. The corresponding inputs of the fractionated cell extract samples are shown in Fig. 7C. Note that a substantial residual full-length HA-L16 protein is still detected in cells expressing the L16B-N168 and L16B-N147 variants (indicated by asterisks).

N168 or L16B-N147 does not ameliorate the impairment of nuclear export of pre-60S r-particles caused by the depletion of L16, while assembly of L16B-N180 fully complements this failure.

Finally, to directly examine whether the truncated L16B variant proteins get incorporated into mature ribosomes, we obtained extracts from cells expressing wild-type or the truncated L16B proteins, subjected them to sucrose gradient fractionation, and the fractions analysed by SDS-PAGE and western blotting using polyclonal anti-L16 antibodies.

As shown in **Fig. 10** and as expected, the full-length L16B and L16B-N180 proteins got efficiently incorporated into mature 60S r-subunits and engaged in active translation. Moreover, both L16B-N168 and L16B-N147 proteins, which inefficiently accumulated as previously shown (see **Fig. 7C**), were found associated with high-molecular-mass complexes sedimenting at positions equivalent to 80S monosomes and light polysomes **(Fig. 10)**. We conclude that the truncated L16B-N168 or L16B-N147 could also get incorporated into pre-60S/60S r-subunits, which are likely not as translationally competent as those derived from wild-type or rpl16-N180 cells.

EXPERIMENTAL PROCEDURES

Strains and microbiological methods

The yeast strains used in this study **(Table 1)** are derivatives of the diploid strain W303 [206]. Heterozygous diploid strains disrupted for one *RPL16A* ORF copy or one *RPL16B* ORF copy, respectively, with the HIS3MX6 marker were obtained by following a standard procedure [207]. FEY206 (*rpl16a*::HIS3MX6) and FEY206 (*rpl16b*::HIS3MX6) are meiotic segregants the corresponding diploid strains. To construct the *GAL::RPL16* strain, FEY206 and FEY206 were crossed and the resulting diploid transformed with a YCplac33-RPL16B plasmid. After sporulation and tetrad dissection, we selected the FEY251 strain, which is a representative double *rpl16a*Δ *rpl16b*Δ mutant that contains YCplac33-RPL16B. FEY251 was transformed with the pGAL1-RPL16B plasmid [175], and subsequently, YCplac33-RPL16B was counter-selected on 5-FOA plates containing galactose. We also refer to this strain as GAL::RPL16. C-terminal truncations of *RPL16B* were performed in the genomic *RPL16B* locus by a standard replacement procedure [207]. Details about the construction of the different strains are available upon request.

Strains were grown at selected temperatures either in rich YP medium (1% yeast extract, 2% peptone) supplemented with 0.2% adenine and containing either 2% glucose (YPD) or 2% galactose (YPGal) as carbon source or in synthetic minimal medium (0.15% yeast nitrogen base, 0.5% ammonium sulphate) supplemented with the appropriate amino acids and bases as nutritional requirements, and containing either 2% glucose (SD) or 2% galactose (SGal) as carbon source. Yeast was transformed by the lithium acetate method [208]. Tetrad dissections were performed using a Singer MS micromanipulator. All recombinant DNA techniques were done according to established procedures using *E. coli* DH5α for cloning and propagation of plasmids.

Plasmids

To construct YCplac33-RPL16B and YCplac111-RPL16B, a PCR was performed using yeast genomic DNA as a template and oligonucleotides placed plus-minus 1 kbp upstream and downstream from the start-stop codon of the RPL16B ORF, respectively; after the appropriate restriction digestion, the PCR product was cloned into the respective vectors. Different C-terminal truncations of L16B were also cloned into YCplac111. To construct pAS25-RPL16B, which allows expression of N-terminally HA-tagged L16B under the control of a *GAL* promoter, a PCR product containing the *RPL16B* ORF plus 500 bp downstream the stop codon was cloned into the empty pAS25 vector [209]. The correctness of all resulting plasmids was confirmed by DNA sequencing. Detailed information on the plasmids is

available upon request. Other plasmids used in this study were: pRS316-RPL25-eGFP-NOP1-mRFP and pRS316-RPS3-eGFP-NOP1-mRFP (gifts from J. Bassler and E. Hurt) [210] and pGAL1-RPL16B (TK810) (gift from JP. Milkereit) [175].

Polysome profile analyses

Polysome preparations were performed as exactly described in [211]. Sucrose gradients were analysed using an ISCO UA-6 system with continuous monitoring at A_{254}. When required, fractions of 0.5 ml were collected from the gradients and proteins were extracted and analysed by western blotting as described [212].

Western blotting analyses

Total cell extracts were obtained by disrupting cells by vigorous shaking with glass beads in a Fastprep-24TM 5G (MP Biomedicals) at 4 ºC, in a standard lysis buffer (50 mM Tris-HCl, pH7.5; 1.5 mM $MgCl_2$; 150 mM NaCl; 1 mM DTT) containing a protease inhibitor cocktail (Complete, Roche); extracts were clarified by centrifugation in a microcentrifuge at the maximum speed (ca. 16100 x g) for 15 min at 4 ºC. Total cell extracts were analysed by western blotting according to a standard procedure using the following primary antibodies: mouse monoclonal anti-Nop1 (MCA28F2, EnCor Biotechnology) and rabbit polyclonal anti-L16 (gift from S. Rospert) [213], anti-L1 (gift from F. Lacroute) [214], anti-Has1 (gift from P. Linder) [215], anti-Mrt4 (gift from J.P.G. Ballesta) [115], anti-L5 (gift from S.R. Valentini) [216] and anti-L10 (gift from B. Trumpower) [217]. Goat anti-mouse or anti-rabbit horseradish peroxidase-conjugated antibodies (Bio-Rad) were used as secondary antibodies. Proteins were detected using a chemiluminescence detection kit (Super-Signal West Pico, Pierce) and a ChemiDocTM MP system (Bio-Rad).

RNA extractions, northern hybridization and primer extension analyses

RNA extraction, northern hybridization and primer extension analyses were carried out as previously described [218, 219]. Total RNA was extracted from samples corresponding to 10 OD_{600} units of cells grown to mid-log phase. Equal amounts of total RNA were loaded on gels or used for primer extension reactions. Specific oligonucleotides, were 5'-end labelled with [γ-^{32}P] ATP and used as probes. The following probes were used: Probe a (5' A_0) 5'-GGTCTCTCTGCTGCCGG-3', Probe b (18S) 5'-CATGGCTTAATCTTTGAGAC-3',

Probe c (3-D/A_2) 5'-GACTCTCCATCTCTTGTCTTCTTG-3', Probe d (A_2/A_3) 5'-TGTTACCTCTGGGCCC-3', Probe e (5.8S) 5'-TTTCGCTGCGTTCTTCATC-3', Probe f (E/C_2) 5'-GGCCAGCAATTTCAAGTTA-3', Probe g (C_1/C_2) 5'-GAACATTGTTCGCCTAGA-3', Probe h (25S) 5'-CTCCGCTTATTGATATGC-3' and Probe 5S 5'-GGTCACCCACTACACTACTCGG-3'. Signal intensities were quantified using a FLA-5100 imaging system and Image Gauge (Fujifilm).

Pulse-chase labelling of pre-rRNA

Pulse-chase labelling of pre-rRNA was performed exactly as previously described [219], using 100 µCi of [5,6-^{3}H]-uracil (Perkin Elmer; 45 to 50 Ci/mmol) per 40 OD_{600} of yeast cells. Cells were grown in SGal-Ura medium to mid-log phase at 30 ºC or shifted to SD-Ura medium for 8 h, pulse-labeled for 2 min and chased for different times with SD medium containing an excess of cold uracil. Total RNA was extracted as above. Radioactive incorporation was measured by scintillation counting and about 20000 cpm per RNA sample were loaded and resolved on 1.2% agarose-6% formaldehyde and 7% polyacrylamide-8M urea gels. RNA was then transferred to nylon membranes and visualized by fluorography [219].

Fluorescence Microscopy

To test pre-ribosomal particle export, the appropriate *GAL::RPL16* strain derivatives were transformed with plasmids expressing either GFP-tagged L25 or S3 and Nop1-mRFP (see above). Transformants were grown in selective SGal medium and shifted to selective SD for 6 h to deplete L16. Cells were washed, resuspended in PBS buffer (140 mM NaCl, 8 mM Na_2HPO_4, 1.5 mM KH_2PO_4, 2.75 mM KCl, pH 7.3), and examined with a Leica DMR fluorescence microscope equipped with a DC350F digital camera and its software. Adobe Photoshop CS2 (Adobe Systems Inc.) was used to process the images.

Affinity Purification of GFP-tagged Proteins

GFP-tagged factors representative of 90S and pre-60S r-particles were purified following a one-step GFP-Trap_A procedure (Chromotek), as exactly described in [134]. The proteins from purified particles were extracted by boiling the beads with Laemmli buffer and analyzed by western blotting. To normalize the amount of purified complexes to be loaded for comparative studies, aliquots of the samples were first resolved and visualized by silver staining according to the manufacturer's instructions (Bio-Rad).

Table 1. Yeast strains used in this study.

Strain	Relevant genotype	Reference
W303-1A	*MAT***a** *ade2-1 his3-11,15 leu2-3,112 trp1-1 ura3-1*	[206]
W303-1B	As W303-1A but *MAT*a	[206]
FEY206	As W303-1B but *rpl16a::*HIS3MX6	This work
FEY209	As W303-1A but *rpl16b::*HIS3MX6	This work
FEY251 [(a)]	As W303-1B but *rpl16a::*HIS3MX6 *rpl16b::*HIS3MX6 [YCplac33-RPL16B]	This work
JFY01	As W303-1B but *rpl16b-N180*	This work
JFY02	As W303-1B but *rpl16a::*HIS3MX6 *rpl16b-N180*	This work
YMD5 [(b)]	As W303-1A but *PWP2*-GFP(S65T)::kanMX6	[220]
YMD24 [(b)]	As W303-1A but *NOP58*-GFP(S65T)::*TRP1*	[220]
JDY850	As W303-1A but *SSF1*-GFP(S65T)::natNT2	[220]
JDY854 [(c)]	As W303-1A but *NSA1*-GFP(S65T)::natNT2	This work
JDY851	As W303-1A but *NOP7*-GFP(S65T)::natNT2	[220]
JDY852	As W303-1A but *RIX1*-GFP(S65T)::natNT2	[220]
JDY855	As W303-1A but *ARX1*-GFP(S65T)::natNT2	[220]
JDY853	As W303-1A but *LSG1*-GFP(S65T)::natNT2	[220]
JDY861 [(d)]	As W303-1A but *RPP0*-GFP(S65T)::natNT2	[220]

(a) Depending on the experimental conditions, YCplac33-RPL16B was replaced by other plasmids containing different alleles of *RPL16B*.

(b) Gift from M. Dosil.

(c) Strain JDY854 is a segregant of the genetic cross between W303-1B and strain Y4219 (As W303-1A but *rix7*::kanMX6 *ade3*::kanMX4 *NSA1*-GFP(S65T)::natNT2 pHT4467Δ-*RIX7*; gift from D. Kressler) [96].

(d) Gift from M. Remacha.

CAPÍTULO 2

Ribosomal protein L14 contributes to the early assembly of 60S ribosomal subunit in *Saccharomyces cerevisiae*

INTRODUCTION

Ribosomes are ubiquitous ribonucleoprotein particles that are responsible of protein synthesis (for a review, see [221] and references therein). In all organisms, ribosomes are composed of two ribosomal subunits (r-subunits), the large one about twice the size of the small one [222]. The structure of ribosomes from prokaryotes and eukaryotes has been obtained to atomic resolution [22, 142]. Globally, eukaryotic ribosomes are much larger and complex than prokaryotic ones due to the presence of additional rRNA sequences, named expansion segments (ESs), and the addition of several eukaryote-specific r-proteins [22, 142] and r-protein extensions ([142]; see also [107] and references therein). In this regard, in *Escherichia coli,* the small or 30S r-subunit contains a single 16S rRNA and 21 r-proteins, while, in *Saccharomyces cerevisiae*, the small or 40S r-subunit contains a single 18S rRNA, which is ca. 260 nucleotides (nt) longer than 16S rRNA and 33 r-proteins. In turn, the large or 50S r-subunit from *E. coli* is made up of two rRNAs, the 23S (2904 nt in lenght) and 5S (120 nt) rRNAs, and 33 r-proteins, while the large or 60S r-subunit from *S. cerevisiae* contains three rRNAs, 25S (3396 nt), 5.8S rRNA (158 nt) and 5S rRNA (121 nt), and 46 r-proteins [78, 188]. Despite these generalities, it is remarkable that ribosomes are not unchangeable entities; indeed in both prokaryotes and eukaryotes, multiples examples of ribosome heterogeneity including variations in the r-protein complement, alternative rRNA molecules, differential degree of r-protein and/or rRNA modification, and presence of more than one copy of selected r-proteins per subunit have been reported [64, 223-228].

Ribosome synthesis is a highly energy-consuming dynamic process [78, 188]. In eukaryotes, the synthesis of cytoplasmic ribosomes is a compartmentalized pathway that takes place largely in the nucleolus (for reviews, see [30, 106, 185, 229, 230]), although late steps occur in the nucleoplasm and in the cytoplasm [78, 184, 231]. Ribosome synthesis proceeds *via* the formation of pre-ribosomal intermediates [232, 233] that contain r-proteins and many non-ribosomal RNA or protein factors, known as ribosome assembly or *trans*-acting factors, which provide this pathway with the enough speed, accuracy and directionality [29, 230, 234]. Within the pre-ribosomal particles and along the maturation path, the precursors rRNAs (pre-rRNAs) are modified, processed and folded (see **Figure 1**); concomitantly, the r-proteins assemble in a hierarchical manner. Thus, distinct r-proteins, the so-called primary binding proteins, stably bind directly to the nascent pre-rRNAs, while secondary and ternary binding proteins require the previous binding of one or more r-proteins (see [78, 188]. Apparently, the initial interactions of r-proteins with nascent pre-rRNAs are weak but become reinforced as assembly proceeds (e.g. [77, 125, 235]). Different reports have given rise to the interpretation that assembly of r-proteins occurs *via* the hierarchical but not linear formation of discrete folding modules or blocks containing neighbouring r-proteins

and rRNAs that respectively assemble or fold in an interdependent fashion (e.g. [77, 140, 236, 237]). In *S. cerevisiae*, the eukaryote where ribosome biogenesis has perhaps been best studied [30], the course of r-protein assembly has been tackled *in vivo* by different approaches. (i) The pioneering work, led primarily by the laboratories of R.J. Planta and J.R. Warner, undertook the order in which r-proteins are incorporated into early or late nuclear pre-ribosomal particles. From these studies, it became evident that r-proteins can be grouped roughly into three classes: most r-proteins early assemble into distinct 66S and 43S nucleolar pre-ribosomal particles, some r-proteins are added later but still in the nucleus, and few r-proteins assemble in the cytoplasm ([195, 238], see also [239, 240]). (ii) The timing of r-protein assembly has tentatively been deduced by the compositional analyses of distinct pre-ribosomal particles purified using selected tagged *trans*-acting factors as baits by affinity purification methods, especially by the TAP procedure (for examples, see [81, 90, 197, 241]). The fact that r-proteins were found as frequent contaminants of TAP purifications of protein complexes (e.g. [242, 243]) made less reliable these results until the use of more careful analyses of affinity purification and/or protein identification methods (e.g. [77, 125, 244]). (iii) The timing of r-protein assembly has also been studied by the affinity purification of complexes using specific tagged r-proteins as baits and the determination of the co-purified pre-rRNA intermediates (e.g. [131, 134, 166]). (iv) The *in vivo* function of most r-proteins in ribosome assembly has also been studied by the examination of the defects on pre-rRNA processing and nucleocytoplasmic export of pre-ribosomal particles upon their depletion (for few representative examples, see [76, 127-129, 136, 175, 245, 246]). From these studies, r-proteins were classified as early, intermediate, late or cytoplasmic-acting components affecting specific steps of ribosome maturation. In some cases, in addition to pre-rRNA processing and export of pre-ribosomal particles, the changes in the protein composition, *trans*-acting factors and r-proteins, of pre-ribosomal particles upon depletion of selected r-proteins have also been determined [77, 125, 135, 140]. Together, these studies indicate that the timing of action of r-proteins remarkably correlates with their specific location within mature r-proteins and provide a scenario of the sequential assembly of r-subunits (see below). (v) The interaction of each r-protein with the rRNAs and other r-proteins within mature ribosomes has been resolved at atomic resolution within mature yeast ribosomes [10-12]. Importantly, the structure of many ribosome assembly intermediates has also been elucidated by cryo-electron microscopy (cryo-EM) at near-atomic resolution (e.g. [112, 147, 150, 153, 247-250], reviewed in [251, 252]). The comparison of the structure of these intermediates with that of the respective mature r-subunits and/or the structure that some r-proteins adopt when bound to their specific chaperones (e.g. [118, 152, 253, 254]) is providing for the first time molecular clues on how r-proteins undertake different structural rearrangements to acquire their final and stable position within mature r-subunits. These

rearrangements are best exemplified by the incorporation of the 5S RNP into early pre-60S r-particles and its rotation to reach its final position in mature 60S r-subunits [130, 153, 255]. Altogether, all these approaches have ended with the following model for the maturation of the r-subunits (reviewed in [78]). The small r-subunit seems to assemble in a bipartite manner: first, it occurs the co-transcriptional formation of the body of the r-subunit that comprise the association of the set of r-proteins that bind the 5' domain of 18S rRNA; later, the formation of the head of the r-subunit takes place by the assembly of those r-proteins that bind the 3' domain of the 18S rRNA. The construction of the head structure is necessary for the proper export of the pre-40S r-particle to the cytoplasm, where the assembly of the last r-proteins occurs [76, 77]. This outline has largely been preserved in higher eukaryotes [111] and it is reminiscent of the classical *in vitro* assembly pathway initially designed by M. Nomura and co-workers [68, 188]. The development of new purification techniques for capturing intermediates in the progression of 90S pre-ribosomal particles [87, 88] and the cryo-EM determination of intermediates during the maturation of small r-subunits [82, 83, 250, 256] will certainly help, among other challenges, in the better understanding of the small r-subunit assembly. The large r-subunit assembles hierarchically and its construction occurs parallel to the maturation of the 25S/5.8S rRNAs (see **Figure 1**). The earliest assembly steps of large r-subunit likely involve the initial compaction of $27SA_2$ pre-rRNA aided by the binding of at least primary r-protein L3 (uL3 according to the recently proposed r-protein nomenclature [79]). Next, and coupled to the removal of ITS1, those r-proteins that bind mainly domains I and II in the 25S/5.8S rRNAs get associated to the particles. All these r-proteins, including L4, L6, L7, L8, L9, L13, L16, L18, L20, L32 and L33 (uL4, eL6, uL30, eL8, uL6, eL13, uL13, eL18, eL20, eL32 and eL33, respectively), form a belt around the equator of the solvent-exposed surface of the large r-subunit. Intermediate steps of assembly include cleavage at the C_2 site in the ITS2 spacer and association of some r-proteins in the vicinity to 5.8S rRNA and the perimeter of the solvent-exposed part of the peptide exit tunnel, among them L17, L19, L23, L26, L27, L35 and L37 (uL22, eL19, uL14, uL24, eL27, uL29 and eL37, respectively). It has been reported that association of L2, L39 and L43 (uL2, eL39 and eL43, respectively) with pre-60S r-particles is likely specifically stabilised after cleavage at the site C_2, event that might required the previous assembly of the above middle-acting r-proteins. The next reactions in 60S r-subunit assembly are described as late nuclear steps and include the maturation of 25.5S and 7S pre-rRNAs and the rotation of the central protuberance, which contains 5S rRNA and r-proteins L5 and L11 (uL18 and uL5, respectively), that was rotated 180º from its final conformation in mature r-subunits. At this stage, pre-60S r-particles are competent for nuclear export. The final steps of assembly occur in the cytoplasm and include, among other events, the processing of 6S pre-rRNAs to mature 5.8S rRNAs and the assembly of few r-proteins, among them L10, L24, L29, L40, L42, P1 and P2 (uL16, eL24,

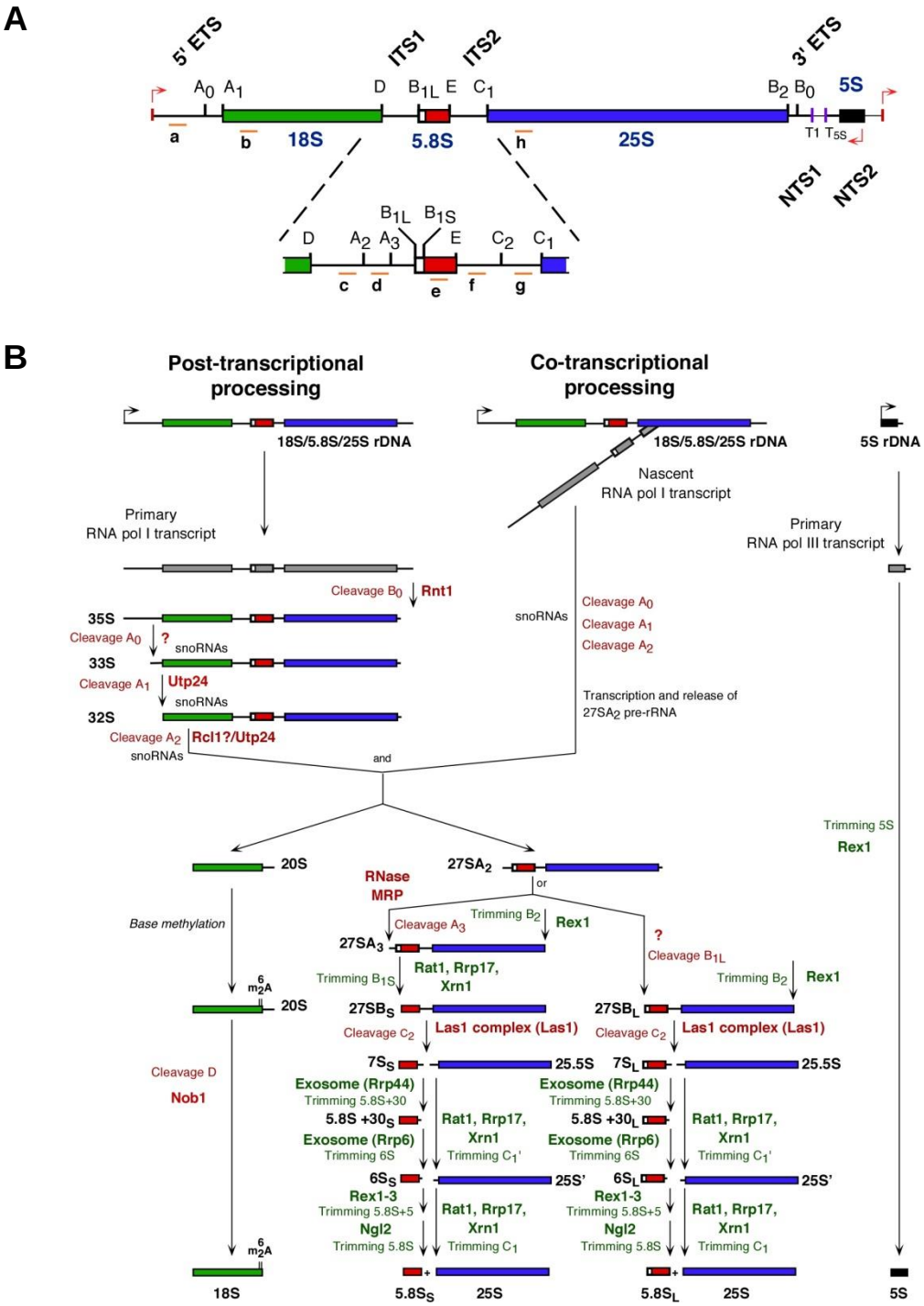

Fig 1. Pre-rRNA processing pathway in *S. cerevisiae*. (A) Structure and processing sites of the 35S and pre-5S pre-rRNAs. Mature 18S, 5.8S and 25S rRNAs are flanked by external transcribed (ETS) and separated by internal transcribed (ITS) spacer sequences; pre-5S rRNA is separated from 35S pre-rRNA by non-transcribed sequences (NTS). Processing sites and location of the different probes used in this study are indicated. (**B**) Pre-rRNA processing pathway. Endo- and exonucleolytic reactions are indicated. The known nucleases responsible of the processing reactions are highlighted. For more details on yeast pre-rRNA processing, see [35, 48, 181].

eL29, eL40, eL42, P1 and P2, respectively), which are located at the r-subunit interface (for references, see [78, 125, 140, 257]). As for 40S r-subunits, the sequence of r-protein incorporation into 60S r-subunits has been well conserved in higher eukaryotes [258].

The role of few r-proteins on pre-rRNA processing and ribosome assembly remains undefined or has only been poorly characterised. Among these orphan proteins is L14 (eL14). L14 is an eukaryote-specific r-protein from the 60S r-subunit, which is conserved in some but not all archaea [222, 259]. In addition, eukaryotic L14 contains a specific C-terminal extension, absent in the archaeal orthologues (see [176]), whose role is unknown. L14 forms a eukaryote-specific structure, close to the r-stalk, on the solvent-exposed surface of the 60S r-subunits together with the ES7^{L} and ES39^{L} of domain II and VI of 25S rRNA, respectively, H41 of domain II of 25S rRNA, its interacting r-proteins L6, L9, L16, L20, and its neighbouring r-proteins L7, L32 and L33. (**Figure 2**). Knockdown of *RPL14* expression by

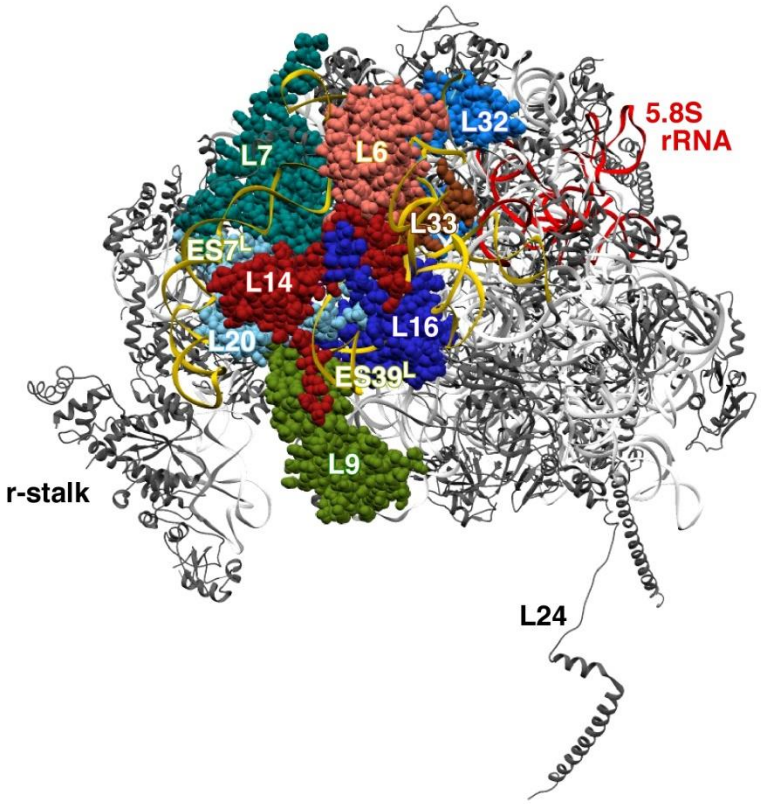

Fig. 2. Molecular environment of L14 in the yeast 60S r-subunit. Position of L14 and its rRNA/protein neighbourhood in the solvent-exposed surface of the yeast 60S r-subunit. The r-proteins L6 (salmon), L7 (cyan), L9 (green), L14 (red), L16 (marine blue), L20 (light blue), L32 (brown) and L33 (middle blue) are shown. The rRNA expansion segments ES7^{L} and ES39^{L} are shown in gold and 5.8S rRNA in red. The remaining 60S r-proteins are coloured in black and rRNA in pale grey. The representation were rendered with UCSF Chimera [193], using the atomic model for the crystal structure of the yeast 80S ribosome at 3.0 Å (PDB ID: 3U5I and 3U5H; [10]). Note that ES7^{L}a is not resolved in this model.

siRNA in human HeLa or HCT116 cancer cells impairs 28S and 5.8S rRNA synthesis and formation of 60S r-subunits [139, 258]. In this study, we have examined the precise role of the otherwise uncharacterised yeast L14 r-protein in ribosome biogenesis. Our data indicate that yeast L14 assembles in the nucleolus within earliest pre-60S r-intermediates. Depletion of L14 causes a shortage of 60S r-subunits, which is due to defective production and accelerated turnover of early and intermediate pre-60S r-particles. Consistently, pulse-chase analyses demonstrate impaired production of mature 25S and 5.8S rRNAs, northern blot hybridization shows mild accumulation of 27SA pre-rRNAs and low steady-state of 27SB and 7S pre-rRNAs, and fluorescence microscopy suggests a defect in the nuclear export of pre-60S r-particles. We have also analysed the impact of the L14 depletion on the protein composition of early pre-60S r-particles, which were affinity-purified using TAP-tagged Noc2 as a bait. Our results clearly show that L14 is required for the stably assembly of a subset of r-proteins, mainly located in its immediate neighbourhood, such as L6, L20 and L33 or surrounding the solvent-exposed part of the peptide exit tunnel such as L17, L26, L37 and L39. L14 is also particularly required for the association of few late-acting ribosome assembly factors, most of them essential for cleavage at site C_2 in ITS2. Finally, we also discuss on the role of the eukaryote-specific C-terminal extension of yeast L14 in ribosome biogenesis and function.

RESULTS

Yeast L14 assembles in the nucle(ol)us within early pre-60S r-particles

Assembly of most r-proteins occurs primarily in the nucle(ol)us, although few ones appear to load preferentially or exclusively in the cytoplasm (reviewed in [78]). No specific information was available on the course of the incorporation of yeast L14 into pre-60S r-particles. We suspect it should occur into the nucleus despite the fact that no nuclear localisation sequence can apparently be predicted in L14 (cNLS mapper programme, [260]; NucPred tool, [261]). Indeed, one of us has previously shown that L14 is included in the broad list of r-proteins that are roughly equally enriched in early to late pre-60S r-particles [125]. Consistently, L14 has been identified at its final location in cryo-EM maps of distinct nuclear pre-60S r-particles (e.g. [153, 262, 263]).

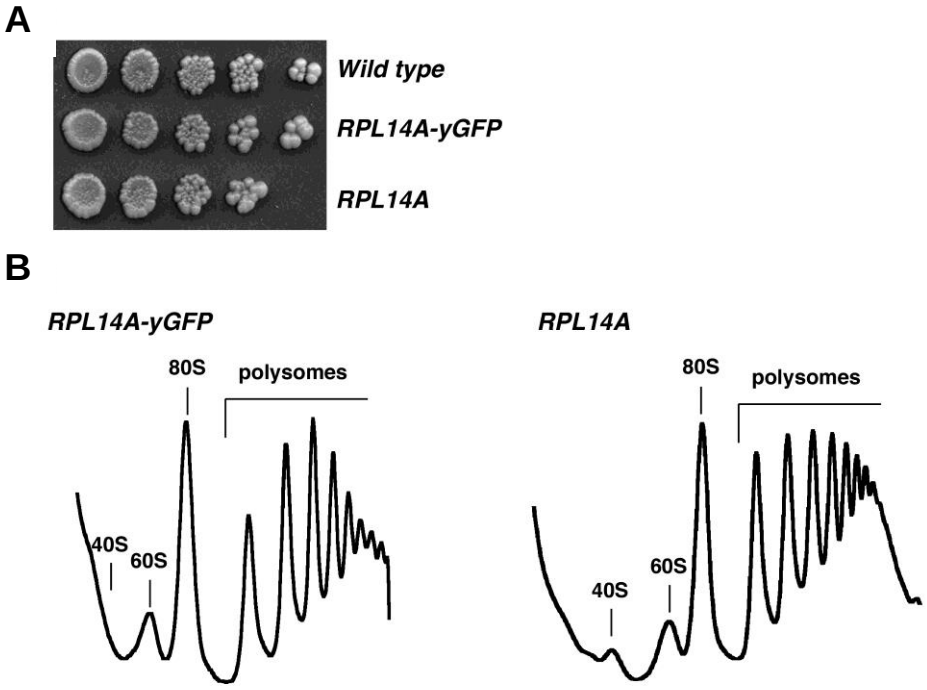

Fig 3. Functional analysis of the L14A-yGFP construct. (A) Strains W303-1B (*Wild type*) and FEY229, which is a *rpl14A*Δ *rpl14B*Δ null strain, expressing either L14A (*RPL14A*) or L14A-yGFP (*RPL14A-yGFP*) from a centromeric YCplac111 plasmid were grown in YPD and diluted to an OD_{600} of 0.05. A 5-fold series of dilutions were performed and 5 μl drops were spotted onto YPD plates. Plates were incubated at 30 ºC for 3 days. **(B)** Polysome profiles of the *RPL14A* and *RPL14A-yGFP* strains. These strains were grown in YPD at 30 ˚C to an OD_{600} of 0.8. Cell extracts were prepared, and 10 A_{260} of each extract were resolved in 7-50% sucrose gradients. The A_{254} was continuously measured. Sedimentation is from left to right. The peaks of free 40S and 60S r-subunits, 80S vacant ribosomes/monosomes, and polysomes are indicated.

To explore in further detail the timing of incorporation of L14 into pre-60S r-particles, we first monitored the localisation of an L14A-yGFP construct upon induction of dominant negative *NMD3-Δ100* allele, which has been proven to trap nascent pre-60S r-particles in the nucleus [264]. The L14A-yGFP construct fully complemented the growth and ribosome biogenesis defects of the null *rpl16AΔ rpl16BΔ* strain (**Figure 3**). As shown in **Figure 4**, L14A-yGFP accumulated in the nucleus of most of the cells examined upon overexpression of the Nmd3-Δ100 protein but it was found in the cytoplasm under non-inducible conditions. No changes in the cytoplasmic distribution of L14A-yGFP was observed upon overexpression of a wild-type Nmd3 protein (**data not shown**).

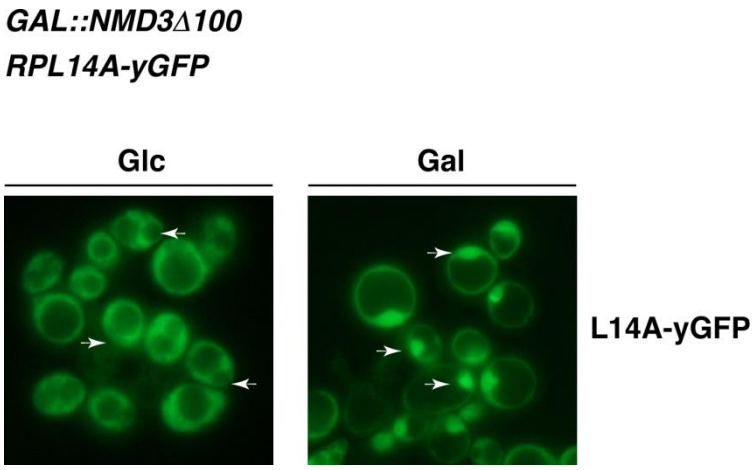

Fig. 4. Nuclear assembly of L14A-yGFP. Localization of L14A-yGFP upon induction of the dominant-negative *NMD3Δ100* allele. Cells of the *rpl14* null strain expressing GFP-tagged L14A as the sole source of L14 was transformed with the pRS316-GAL-NMD3Δ100 plasmid. Transformants were grown in SD-Ura (Glc) or shifted for 12 h to SGal-Ura (Gal) to induce the Nmd3Δ100 protein. The GFP signal was inspected by fluorescence microscopy. Arrows point to nuclei. Approximately 200 cells were examined for the reporter and practically all cells gave the results shown in the representative pictures.

Next, we tested for the presence of L14 within different GFP-affinity purified pre-ribosomal particles on the road of maturation of 60S r-subunits. The specificity of the purification was evaluated by assessing the presence of the selected *trans*-acting factors Nop1, Has1 and Mrt4 by western blot using specific antibodies (**Figure 5**). Western blot analyses also showed that L14 significantly co-enriched with practically all tested particles (**Figure 5**), as did L1, which was used as a control of an early assembling r-protein [125, 166]. In contrast, L10, which has been reported to assemble in the cytoplasm [125, 200], only co-enriched with late and cytoplasmic pre-60S r-particles and P0-GFP-containing particles that correspond mainly to mature ribosomes [134]. Interestingly, L14 seemed not to be as

stably associated with early 90S particles, which were purified using GFP-tagged Pwp2/Utp1 as L16 or L1; similar results to those of L14 were obtained for L6, a r-protein that directly interacts with L14 [265], which was also found even poorer represented in 90S/66S particles purified using GFP-tagged Nop58/Nop5 than L14 (**Figure 5**). Together, these data indicate that L14 assembles in early nucle(ol)ar pre-60S r-particles.

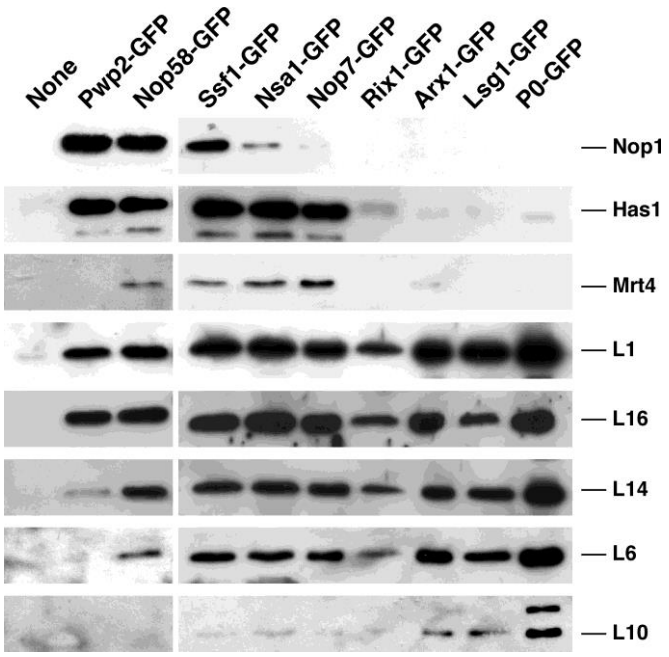

Fig. 5. Association of L14 with maturing 60S r-subunits. 90S and pre-60S r-particles from early to late intermediates were affinity-purified by using the GFP-Trap® immunoprecipitation procedure with the indicated bait proteins. Equivalent amounts of immunoprecipitates were analyzed by 12% SDS-PAGE and western blot analysis. Specific antibodies were used to detect the Nop1, Has1 and Mrt4 *trans*-acting factors and the L1, L6, L10, L14 and L16 r-proteins. Note that the Rix1-GFP and Lsg1-GFP are slightly underloaded. The affinity-purified complexes and all protein signals, except those of L14 and L6, have been previously shown in [137].

In agreement with these results, when we affinity purified L14A-yGFP-containing particles and assayed those pre-rRNA intermediates that co-purified by northern blot hybridization, we detected 27SB and 7S pre-rRNAs clearly above background levels (**Figure 6**). As previously shown for other 60S r-proteins [131, 133, 136], L14A-yGFP also co-purified substantial amounts of mature rRNAs (**Figure 6**). The $27SA_2$ pre-rRNA was also detected, albeit slightly above background levels (**Figure 6**), suggesting that either L14A associates with pre-60S r-particles once cleavage at site A_2 has occurred or more likely that the assembly of L14A is only stabilised after some reorganization of the pre-rRNAs that takes place concomitantly to the formation of 27SB pre-rRNAs. Taken together, all these results suggest that L14 assembles into early pre-60S r-particles and appears to become stable only in those containing the 27SB pre-rRNAs.

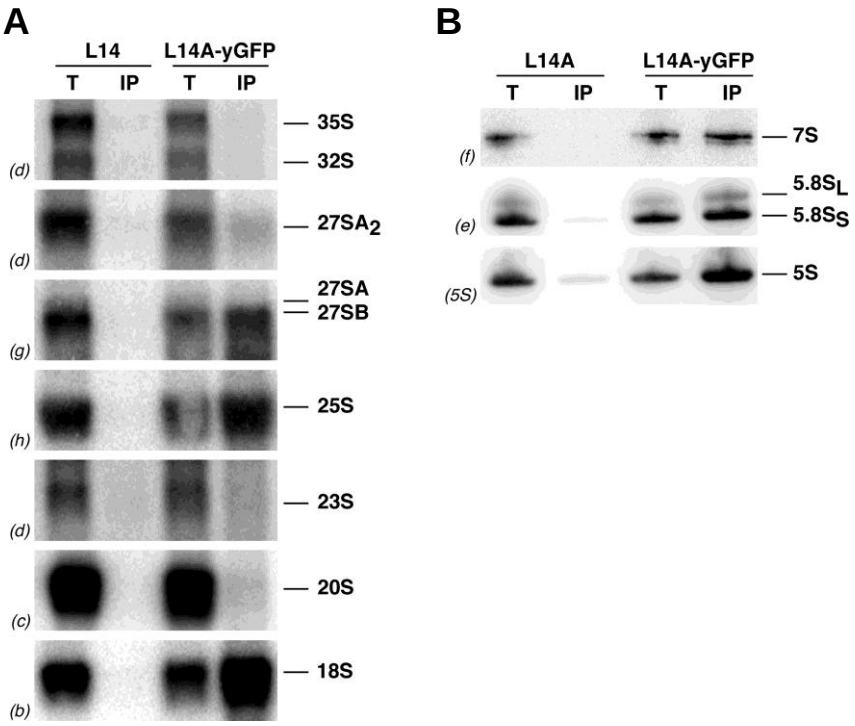

Fig. 6. L14-yGFP stably assembles within pre-60S r-particles containing 27SB pre-rRNAs. Affinity-purification of ribosomal particles was performed from cells expressing L14A-yGFP *via* the GFP-Trap® immunoprecipitation procedure. Wild-type cells (untagged L14) were used as a negative control. Total RNA was extracted from whole cell extracts (T) and immunoprecipitates (IP) and analysed by northern blotting. **(A)** Northern blot analysis of high-molecular-mass or **(B)** low-molecular-mass pre- and mature rRNAs. The indicated probes, between parentheses, were used to detect the different pre- and mature rRNA species (see Fig. 1A and Table 3).

L14 is required for normal accumulation of 60S ribosomal subunits

L14, as most r-proteins (e.g. [266]), is essential for cell viability, and is encoded by two different paralogous genes, *RPL14A* and *RPL14B*. Deletion of *RPL14A* caused a severe defect on growth, while deletion of *RPL14B* led to a minor growth defect (**Figure 7A**, see also [266]). These defects seemed to be exacerbated at lower temperatures (**Figure 7A**). As shown in **Figure 7B**, both deletions led to polysome profiles alike to those for mutants showing a deficit on the content of 60S r-subunits. Thus, for the profiles of both deletion strains, we observed a decrease in the amount of free 60S r-subunits relative to free 40S r-subunits and the appearance of half-mer polysomes. The overall defects were apparently more pronounced for the *rpl14A*Δ than for the *rpl14B*Δ null strain. These data are in agreement with those previously described by [176].

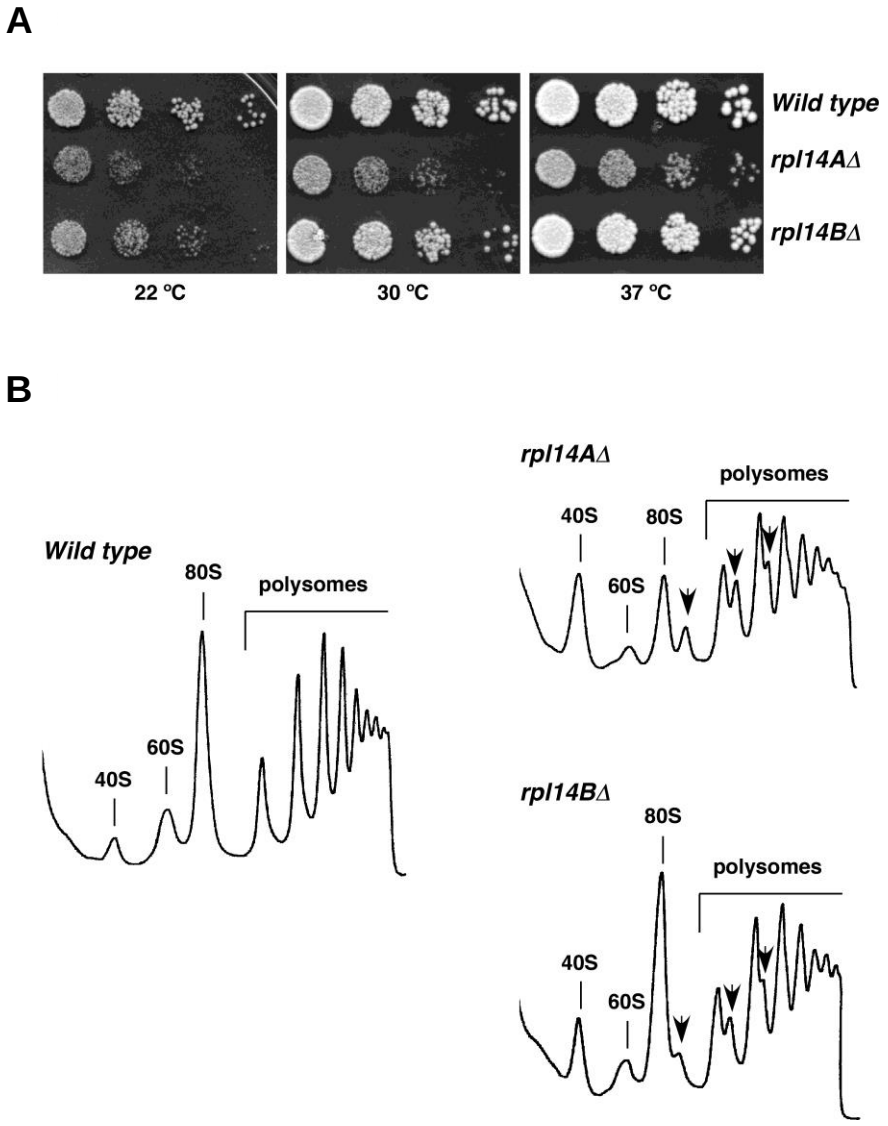

Fig 7. Deletion of either *RPL14A* or *RPL14B* leads to a deficit in 60S r-subunits. (A) Growth phenotypes of the *rpl14A* and *rpl14B* null mutants. Strains W303-1B (*Wild type*), FEY204 (*rpl14AΔ*), FEY203 (*rpl14BΔ*) were grown in YPD and diluted to an OD_{600} of 0.05. A 5-fold series of dilutions were performed and 5 μl drops were spotted onto YPD plates. Plates were incubated at 22 ºC, 30 ºC and 37 ºC for 3 days. **(B)** Polysome profiles of the above strains. These strains were grown in YPD at 30 ºC to an OD_{600} of 0.8. Cell extracts were prepared, and 10 A_{260} of each extract were resolved in 7-50% sucrose gradients. The A_{254} was continuously measured. Sedimentation is from *left* to *right*. The peaks of free 40S and 60S r-subunits, 80S vacant ribosomes/monosomes, and polysomes are indicated. Half-mers are labeled by arrows.

For the phenotypic analysis of the complete loss-of-function of L14, we constructed a conditional strain, named *GAL::RPL14* strain, that expressed a double HA-tagged variant of L14A as the sole source of L14 under the control of a *GAL* promoter. This strain grew as the

isogenic wild-type strain or a isogenic *GAL::RPL16* control strain (see [137]) on YPGal plates but was unable to grow on YPD plates (**Figure 8A**). After shifting a culture of the

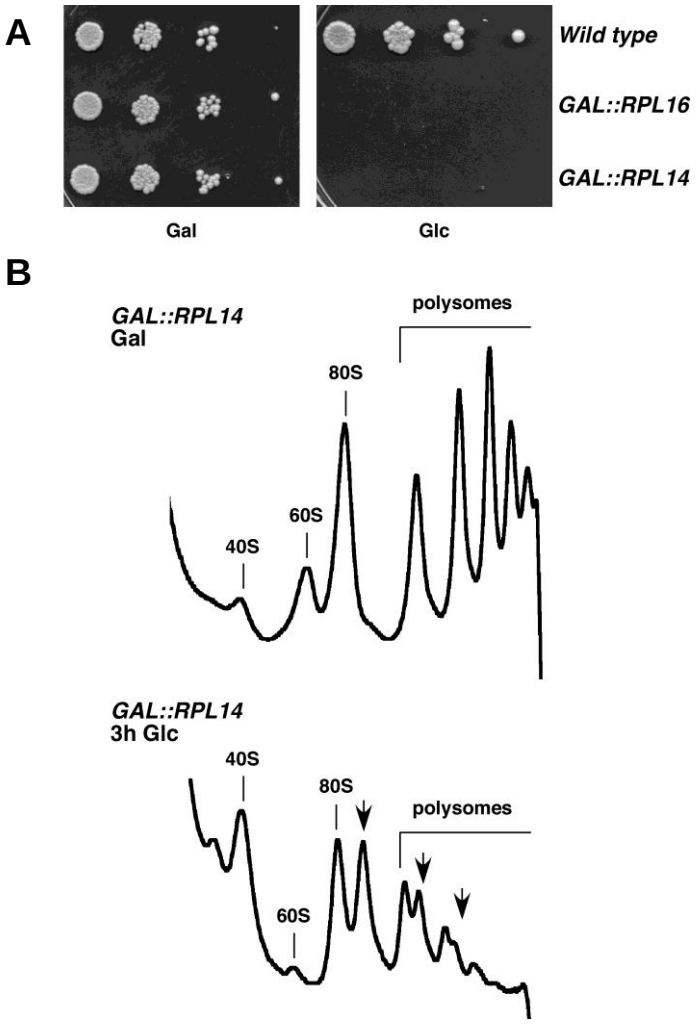

Fig. 8. Depletion of L14 results in a deficit in 60S r-subunits. (A) Growth comparison of the strains W303-1B (*Wild type*), FEY251 [pAS24-RPL16B] (*GAL::RPL16*) and FEY229 [pAS24-RPL14A] (*GAL::RPL14*). The cells were grown in YPGal and diluted to an OD_{600} of 0.05. A 5-fold series of dilutions were performed and 5 μl drops were spotted onto YPGal (Gal) and YPD (Glc) plates. Plates were incubated at 30 ºC for 3 days. Note that the growth of wild-type and *GAL::RPL16* strains has been previously shown in [137]. **(B)** Polysomes profile analysis of *GAL::RPL14* cells grown in YPGal (Gal) or shifted to YPD (Glc) for 3 h. Cells were harvested at an OD_{600} of around 0.8, whole cell extracts were prepared and 10 A_{260} units of each extract were resolved in 7-50% sucrose gradients. The A_{254} was continuously measured. Sedimentation is from *left* to *right*. The peaks of free 40S and 60S r-subunits, 80S vacant ribosomes or monosomes and polysomes are indicated. Half-mers are labelled by arrows.

GAL::RPL14 strain from liquid YPGal to YPD medium, the rate of cell division slowed down significantly in few hours and practically stopped after 8-10 h in YPD (**data not shown**). When we analysed polysome profiles from cell extracts of the *GAL::RPL14* strain grown in

YPGal, normal wild-type profiles were obtained (**Figure 8B**). However, when shifted for about 3 h to YPD, extracts showed abnormal polysome profiles, consisting of a clear decrease in the levels of free 60S *versus* free 40S r-subunits, a decrease in the 80S peak and polysomes and the appearance of half-mer polysomes (**Figure 8B**). Taken together, these results indicate that L14 is essential for growth and for normal accumulation of 60S r-subunits.

L14 is required for 27S pre-rRNA processing and normal production of 25S and 5.8S rRNAs

To study whether the deficit of 60S r-subunits caused by the depletion of L14 is attributed to a defective production or/and an excessive degradation of 60S r-subunits, we analysed the effects of L14 depletion on the synthesis and processing of pre-rRNAs by [^{3}H]uracil pulse-chase labelling experiments. For this purpose, the *GAL::RPL14* and an isogenic wild-type control strain were grown in YPGal and shifted to SD-Ura for 6 h. In wild-type cells, the 35S pre-rRNA was processed rapidly into 32S pre-rRNA, and then into 27S and 20S pre-rRNAs, which were subsequently converted into mature 25S and 5.8S, and 18S rRNAs, respectively (**Figure 9**). In contrast, in the *GAL::RPL14* strain, processing of the 35S pre-rRNA was delayed; as a consequence, less 27SA and 20S pre-rRNAs were formed and traces of 23S pre-rRNA were detected, but while enough mature 18S rRNA was still made, some 27SB pre-rRNAs persisted even after the 60 min of chase and practically no labelled mature 25S and 5.8S rRNAs were detected (**Figure 9**). These defects were apparently specific since no changes in the kinetics of production of mature 5S rRNA or tRNAs or their levels were observed upon the depletion of L14 (**Figure 9**). These results indicate that the deficit in 60S r-subunits following depletion of L14 was due to impaired processing and increased turnover of 27SB pre-rRNAs. As a consequence, reduced levels of both mature 25S and 5.8S rRNAs were synthesized. Most likely as a side effect (for further discussion, see [137] and references therein), earlier processing reactions at sites A_0, A_1 and A_2 were also delayed upon depletion of L14; however, this delay impacted only slightly 18S rRNA production.

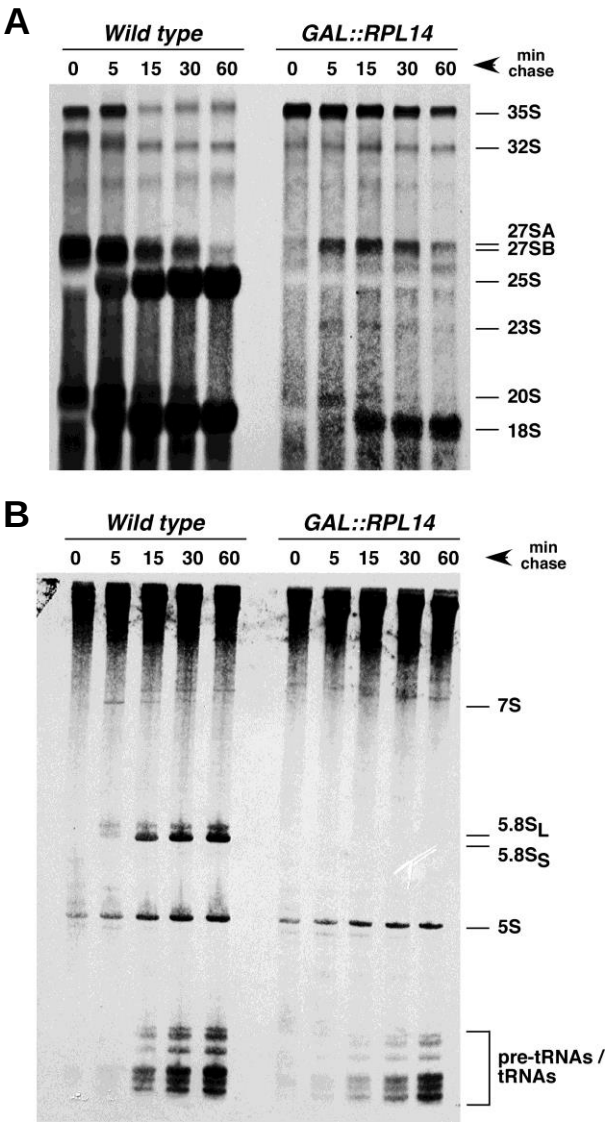

Fig. 9. Depletion of L14 impairs 27S pre-rRNA processing. (A) Wild-type strain W303-1B (*Wild type*) and FEY229 [pAS24-RPL14A] (*GAL::RPL14*) were transformed with YCplac33 (*CEN URA3*), grown at 30 ºC in SGal-Ura to mid log phase and shifted to SD-Ura for 6 h. Cells were pulse-labelled with [5,6-^{3}H]uracil for 2 min followed by a chase with a large excess of unlabelled uracil for the times indicated. Total RNA was extracted from each sample and 20,000 cpm was loaded and separated on **(A)** a 1.2% agarose-6% formaldehyde gel or **(B)** a 7% polyacrylamide-8M urea gel, transferred to nylon membranes and visualized by fluorography. The positions of the different pre- and mature rRNAs are indicated.

Depletion of L14 affects negatively 27S pre-rRNA processing

To define the exact pre-rRNA processing steps that are affected upon depletion of L14, we evaluated changes in the steady-state levels of mature rRNA and pre-rRNA intermediates. For this purpose, total RNA was isolated from the *GAL::RPL14* and an isogenic wild-type control strain grown in YPGal or at various time points after a shift to YPD and analysed by northern blotting and primer extension.

As shown in **Figure 10A**, and consistently with the pulse-chase data, depletion of L14 resulted in a minor decrease in 18S rRNA and in a more drastic decrease in 25S rRNA. Slight changes in the levels of different pre-rRNAs were observed for the wild-type strain grown in YPGal or shifted to YPD, which are most likely due to the effects of the nutritional up-shift from the galactose- to the glucose-containing medium [267]. More significant differences were observed for the *GAL::RPL14* strain, thus, 35S and aberrant 23S pre-rRNAs progressively accumulated with ongoing depletion of L14. However, while levels of

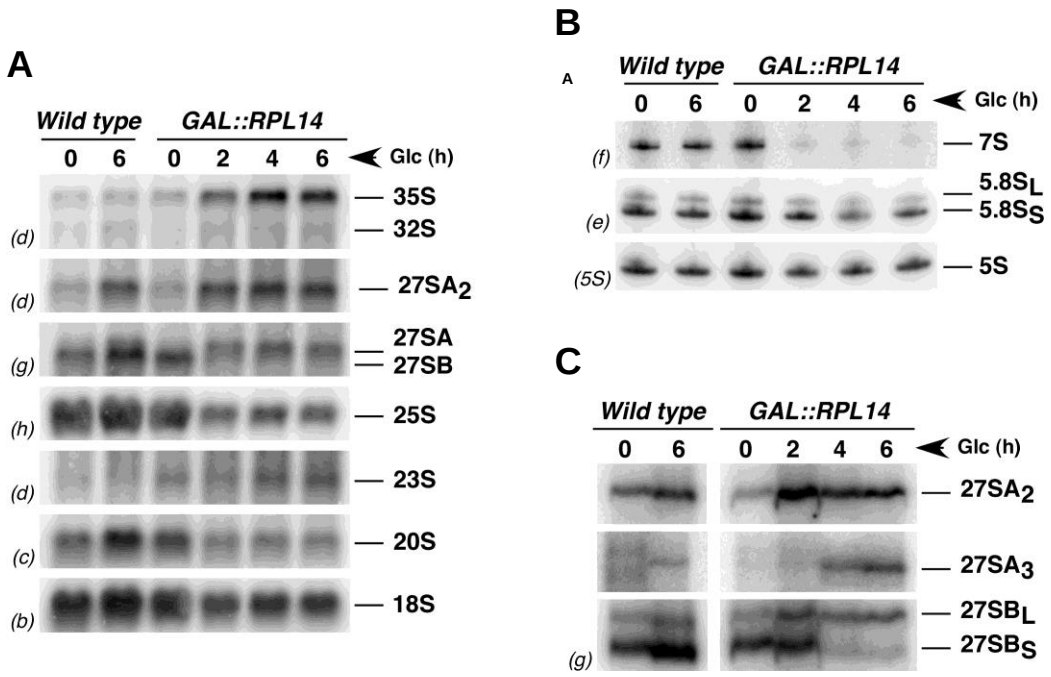

Fig. 10. Depletion of L14 affects the steady-state levels of pre-rRNA and mature rRNA species. Strains W303-1B (*Wild type*) and FEY229 [pAS24-RPL14A] (*GAL::RPL14*) were grown at 30 ºC in liquid YPGal medium and shifted to YPD. Total RNA was extracted from the cultures at the indicated times after the shift and equal amounts (5 µg) were subjected to northern hybridization or primer extension analysis. **(A)** Northern blot analysis of high-molecular-mass or **(B)** low-molecular-mass pre- and mature rRNAs. Probes, between parentheses, are described in the Fig. 1A and Table 3. **(C)** Primer extension analysis with probe g, which is complementary to sequences in ITS2 (Fig. 1A). This probe allows detection of $27SA_2$, $27SA_3$, and both 27SB pre-rRNAs.

20S pre-rRNA mildly decreased, those of $27SA_2$ pre-rRNA initially accumulated but, then, remained apparently unaffected 6 h after transfer to YPD. In contrast, the levels of 27SB pre-rRNAs clear decreased. Analysis of low-molecular-weight rRNAs revealed a significant decrease in the steady-state levels of 7S pre-rRNAs, a slight reduction in those of mature 5.8S rRNAs, but no alteration in the levels of 5S rRNA in the L14-depleted strain (**Figure 10B**). Importantly, the ratio of $5.8S_L$ *versus* $5.8S_S$ rRNA was not affected by the depletion of L14.

We also performed primer extension assays to identify $27SA_3$ pre-rRNA and to distinguish between $27SB_L$ and $27SB_S$ pre-rRNAs. As shown in **Figure 10C**, primer extension did not shown any differences in the levels of $27SA_2$ pre-rRNA, fully consistent with the results obtained by northern hybridisation. However, a clear but mild accumulation of $27SA_3$ pre-rRNA was observed upon depletion of L14. Moreover, we could also observe a slight accumulation of $27SB_L$ pre-rRNA and a significant reduction in $27SB_S$ pre-rRNA levels with ongoing depletion of L14. Altogether, these results indicate that L14 is required for processing of $27SA_2$ and $27SA_3$ pre-rRNAs to 27SB pre-rRNA species. In addition, the presence of L14 in pre-60S r-particles is needed for the stability of 27SB precursors. Thus, although $27SB_L$ pre-rRNA is still made in L14-depleted cells, it fails to be converted to $7S_L$ pre-rRNA and consequently degraded. In these circumstances, the $27SB_S$ pre-rRNA is even less stable than the $27SB_L$ pre-rRNA and, therefore, it could neither be converted into its subsequent $7S_S$ pre-rRNA.

Depletion of L14 leads to nuclear retention of pre-60S ribosomal particles

Among the distinct phenotypes of most loss-of-function mutants in 60S r-subunit assembly factors and/or 60S r-proteins that lead to an impairment of pre-rRNA processing are the failure in nuclear export of pre-60S r-particles (e.g. [131, 175, 268]). Thus, to test whether depletion of L14 impairs 60S r-subunit export, we studied the localisation of a GFP-tagged L25 r-protein upon depletion of L14. It has been well established the use of the L25-eGFP reporter to trace the nucleo-cytoplasmic transport of 60S r-subunits by fluorescence microscopy [136, 220, 269]. As shown in **Figure 11**, and as expected for an r-protein, a predominantly cytoplasmic distribution of L25-eGFP with vacuolar and nuclear exclusion was observed in *GAL::RPL14* cells grown to early log phase in selective SGal medium. However, *GAL::RPL14* cells shifted to selective SD medium exhibited an accumulation of the reporter in the nucleus, as denoted by its colocalisation with the red fluorescently tagged Nop1 marker. In many cells, the GFP-decorated region mostly coincided with the RFP-decorated one, thus, indicating that L25-eGFP was mainly accumulated in the nucleolus. We did not observe nuclear accumulation of L25-eGFP when the isogenic wild-type control strain was grown in selective SD medium (**data not shown**). Taken together, these results indicate that upon depletion of L14, both intranuclear transport from the nucleolus to the nucleoplasm and nucleocytoplasmic export of pre-60S r-particles are blocked.

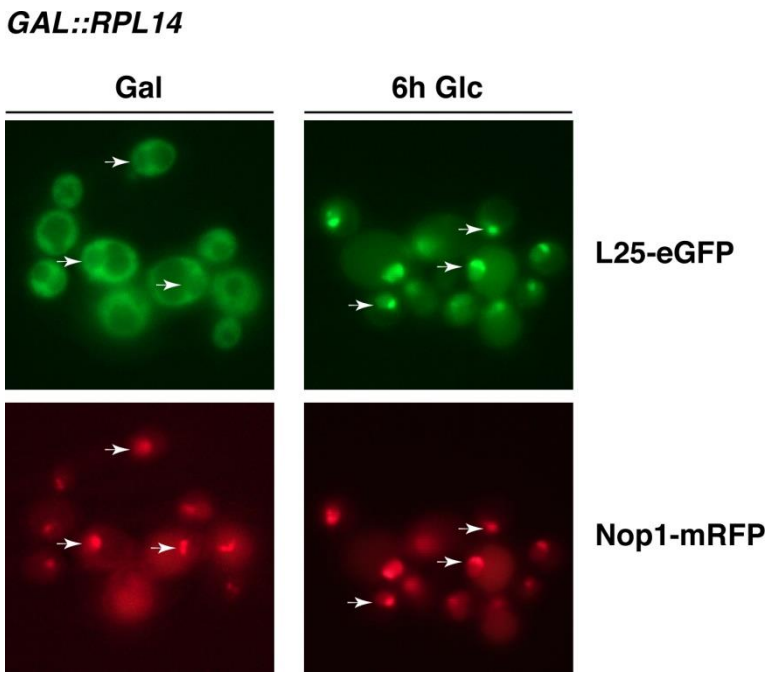

Fig. 11. Depletion of L14 results in retention of pre-60S r-subunits in the nucle(ol)us. FEY229 [pAS24-RPL14A] (*GAL::RPL14*) cells co-expressing the nucleolar Nop1-mRFP and the 60S r-subunit reporters were grown in SGal-Trp (Gal) or shifted to SD-Trp up to 6 h. The subcellular localization of the GFP-tagged r-protein and the NOP1-mRFP marker was analysed by fluorescence microscopy. Arrows point to nucleolar fluorescence. Approximately 200 cells were examined for each reporter, and practically all cells gave the results shown in the pictures.

L14 is required for the stable assembly of 60S r-proteins located at its immediate neighbourhood and surrounding the polypeptide exit tunnel

To further study the role of L14 in 60S r-subunit biogenesis, we determine how the depletion of L14 affected the assembly of other 60S r-proteins to pre-60S r-particles. For this purpose, we chromosomally TAP-tagged Noc2 in the *GAL::RPL16* strain, affinity purified TAP-tagged Noc2-containing pre-ribosomal particles in the presence of L14 or upon its depletion, and compared the rRNA and protein composition in both conditions. Noc2 is an early 60S r-subunit assembly factor present in early to intermediate pre-60S r-particles that apparently weakly associates with 90S pre-ribosomal particles and dissociated from particles before or concomitantly with 27SB pre-rRNA processing at site C_2 [92, 125, 270]. In both conditions, before or after depletion of L14, Noc2-TAP co-purified early to intermediates pre-60S r-particles with similar efficiency; pre-rRNA content of these particles was in consistence to the relative abundance of the same pre-rRNAs in the total cell extracts of the undepleted or L14-depleted cells; thus, enlarged co-purification of 35S pre-rRNA and reduced co-purification of 27SB pre-rRNA with Noc2-TAP was observed upon depletion of L14 (see

Figure 10; **data not shown**). We also compared changes in protein composition of TAP-tagged Noc2-containing particles purified from L14-depleted *versus* L14-undepleted cells focusing first in the category of r-proteins. As shown in **Figure 12A**, and as expected, L14 itself was the r-protein whose levels most severely diminished. Levels of about a dozen of other different r-proteins were also mild but significantly reduced upon depletion of L14. These proteins can be classified into different groups: (i) L6, L16, L20 and L33 r-proteins, which all belong to the neighbourhood area of L14. L14 direct interacts with L6, L9, L16 and L20 r-proteins [10, 265], but while L6 and L20 appeared substantially underrepresented, L9 could not be detected in our analysis, and strikingly, L16 was very minor affected upon depletion of L14 (see Discussion). All these r-proteins are involved in early steps of 60S r-subunit assembly and their respective depletion led to practically identical pre-rRNA processing defects to those we have described for the depletion of L14 [140, 175, 192]. (ii) L17, L19, L26, L37 and L39, which all located around the polypeptide exit tunnel or its nearby region [10]. All these proteins are middle-acting r-proteins required for 27SB pre-rRNA processing ([131, 133, 136, 175] and our unpublished results). (iii) A miscellaneous group composed by L1 (uL1), L2, L28 (uL15), L34 (eL34) and L36 (eL36). Remarkably, L28 and L36 interact each other directly in the mature 60S r-subunit [10, 265], and L34 and L36 form part of the same functional network of the *trans*-acting factor Ebp2 [271]. Depletion of L36 leads to practically identical pre-rRNA processing defects than depletion of L14 [271]. In turn, L34 is required for 27SB pre-rRNA processing [175]. (iv) L10 and L24, which, as mentioned above, assembles in the cytoplasm [78]. Decreased representation of these two r-proteins upon depletion of L14 could likely be the artefactual result of some minor mature 60S r-subunit contamination after Noc2-TAP purification from L14-undepleted extracts.

In turn, levels of several other r-proteins significantly increased with Noc2-TAP purified complexes upon depletion of L14. These include many early-acting r-proteins such as L3, L7, L8, L13, L15, L18 or L32, the r-proteins components of the 5S rRNP (L5 and L11), and the r-stalk protein P0 (uL10) and its base L12 (uL11). Likely, these proteins either assemble earlier than L14 into pre-60S r-particles (i.e. L3), thus, not being affected by the depletion of L14 or belong to ribosomal modules whose assembly occur regardless of the presence or the absence of L14 in pre-ribosomal particles.

Together, these results indicate that L14 contributes to the optimal formation of an early pre-ribosomal structure that comprises mostly those r-proteins located at the central solvent interface of 60S r-subunits and the adjacent region surrounding the polypeptide exit (see **Figure 13**). All these r-proteins are either involved in $27SA_2$ and $27SA_3$ pre-rRNA processing reactions as L14 or in the immediately downstream step of 27SB pre-rRNA processing.

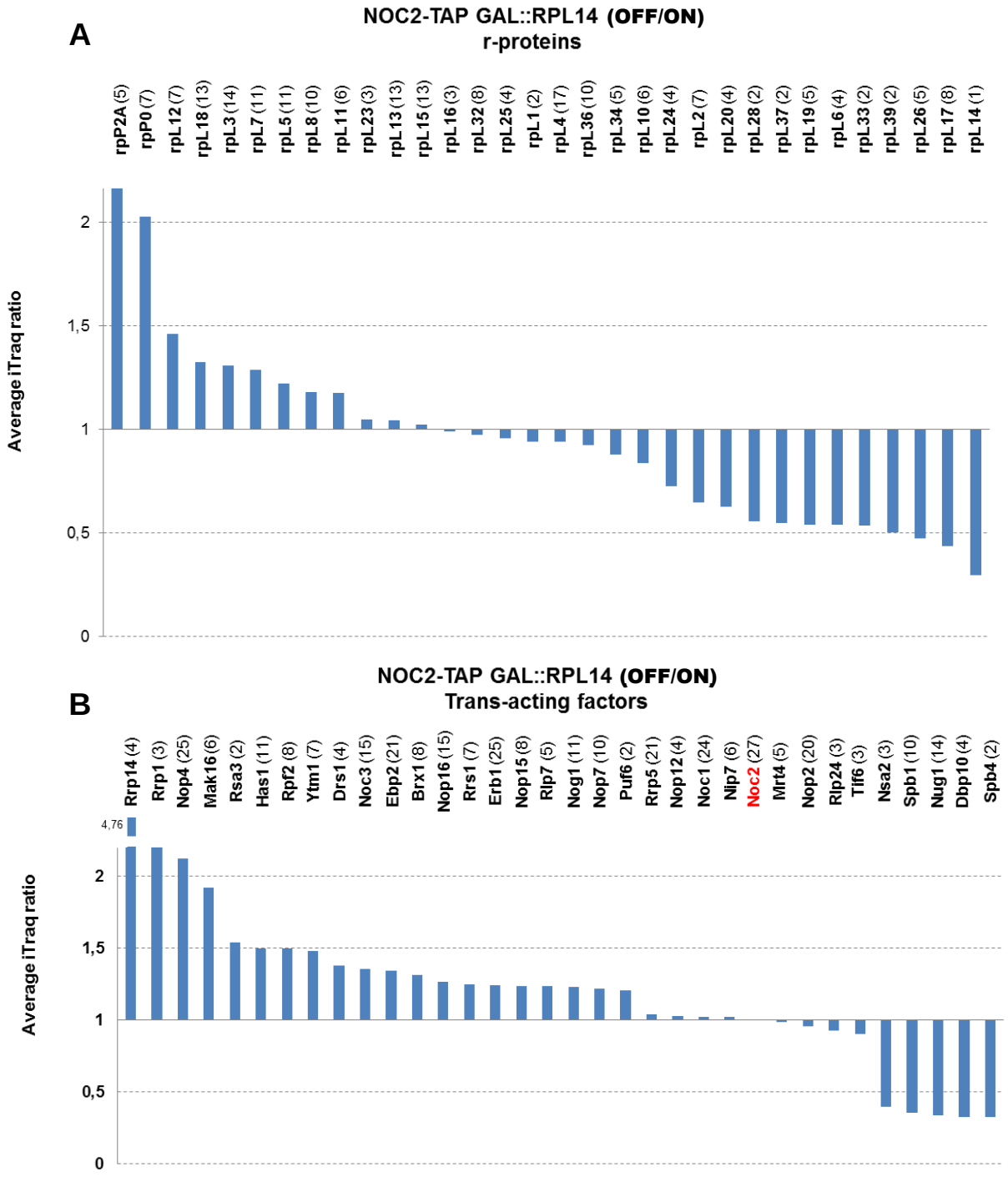

Fig. 12. Changes in composition of pre-ribosomal particles upon depletion of L14. FEY320 strain, which expresses a genomic *NOC2-TAP* allele from its cognate promoter and harbour a plasmid-borne *HA-RPL14A* allele driven by the *GAL1-10* promoter was cultivated at 30 ºC in YPGal and shifted to YPD for 6 h to shut down the expression of L14. Whole cell extracts were done for each condition, complexes associated to Noc2-TAP affinity purified and the co-purifying proteins processed for comparative protein analysis by semiquantitative mass spectrometry using iTRAQ (see Experimental Procedures). Average iTRAQ ratios of all respective proteins identified by more than one peptide are indicated. Numbers in parentheses indicate the number of peptides by which the respective protein was identified. (**A**) Relative enrichment/deprivation of r-proteins purified before or after depletion of L14. (**B**) Relative enrichment/deprivation of *trans*-acting factors purified before or after depletion of L14.

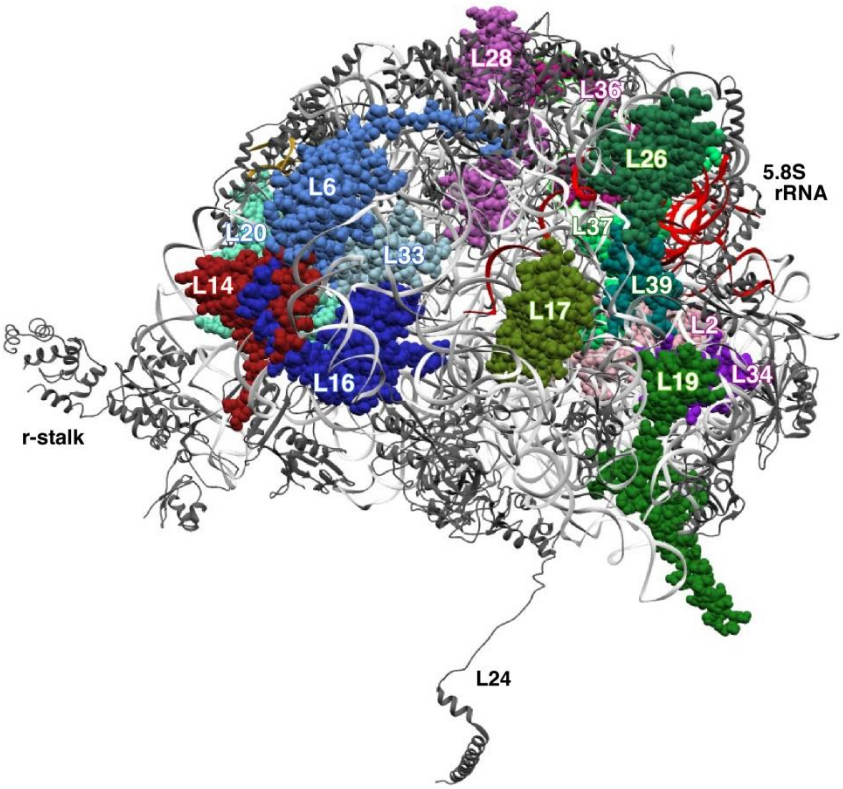

Fig 13. Ribosomal proteins that significantly diminish from Noc2-TAP containing pre-ribosomal particles upon depletion of L14. Different subset of r-proteins are shown: (i) L14 (red), (ii) L6, L16, L20, L33 (different blue tones), which are r-proteins nearby L14 that fail to associate upon depletion of L14. (iii) L17, L19, L26, L37 and L39 (different green tones), which are r-protein that surround the polypeptide exit tunnel. (iv) L28, L36, L34 and L2 (different pink tones). 5.8S rRNA was coloured in red and 5S in gold. Note that a structure for any early pre-60S r-particles has still not been determined. Thus, r-proteins were represented using the atomic model for the crystal structure of the yeast 80S ribosome at 3.0 Å (PDB ID: 3U5I and 3U5H; [10]).

L14 is required for the stable association of a set of 60S r-subunit biogenesis factors required for processing of 27SB pre-rRNA

We also determine how the depletion of L14 affected the association of *trans*-acting factors to Noc2-TAP affinity-purified pre-ribosomal particles. As shown in **Figure 12B**, very few factors diminished to a different extent. Most of these factors (also known as B-factors), Spb4, Dbp10, Spb1, Nsa2, Tif6, Nip7, Nop2 and Rlp24, are required for 27SB pre-rRNA processing, thus for cleavage at site C_2 within ITS2 [146, 160, 212, 272-277]. Dbp10, Tif6, Rlp24 are among the subset of factors required to recruit Nsa2 to pre-60S r-particles [272]. Nip7 and Nop2 form a heterodimer [272]. Nug1, which is apparently not a B-factor, genetically interacts with and is required for the stable association of Dbp10 with pre-ribosomal particles [278, 279].

Few other factors required for 27SB pre-rRNA processing are enriched upon depletion of L14, among them, Nog1 and the physical and functional related pair of factors Rpf2 and Rrs1 [130], which guides assembly of the 5S rRNP (see [255], and references therein). The significance of the enrichment of Rrp14, Nop4, Nop16, Rsa3, Puf6 and Noc3 is still unclear, although it has been described that Rrp14 delays 27SB pre-rRNA processing and interacts with Epb2 in a two-hybrid assay [280]. Remarkably, practically all A_3-factors so far described were found among the proteins that enriched upon depletion of L14: Has1, Drs1, Rrp1, Nop12, Brx2, Epb2, Nop7, Ytm1, Erb1, Nsa3/Cic1, Nop15 and Rlp7 (for details, see [30]). Depletion of any of these factors leads to defect in $27SA_3$ pre-rRNA processing (e.g. [132]), phenotype that it is the most significant feature of the L14 depletion (see **Figure 10C**). It has been shown that factors Nop7, Ytm1 and Erb1 form a stable sub-complex to which Drs1 associates [281, 282]. This sub-complex together with Nsa3, Nop15 and Rlp7 has been described to be mutually interdependent for association with pre-60S r-particles [132]. Has1 interacts with Nop15 in a two-hybrid assay [283].

In conclusion, depletion of L14 prevents stable association of a set of factors required for 27SB pre-rRNA processing with early pre-60S r-particles. Consequently, these particles are unable to progress in their maturation at ITS2 of the pre-rRNAs. In contrast, these particles still associate with most factors required for $27SA_3$ pre-rRNA processing, but strikingly, they are also unable to support this pre-rRNA processing reaction, as evidenced for the pre-rRNA processing defects observed for a L14-depleted strain. Likely as the direct consequence of these impairments, early pre-60S r-particles are subjected to nuclear retention and efficient turnover following depletion of L14.

Disruption of the interaction between the eukaryote-specific C-terminal extensions of L14 and L16 r-proteins causes paromomycin hypersensitivity

In both late pre-60S r-particles and mature 60S r-subunits, an interaction between the most distal α-helices of the eukaryote-specific C-terminal extensions of L14 and L16 is produced. This interaction is maintained by apolar contacts between amino acids of both helices and two salt bridges, one between the carboxylic group of L14[A138] and the ε-amino group of L16[K177] and another between the guanidinium group of L14[R109] and the carboxylic group of L16[Y199] (**Figure 2**). To study the relevance of this interaction in cell growth and ribosome biogenesis, we tested the genetic interaction between two distinct and previously reported truncated alleles: *rpl14A-L123**, which expressed a truncated L14A variant lacking the last 16 amino acids [176] and *rpl16B-N180*, which expressed a truncated L16B variant lacking the last 18 amino acids [137]. These two alleles confer a practically

wild-type phenotype at 30 ºC but a 60S r-subunit deficit when expressed as the sole copy of each respective r-protein in yeast cells [137, 176] (see also **Figure 14A**). Moreover, combination of these two alleles as the sole sources of L14 and L16 in double mutant cells did not cause any synergistic growth defect phenotype in either rich or synthetic media at either 30 ºC, 37 ºC or 22 ºC (**Figure 14A** and **data not shown**), and both protein variants were expressed to wild-type levels (**Figure 14B**). Interestingly, the double mutant but neither of the single ones displayed increased sensitivity to paramomycin (**Figure 14A**). This observation suggest that, despite, its practically wild-type growth rate at 30 ºC, cells lacking the most distal parts of the C-terminal extensions of L14 and L16 produce 60S r-subunits that might be enough structurally abnormal to manifest slight dysfunctions when subjected to certain stresses, such as the presence of distinct antibiotics that inhibit translation.

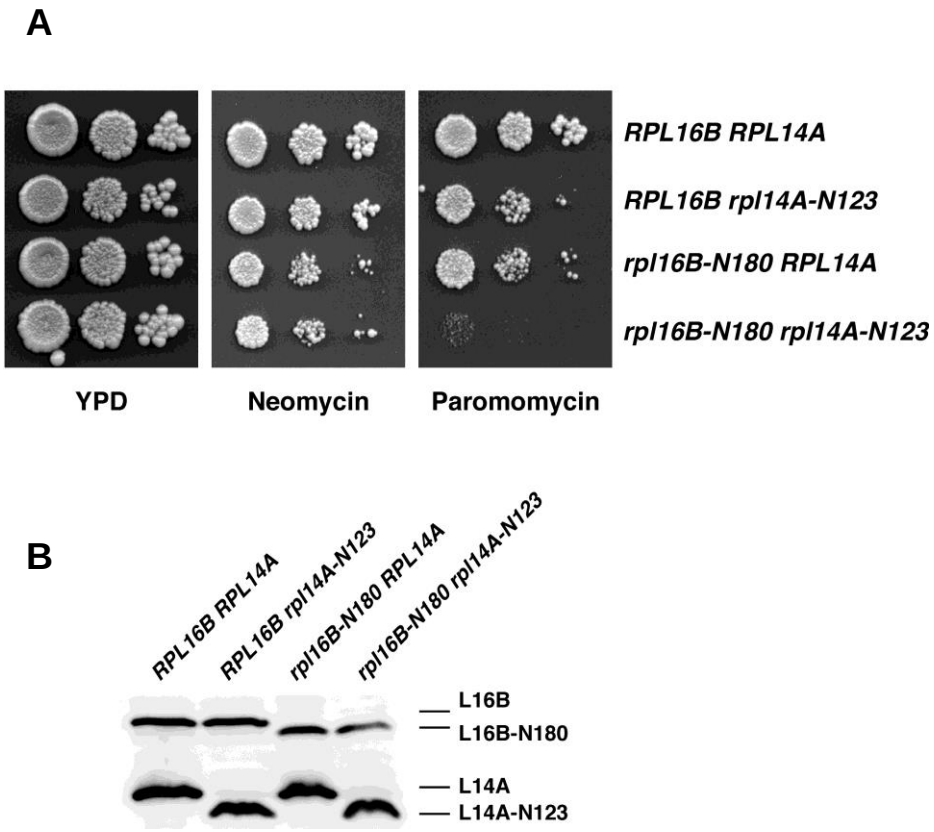

Fig. 14. The *rpl14A-N123 rpl16B-N180* mutant is hypersensitive to paromomycin. (A) Growth phenotypes of the indicated strains on YPD plates without antibiotics or containing 5 mg/ml neomycin or 1 mg/ml paromomycin. A triple *rpl14A*Δ *rpl14B*Δ *rpl16A*Δ null mutant containing the indicated combinations of plasmid-borne *RPL14A and rpl14A-N123 allele and genomic RPL16B* and *rpl16B-N180* alleles as sole sources of L14 and L16 respectively, were grown in YPD medium and spotted in 10-fold serial dilution steps onto YPD plates with or without the indicated antibiotics. Plates were incubated at 30 ºC for 3 days. **(B)** Expression levels of the plasmid-borne wild-type and indicated mutant alleles of both *RPL14A* and *RPL16B* genes as sole sources of L14 and L16. Equivalent amounts of cell extracts of the above strains were separated by SDS-PAGE and levels of the L14 and L16 r-proteins variants were determined by western blot analysis using specific anti-L14 and anti-L16 antibodies.

EXPERIMENTAL PROCEDURES

Strains and microbiological methods

The *S. cerevisiae* strains used are listed in **Table 1** and are derived from W303 [206]. The deletion disruption of the *RPL14A* and *RPL14B* genes and the C-terminal TAP-tagging of *NOC2* at the genomic locus were performed as previously described [125, 207, 284]. FEY204 (*rpl14A*::HIS3MX6) and FEY203 (*rpl14B*::HIS3MX6) are meiotic segregants of the corresponding diploid strains. To construct the *GAL::RPL14* strain, FEY203 and FEY204 were crossed and the resulting diploid transformed with the YCplac33-RPL14A plasmid. After sporulation and tetrad dissection, we selected the FEY229 strain, which is a representative double *rpl14A*Δ *rpl14B*Δ mutant that contains YCplac33-RPL14A. Then, FEY229 was transformed with the pAS24-RPL14A plasmid, and subsequently, YCplac33-RPL14A was counter-selected on 5-FOA plates containing galactose. The correct genomic integration of the *TAP-URA3* cassette in the FEY320 strain was verified by PCR and the expression of the Noc2-TAP fusion protein by western blot analysis. Strains JFY136 and JFY137 are also meiotic segregants; YKL516 and JFY01 were crossed, the resulting diploid was sporulated, and tetrads were dissected. In spore clones with the appropriate markers, the presence of the wild-type or mutant variant alleles of *RPL14A/B* and *RPL16A/B* genes were analysed by PCR. The expression of the wild-type L14A and L16B or the truncated variants L14A-N123 and L16B-N180 proteins was tested by western blot analysis.

Strains were grown at selected temperatures either in rich YP medium (1% yeast extract, 2% peptone) supplemented with 0.2% adenine and containing either 2% glucose (YPD) or 2% galactose (YPGal) as carbon source or in synthetic minimal medium (0.15% yeast nitrogen base, 0.5% ammonium sulphate) supplemented with the appropriate amino acids and bases as nutritional requirements, and containing either 2% glucose (SD) or 2% galactose (SGal) as carbon source. Preparation of media and genetic manipulations were done according to established procedures. Antibiotic-containing plates were prepared by adding the drugs from stocks solution into 2% YPD-agar medium before pouring the plates [133]. Yeast cells were transformed by the lithium acetate method [208]. Tetrad dissections were performed using a Singer MS micromanipulator.

Plasmids

All recombinant DNA techniques were done according to established procedures using *E. coli* DH5α for cloning and propagation of plasmids. Plasmids used in this study are listed in **Table 2**. To construct YCplac33-RPL14A, YCplac111-RPL14A, pAS24-RPL14A and

YCplac111-RPL14A-yGFP, specific DNA fragments were PCR-amplified using yeast genomic DNA as a template and the appropriate oligonucleotides. The oligonucleotides used in this study are listed in **Table 3**. After restriction digestion, the PCR products were cloned into the respective vectors. All cloned DNA fragments generated by PCR were verified by sequencing. Detailed information on the plasmids is available upon request. YCplac22-RPL14A and YCplac22-rpl14A-N123, a generous gift from D. Kressler, have been previously reported [176]. Other plasmids used in this study were: pRS314-RPL25-eGFP-NOP1-mRFP and pRS314-RPS3-eGFP-NOP1-mRFP, gifts from J. Bassler and E. Hurt, [210] and pRS316-GAL-NMD3Δ100, gift from A. Jacobson [285].

Polysome profile analyses

Cell extracts for polysome proflle analyses were performed as described previously [211]. 7-50% sucrose gradients were centrifuged at 39,000 rpm in a Beckman Coulter rotor SW41 Ti at 4 ºC for 2 h 45 min and fractionated using a Teledyne-ISCO UA-6 system with continuous monitoring at A_{254}.

Pulse-chase labeling of pre-rRNA

Pulse-chase labelling of pre-rRNA was performed exactly as previously described [219], using 100 µCi of [5,6-^{3}H] uracil (Perkin Elmer; 45 to 50 Ci/mmol) per 40 OD_{600} of yeast cells. Cells were grown in SGal-Ura medium at 30 ºC to mid-log phase or shifted to SD-Ura medium for 6 h, pulse-labeled for 2 min and chased for different times with SD medium containing an excess of cold uracil. Total RNA was extracted by the hot acidic phenol-chloroform procedure [286]. Radioactive incorporation was measured by scintillation counting and about 20,000 cpm per RNA sample were loaded and resolved on 1.2% agarose-6% formaldehyde and 7% polyacrylamide-8M urea gels. RNA was then transferred to nylon membranes and visualized by fluorography [219].

Steady-state analysis of pre-rRNA

Northern hybridization and primer extension analyses were carried out as previously described [218, 219]. Total RNA was extracted from samples corresponding to 10 OD_{600} units of cells grown to mid-log phase. Equal amounts of total RNA were loaded on gels or used for primer extension reactions. Specific oligonucleotides (see **Table 3**), were 5'-end labelled with [γ-^{32}P] ATP and used as probes. Hybridization signals were detected using a Typhoon™ FLA9400 imaging system (GE Healthcare) and quantified using the GelQuant.NET software (biochemlabsolutions.com).

Affinity Purification of GFP-tagged Proteins

GFP-tagged factors representative of 90S and pre-60S r-particles were purified following a one-step GFP-Trap_A procedure (Chromotek), as described previously [220]. The proteins from purified particles were extracted by boiling the beads with Laemmli buffer and analyzed by western blotting. To normalize the amount of purified complexes to be loaded for comparative studies, aliquots of the samples were first resolved by SDS-PAGE and visualized by silver staining.

Affinity purification of particles containing L14A-yGFP was also performed by the one-step GFP-Trap_A procedure. The pre- and mature rRNAs associated with the particles were recovered by the hot phenol-chloroform method and analysed by northern blotting as described above.

Fluorescence Microscopy

To test pre-ribosomal particle export, the *GAL::RPL14* strain was transformed with plasmids expressing either GFP-tagged L25 or S3 and Nop1-mRFP (see above). Transformants were grown in selective SGal medium and shifted to selective SD for 6 h to deplete L14. Cells were washed, resuspended in PBS buffer (140 mM NaCl, 8 mM Na_2HPO_4, 1.5 mM KH_2PO_4, 2.75 mM KCl, pH 7.3), and examined with an Olympus BX61 fluorescence microscope equipped with a digital camera. Images were analysed using the Olympus cellSens software and processed with Adobe Photoshop CS2 (Adobe Systems Inc.).

Protein extracts and western blotting analyses

Total yeast protein extracts were prepared as described previously [137]. Total protein extracts and samples from purified particles were analysed by western blotting according to standard procedures. The following primary antibodies were used in this study: mouse monoclonal anti-GFP (clones 7.1 and 13.1, Roche) and anti-Nop1 (MCA28F2, EnCor Biotechnology); rabbit polyclonal anti-L1 (gift from F. Lacroute) [214], anti-L6 (gift form G, Dieci) [287], anti-L10 (gift from B. Trumpower) [217], anti-L14 (gift from G. Dieci) [287], anti-L16 (gift from S. Rospert) [213], anti-Has1 (gift from P. Linder) [215], anti-Mrt4 (gift from J.P.G. Ballesta) [115]. Secondary goat anti-mouse or anti-rabbit horseradish peroxidase-conjugated antibodies (Bio-Rad Laboratories, Inc.) were used as secondary antibodies. Proteins were visualized using a chemiluminescence detection kit (Super-Signal West Pico, Pierce) and a ChemiDoc™ MP imaging system (Bio-Rad Laboratories, Inc.). Images were processed with Adobe Photoshop CS2 (Adobe Systems Inc.).

Affinity-purification of Noc2-TAP containing pre-ribosomal particles

The FEY320 strain, which expresses a chromosomally-encoded Noc2-TAP fusion protein and harbours a *GAL::HA-RPL14A* allele as the sole source of L14 r-protein, was grown in YPGal to an OD_{660} of ca. 0.8 and shifted to YPD for 6-8 h to shut down *RPL14A* expression. Noc2-TAP and associated pre-ribosomal particles were then affinity purified from total cell extracts using a matrix of rabbit IgG covalently coupled to magnetic beads (Sigma-Aldrich) as described previously [125] with some minor modifications. The cell pellet corresponding to one litre of yeast culture was resuspended in 1.5 ml of cold MB buffer (20 mM Tris HCl pH 8,0, 200 mM KCl, 5 mM $(CH_3COO)_2Mg$, 2 mM benzamidine, 1 mM PMSF, and 0.02 U/ml RNasin®) per g of cell pellet. Cells were broken by vigorous shaking with glass beads (1.4 g beads of 0.75-1 mm diameter per 0.8 ml of cell suspension) in a Vibrax VXR shaker (IKA) for 10 min at 4°C, followed by 2 min on ice. This procedure was repeated twice. Total cell extracts were clarified by two consecutive centrifugation steps in a microfuge at the maximum speed (ca. 16000 x *g*) for 5 min and 10 min, respectively. The protein concentration of the cleared lysated was determined using the Bradford protein assay (Bio-Rad). To each of the resulting supernatant (typically 1 ml with ca. 50 mg of total protein), Triton X-100 (0.5% final), Tween 20 (0.1% final) and 200 ml of IgG-coupled magnetic beads slurry, equilibrated with MB buffer containing 0.5% Triton X-100 and 0.1% Tween, were added, and the mixture was incubated for 2 h 30 min at 4 ºC with end-over-end tube rotation. After incubation, the beads were washed four times with 700 µl cold MB buffer with 0.5% Triton X-100 and 0.1% Tween 20. RNA was extracted from the 20% of the mixture to perform northern blot analyses. The remaining 80% mixture was washed two times with 1 ml AC buffer (100 mM CH_3COONH_4, pH 7.4, 0.1 mM $MgCl_2$) to remove excess of salt from the samples and bound proteins eluted two times with 500 µl of freshly prepared 500 mM NH_4OH solution for 20 min at room temperature, pooled and lyophilised overnight.

Semiquantitative mass spectrometric analyses

Lyophilised eluates were further processed for iTRAQ (isobaric tags for relative and absolute quantitation) and mass spectrometric protein analyses, as previously described [288]. Proteins identified by only one peptide were discarded. iTRAQ ratios (depleted versus non-depleted sample) were determined and normalized to the ratio of the Noc2 bait protein.

Table 1. Yeast strains used in this study.

Strain	Relevant genotype	Source
W303-1A	*MAT***a** *ade2-1 his3-11,15 leu2-3,112 trp1-1 ura3-1*	[206]
W303-1B	As W303-1A but *MAT*α	[206]
FEY204	As W303-1A but *rpl14A*::HIS3MX6	This study
FEY203	As W303-1B but *rpl14B*::HIS3MX6	This study
FEY229 [(a)]	As W303-1B but *rpl14A::*HIS3MX6 *rpl14B::*HIS3MX6 [YCplac33-RPL14A]	This study
YKL516 [(b)]	As W303-1A but *rpl14A::*natNT2 *rpl14B::*HIS3MX6 [YCplac33-RPL14A]	[176]
FEY320	As FEY229 but *noc2*::*NOC2-TAP*-URA3 [pAS24-RPL14A]	This study
JFY01	As W303-1B but *rpl16A::*HIS3MX6 *rpl16B-N180::*HIS3MX6	[137]
JFY137 [(a)]	As W303-1B but *rpl14A::*natNT2 *rpl14B::*HIS3MX6 *rpl16A::*HIS3MX6 [YCplac22-RPL14A]	This study
JFY136 [(a)]	As W303-1B but *rpl14A::*natNT2 *rpl14B::*HIS3MX6 *rpl16A::*HIS3MX6 *rpl16B-N180::*HIS3MX6 [YCplac22-RPL14A]	This study
YMD5 [(c)]	As W303-1A but *PWP2*-GFP(S65T)::kanMX6	[220]
YMD24 [(c)]	As W303-1A but *NOP58*-GFP(S65T)::*TRP1*	[220]
JDY850	As W303-1A but *SSF1*-GFP(S65T)::natNT2	[220]
JDY854	As W303-1A but *NSA1*-GFP(S65T)::natNT2	[137]
JDY851	As W303-1A but *NOP7*-GFP(S65T)::natNT2	[220]
JDY852	As W303-1A but *RIX1*-GFP(S65T)::natNT2	[220]
JDY855	As W303-1A but *ARX1*-GFP(S65T)::natNT2	[220]
JDY853	As W303-1A but *LSG1*-GFP(S65T)::natNT2	[220]
JDY861 [(d)]	As W303-1A but *RPP0*-GFP(S65T)::natNT2	[220]

[(a)] Depending on the experimental conditions, the corresponding plasmid was replaced by other plasmids containing different alleles of *RPL14A*. [(b)] Gift from D. Kressler. [(c)] Gift from M. Dosil. [(d)] Gift from M. Remacha.

Table 2. Plasmids used in this study.

Name	Relevant information	Source
YCplac33	*CEN, URA3*	[289]
YCplac111	*CEN, LEU2*	[289]
YCplac33-RPL14A	*RPL14A, CEN, URA3*	This study
YCplac111-RPL14A	*RPL14A, CEN, LEU2*	This study
YCplac22-RPL14A [(a)]	*RPL14A, CEN, TRP1*	[176]
YCplac22-rpl14A-N123 [(a)]	*rpl14A-N123, CEN, TRP1*	[176]
pAS24 [(b)]	*promoter GAL1-10, N-terminal 2xHA tag, CEN, LEU2*	[209]
pAS24-RPL14A	*GAL::2xHA-RPL14A, CEN, LEU2*	This study
YCplac111-yGFP/TCYC1	*C-terminal yGFP tag, TCYC1, CEN, LEU2*	D. Kressler
YCplac111-RPL14A-yGFP	*RPL14A-yGFP, TCYC1, CEN, LEU2*	This study
pFA6a-HIS3MX6	HIS3MX6 cassette	[207]
pRS314-RPL25-eGFP-NOP1-mRFP [(c)]	*RPL25*-eGFP, *NOP1*-mRFP, *CEN, TRP1*	[210]
pRS314-RPS3-eGFP-NOP1-mRFP [(c)]	*RPS3*-eGFP, *NOP1*-mRFP, *CEN, TRP1*	[210]
pRS316-GAL-NMD3Δ100 [(d)]	*GAL::NMD3Δ100, CEN, URA3*	[285]

[(a)] Gift from D. Kressler. [(b)] Gift from M. N. Hall. [(c)] Gift from J. Bassler and E. Hurt. [(d)] Gift from A. Jacobson.

Table 3. Oligonucleotides used in this study.

Name	5'-3' Sequence	Use
Probe a (5' A_0)	GGTCTCTCTGCTGCCGG	pre-rRNA hybridization
Probe b (18S)	CATGGCTTAATCTTTGAGAC	18S rRNA hybridization
Probe c (3-D/A_2)	GACTCTCCATCTCTTGTCTTCTTG	pre-rRNA hybridization
Probe d (A_2/A_3)	TGTTACCTCTGGGCCC	pre-rRNA hybridization
Probe e (5.8S)	TTTCGCTGCGTTCTTCATC	5.8S rRNA hybridization
Probe f (E/C_2)	GGCCAGCAATTTCAAGTTA	pre-rRNA hybridization
Probe g (C_1/C_2)	GAACATTGTTCGCCTAGA	pre-rRNA hybridization
Probe h (25S)	CTCCGCTTATTGATATGC	25S rRNA hybridization
Probe 5S	GGTCACCCACTACACTACTCGG	5S rRNA hybridization
RPL14A +/- 1kb up	GGAATTCTCTCCCATATACAAGGAAGG	PCR cloning *RPL14A*
RPL14A +/- 1kb dwn	CGGATCCCCTACAACCACTGCTGCTGC	PCR cloning *RPL14A*
RPL14B+/- 1kb up	CGGATCCGGTGGAAGGGAGCTCTTCG	PCR verification *RPL14B*
RPL14B +/- 1kb dwn	CACATCCCTTCTTTGTTGACG	PCR verification *RPL14B*
RPL16A +/- 1kb up	GTACCGCCAACCCTTCCAG	PCR verification *RPL16A*
RPL16A +/- 1kb dwn	CGAACGAACTGTATCGCGG	PCR verification *RPL16A*
RPL16B +/- 1kb up	AGATAGCGGAGGCAACAAGAG	PCR verification *RPL16B*
RPL16B +/- 1kb dwn	ACTAGTTCCCTCTTATCTCTC	PCR verification *RPL16B*
L14A up DEL	GTTTGTCTTAGTGAACAAAGAGAGTCGTGAAAAATAAAATAAACACGTACGCTGCAGGTCGAC	Genomic deletion *rpl14A*::HIS3MX6
L14A dwn DEL	AAATTACATACGAAATATATCAGAATTAAAGATCATGTACATATTATCGATGAATTCGAGCTCG	Genomic deletion *rpl14A*::HIS3MX6
L14B up DEL	GCATTTAAAGTAACTTCAGGAAATAAACGCGCAAATAAACCAAAACGTACGCTGCAGGTCGAC	Genomic deletion *rpl14B*::HIS3MX6
L14B dwn DEL	TGCTTTCAGTACTTACCTATGGATTTTAGAATTATTCTTCTTTTTATCGATGAATTCGAGCTCG	Genomic deletion *rpl14A*::HIS3MX6
pGAL-L14A up	GCGTCGACATGTCCACCGATTCTATTGTC	PCR cloning GAL::*RPL14A*
pGAL-L14A dwn	GGCGTGTACTTTCACGAC	PCR cloning GAL::*RPL14A*
GFP-L14A dwn	CGGATCCAGCCTTAGCCAAAGCCTTC	PCR cloning *RPL14A-yGFP*
NOC2 up100	CGTGAAGTTAAGGAAGAAAAGGCC	Genomic tagging *NOC2-TAP-URA3*
NOC2 dwn100	GCTTGGAGTGCTCACATGTTAGC	Genomic tagging *NOG2-TAP-URA3*

DISCUSIÓN

En estos últimos años se ha profundizado bastante en el conocimiento que se tiene de la contribución de las proteínas ribosómicas de la subunidad 60S a la biogénesis del ribosoma [144]. Solo unas pocas proteínas ribosómicas de la subunidad 60S, especialmente algunos no esenciales para el crecimiento, quedan aún por estudiar.

En esta Tesis, hemos abordado la caracterización funcional de dos proteínas ribosómicas que componen la subunidad grande del ribosoma de *S. cerevisiae,* la proteína L16 (**Capítulo I**) y la proteína L14 (**Capítulo II**).

Ambas proteínas ribosómicas son esenciales y están evolutivamente conservadas. L16 (uL13) presenta una gran similitud estructural a su homóloga procariota L13 en lo referente a su parte globular central y su región amino-terminal; sin embargo, L16 contiene una extensión carboxilo-terminal específica de organismos eucariotas que forma dos α-hélices consecutivas, las cuales están estabilizadas en el ribosoma por la interacción que presentan con el extremo carboxilo-terminal específico de eucariotas de la proteína ribosómica L14 y el segmento de expansión del rRNA $ES39^{L}$ [10, 11]. L14 (eL14) se encuentra conservada sólo en eucariotas y algunas arqueas, pero no está presente en el ribosoma bacteriano. En eucariotas, L14 presenta una extensión C-terminal que está ausente en los ortólogos de arqueas [176]. Como anteriormente se ha demostrado para la proteína L13a de mamíferos (ortóloga de la proteína L16 de levadura) [190], nuestros resultados indican que la proteína L16 se ensambla establemente en partículas pre-ribosómicas tempranas. En el caso de L14 hemos demostrado, como se esperaba inicialmente [125, 147], que L14 igualmente se ensambla en el nucle(ol)o en las partículas ribosómicas pre-60S.

En esta Tesis, hemos estudiado las consecuencias de la represión transcripcional de L16 y L14, los efectos de la truncación seriada de la extensión C-terminal de L16 y la relación funcional existente entre la extensión C-terminal especifica de eucariotas de L14 y L16 en el procesamiento de los pre-rRNAs y el transporte núcleo-citoplasmático de partículas ribosómicas pre-60S. Los perfiles de polirribosomas tras la represión transcripcional de ambas proteínas indican que tanto L14 como L16 son necesarias para la óptima producción de subunidades 60S maduras. Los experimentos de *northern blot, primer extension* y pulso y caza indican que, tras la represión transcripcional de las proteínas L16 y L14, hay una drástica disminución en los niveles de los precursores pre-rRNAs $27SB_s$ pero no en los del pre-rRNA $27SB_L$ así como una bajada en la formación de ambas formas del pre-rRNA 7S y los rRNAs 5.8S maduros. Estos resultados indican que tras la represión transcripcional de estas proteínas, la maduración en ITS2 se encuentra bloqueada. Además,

la represión transcripcional de L14 y L16 provoca una inhibición en el procesamiento del pre-rRNA 27SA3. Estos resultados complementan los datos previamente publicados por el grupo del Prof. Milkereit para la proteína L16, pero son novedosos en el campo para la proteína L14 [175]. Como consecuencia de estos fenotipos la supresión transcripcional de estas proteínas puede ocasionar un ensamblaje defectuoso de partículas pre-60S tempranas e intermedias. Estas partículas defectuosas no serían transportadas de manera correcta al citoplasma, como sugiere la retención del marcador L25-eGFP en el núcleo con cierto enriquecimiento en el nucléolo. Por otro lado, nuestros ensayos de *northern blot* y *pulso-caza* también indican que la represión transcripcional de L16 y L14 causa un leve retraso en los eventos del procesamiento de los pre-rRNAs en los sitios A_0, A_1 y A_2 como revela la acumulación del pre-rRNA 35S y el hecho de que el corte en el sitio A_3 preceda al corte en esos sitios conllevando a una reducción en la formación del pre-rRNA 20S y la aparición del pre-rRNA aberrante 23S. Este último fenotipo es general para casi todos los mutantes que causan una deficiencia en la produccion de subunidades 60S y parece ser debido al secuestro de factores tempranos de ensamblaje de intermediarios pre-60S y/o la perdida especifica del corte co-transcripcional del pre-rRNA naciente en el sitio A_0-A_2 [92, 124, 129, 131, 135, 137, 268, 290, 291].

Los defectos en el procesamiento de los pre-rRNAs $27SA_3$, $27SB_s$ y $7S_{S/L}$, si parecen estar más específicamente relacionados con la represión transcripcional de estas proteínas ribosómicas L16 o L14. Estos defectos en el procesamiento de los pre-rRNAs se parecen bastante a los descritos en las mutaciones de pérdida de función o en la represión transcripcional de diferentes conjuntos de factores de biogénesis de la subunidad 60S, muchos de ellos pertenecientes a la categoría llamada “factores A_3”, los cuales son necesarios para el procesamiento del pre-rRNA $27SA_3$ [30, 137], y que incluye al menos aquellos factores del sub-complejo Pwp1 (Pwp1, Nop12, Ebp2 y Brx1), el sub-complejo Erb1-Nop7-Ytm1, Nop15, Nsa3, Rlp7, Rrp1 y las helicasas de RNA Drs1 y Has1 [114, 215, 283, 292-295] [132, 138, 271, 282, 296-302]. De todos estos factores, solo la represión transcripcional de Ebp2, Pwp1, Erb1, Nop7, Ytm1, Nop15, Nsa3 y Rlp7 provoca una baja acumulación del pre-rRNA $27SB_S$ sin afectar significativamente a los niveles del pre-rRNA $27SB_L$. También se ha observado fenotipos similares tras la mutacion o la represión transcripcional de distintas proteínas ribosómicas tales como L8 y L36, las cuales, junto con L15, son vecinas cercanas en una región del dominio I del rRNA 25S/5.8S donde el extremo 5’ del rRNA 25S se aparea con el extremo 3’ del rRNA 5.8S [135, 271], L4 [175, 202], L6 [140], L7 [135, 175], L8 [135, 175], L16 [137, 175, 192], L18 [140, 175, 192], L20 [175, 192] y L33 [128, 175, 192], las cuales, junto con L14 se localizan alrededor del dominio II de los rRNAs 25S/5.8S. Fenotipos similares pero no idénticos se han observado tras la mutacion o

la represión transcripcional de las proteínas ribosómicas L3 [129, 140, 175], L9 [140], L13 [140], L23 [140], y L32 [175]. En el caso de L3, su represión transcripcional provoca la degradación de los pre-rRNAs $27SA_3$ y $27SB_S$ y de este modo, se ha descrito como la proteína ribosómica más temprana en intervenir en la ruta de procesamiento del pre-rRNA. Aunque no hay un simple escenario que pueda explicar el papel de todos estos factores y proteínas ribosómicas de manera unificada en el procesamiento del pre-rRNA 27S y la maduración de la partícula pre-60S, parece claro que estos defectos son consecuencia del mal plegamiento de las estructuras del pre-rRNA en las partículas pre-60S y/o a la asociación deficiente de factores específicos de ensamblaje o de distintas proteínas ribosómicas a estas partículas. En este sentido, se ha demostrado que tras la represión transcripcional de L8, el conjunto de factores A_3, el factor Has1 y las proteínas ribosómicas L15 y L36 no se unen a las partículas intermedias pre-60S [135]. Como consecuencia de la ausencia de factores A_3, las proteínas ribosómicas L17, L26, L35 y L37, las cuales se unen al dominio I de los rRNAs 25S/5.8S y alrededor del túnel de salida del polipéptido naciente, no se reclutan a partículas pre-60S [135]. De modo similar, la represión transcripcional de la proteína ribosómica L7 da lugar a una considerable disminución en el ensamblaje de sus proteínas ribosómicas vecinas, tales como L6, L14, L20 y L33, y de las proteínas ribosómicas que se localizan alrededor del túnel de salida a partículas intermedias pre-60S; sin embargo, los niveles de factores A_3 solo disminuyen medianamente; el factor Has1 y las proteínas ribosómicas vecinas de L8 permanecen prácticamente inalteradas [135]. En ambos casos, tras la represión transcripcional de L7 ó L8, las partículas pre-60S se degradan rápidamente [135]. Finalmente, la represión transcripcional de algunas de las proteínas ribosómicas que se ensamblan alrededor del dominio II, incluyendo a L16, perjudican mínimamente a la asociación de los factores A_3 y Has1 [192]. Cabe destacar que la asociación de Rrp17 con las partículas tempranas pre-60S se ve negativamente afectada tras la represión transcripcional de muchas de las proteínas ribosómicas mencionadas anteriormente [192].

En el caso concreto de la proteína L14, en esta Tesis hemos comparado la composición de partículas pre-ribosómicas tempranas purificadas usando el factor de actuación en *trans* Noc2 antes y después de reprimir transcripcionalmente la proteína L14. Las partículas purificadas tras la represión transcripcional de L14 pueden corresponder a esos precursores intermediarios que han sido capaces de incorporar a todas las proteínas ribosómicas y factores de actuación en *trans* que no dependen estrictamente del ensamblaje de L14. Como la represión transcripcional de L14 conlleva al reciclaje de los pre-rRNAs 27S y la acumulación de partículas pre-60S en el núcleo, es probable que estos intermediarios sean de hecho esas partículas que hemos observado que se retienen en el nucle(ol)o y que

aún no han sido enviadas a degradación. Estas partículas deben acumularse como consecuencia de un punto de control estructural en el estado conformacional erróneo del pre-rRNA 27S como resultado de la ausencia de L14 que impide la asociación de diferentes factores de actuación en *trans*, especialmente la del factor de exportación Nmd3 [161, 184]. La composición proteica de estas partículas indican que la represión transcripcional de L14 previene el ensamblaje estable de diferentes proteínas ribosómicas, entre ellas se pueden destacar dos grupos de proteínas, primero, aquel formado por las proteínas ribosómicas L17, L39, L26, L37 y L19, todas ellas localizadas alrededor del túnel de salida del polipéptido naciente y predominantemente unidas al dominios I de los rRNAs 25S/5.8S; segundo, el grupo formado por las proteínas ribosómicas L33, L6 y L20, las cuales interaccionan con L14 y se unen al dominio II del rRNA 25S. Interesantemente, L16, que interacciona directamente con L14, L20 y L33 [265], no se ve afectada significativamente por la represión transcripcional de L14. Este resultado sugiere que, a pesar de su íntima interacción, el ensamblaje de L14 y L16 no es interdependiente y que el ensamblaje de L16 es más temprano que el de L14 en las partículas pre-60S.

La asociación estable de la mayoría de los factores de actuación en *trans* perteneciente a la categoría denominada “factores B”, los cuales son importantes para el corte del pre-rRNA 27SB en el sitio C_2 se ve afectada negativamente [30, 272]. Este resultado concuerda con el requerimiento de L14 para la maduración del pre-rRNA 27SB. Paradójicamente, el reclutamiento de la mayoría de los factores conocidos como factores A_3, los cuales se asocian a las partículas pre-60S de manera interdependiente y están involucrados en el procesamiento del pre-rRNA $27SA_3$ como también lo está L14 [132], permanecen inalterados o tienen un leve incremento en las partículas pre-60S purificadas tras la represión transcripcional de L14. Este resultado claramente indica que, a diferencia a otras proteínas ribosómicas como L8, cuyo ensamblaje es necesario para la asociación de los factores A_3 con las partículas pre-ribosomicas [125, 135], L14 no se requiere para la asociación de estos factores con las partículas pre-60S. De este modo, los defectos en el procesamiento del pre-rRNA $27SA_3$ observados tras la represión transcripcional de L14 no se deben directamente a la ausencia en la asociación de factores A_3 con las partículas pre-60S. Sin embargo, la represión transcripcional de L14 debe afectar claramente a la función de este conjunto de factores durante la reorganización de la región ITS1/5.8S/ITS2 del pre-rRNA 27S y el ensamblaje de las proteínas ribosómicas alrededor del túnel de salida que permiten la digestión exonucleolítica 5’-3’ del pre-rRNA $27SA_3$ al pre-rRNA $27SB_S$. Nuestros resultados también indican que el defecto en el ensamblaje de las proteínas ribosómicas alrededor del túnel de salida tras la represión transcripcional de L14 no es la consecuencia de la ausencia de factores A_3 en las partículas pre-60S, sino el resultado de una formación

alterada de sus sitios de unión en el pre-rRNA, defectos que se deben propagar desde la estructura alterada del sitio de unión en el rRNA de L14 tras la represión transcripcional de L14. El procesamiento del pre-rRNA $27SA_2$ al pre-rRNA $27SA_3$ no se ve afectado tras la represión transcripcional de L14. De forma consistente, nuestros resultados muestran que L3, la cual es necesaria para este paso [129], está presente en las partículas pre-60S purificadas. Se ha descrito que *in vitro* el corte endonucleolítico en el sitio A_3 por la RNasa MRP solo requiere un sustrato mínimo de RNA de cadena sencilla ([48, 303, 304]). Así la presencia del pre-rRNA 27SA3 en la cepa mutante indica no sólo que el reclutamiento de la RNasa MRP deser efectivo en las condiciones no permisivas sino que este mínimo sustrato requerido deber estar presente en las partículas pre-60S carentes de L14 para asegurar que la RNasa MRP se encuentre activa.

De forma general, nuestros resultados concuerdan con resultados previos sobre el ensamblaje de proteínas ribosómicas y la asociación de factores de actuación en *trans* tras la represión transcripcional de otras proteínas ribosómicas tales como L7, L16, L18, L20, L32 y L33 que se unen al dominio II del rRNA 25S y son vecinas de L14 [125]. La comparación de los resultados de esta publicación con los datos aquí presentados sugiere que el ensamblaje de L14 en partículas tempranas pre-60S es interdependiente con al menos el de L6, L20 y L33. L16 parece que se ensambla más temprano que L14 y mientras su ensamblaje parece ser que se requiere para la incorporación eficiente de L14, lo contrario parece que no es aplicable. La alteración local de la falta de ensamblaje de algunas de estas proteínas en su entorno más cercano en los dominios II y VI (ES39) del rRNA 25S debe afectar negativamente al ensamblaje del segundo conjunto de proteínas (L17, L19, L26 y L39). Es más, estas alteraciones también deben ser las responsables de afectar específicamente a la asociación a partículas pre-60S de un sub-grupo de factores de actuación en *trans*. Recientemente, se ha resuelto la estructura de partículas pre-60S nucleoplásmicas tardías en levadura a alta resolución por cryo-EM [147, 153, 247] pero desafortunadamente ninguna estructura está disponible para partículas pre-60S tempranas hasta el momento. De este modo, carecemos de recursos moleculares para explicar la lógica para estos efectos específicos en la asociación de estos distintos factores. Finalmente, el hecho de que la represión transcripcional ciertas proteínas ribosómicas tales como L14, L6, L20 y L33 cause entre otras cosas la perdida de estas proteínas de manera conjunta de partículas pre-60S explicando de una manera lógica y sencilla por qué los fenotipos de procesamiento del pre-rRNA detectados tras la represión transcripcional de todas estas proteínas son prácticamente idénticas.

En esta Tesis, también hemos estudiado el efecto de la truncación de la extensión C-terminal de la proteína ribosómica L16 sobre la viabilidad celular, el procesamiento de los

pre-rRNAs y la maduración de la subunidad 60S. De las diferentes truncaciones estudiadas, sólo aquella que implica los últimos 18 aminoácidos de L16B (L16B-N180) fue capaz de permitir el crecimiento, como única fuente de L16 *in vivo*. Nuestros resultados también muestran que, independientemente de su impacto en el crecimiento celular, todas las variantes truncadas de L16B se expresan y son capaces de ensamblarse en partículas pre-60S. Este resultado es compatible con resultados obtenidos para un estudio similar de la extensión C-terminal de la proteína ribosómica L13a de mamíferos, que indican que la extensión C-terminal de L13a no está activamente involucrada en la unión al rRNA o en el ensamblaje a los ribosomas [190]. No obstante, las partículas pre-60S que contienen truncaciones de L16B no viables son claramente defectuosas, ya que en su mayoría fueron retenidas en el nucléolo. Por el contrario, no hemos observado defectos en el procesamiento del pre-rRNA para el mutante viable L16B-N180. Sin embargo, si encontramos defectos en el procesamiento del pre-rRNA para los mutantes truncados no viables. Los fenotipos observados fueron menos pronunciados que los observados tras la represión transcripcional de L16. Por tanto el ensamblaje del dominio globular de L16 debe ser suficiente para promover algún tipo de plegamiento del pre-rRNA 27SA que resulta en una mayor estabilidad de las partículas tempranas pre-60S. Estos resultados coinciden con resultados publicados de manera independiente por el del Prof. Milikereit y colaboradores donde se evalua el impacto de dos truncaciones de la extensión C-terminal de L16, una truncación idéntica a la L16B-N147 y otra similar a L16B-N168 [192].

No se conoce porque la eliminación de los últimos 18 aminoácidos de L16B prácticamente no presenta ningún efecto sobre la producción de subunidades 60S mientras que truncaciones más grandes de la proteína daña fuertemente la biogénesis. Nosotros especulamos que, mientras que en el mutante *rpl16-N180* no afecta a la interacción entre L14-L16, por otro lado en los mutantes rpl16-N168 y rpl16-N147 no permite una eficiente interacción de ambas proteínas ribosómicas, provocando como consecuencia mal plegamiento del rRNA durante el ensamblaje de las subunidades 60S.

Por otro lado, en esta Tesis, hemos estudiado la relación funcional existente entre la extensión C-terminal especifica de eucariotas de L14 y L16 [10, 11]. Para ello, hemos co-expresado la proteína L14A-N123 y la proteína L16B-N180 como fuentes de L14 y L16, respectivamente, en células de levadura. El alelo rpl14A-N123 que carece de los últimos 16 aminoácidos de L14A confiere un defecto leve en la biogénesis de 60S que afecta sutilmente al crecimiento a 30 ºC cuando es expresado como única fuente de L14 desde un plásmido centromérico [176].

Nuestros resultados indican que, aunque esta combinación no produce ningún defecto sinérgico en condiciones normales de crecimiento (medio YPD, 30 ºC), no permite el crecimiento en medio de cultivo que contiene una concentración sub-letal de paromomicina. Este resultado sugiere que la interacción completa de las extensiones C-terminales de L14 y L16 no es estrictamente necesaria para el ensamblaje de subunidades 60S pero es al menos necesaria para algunos aspectos funcionales de las subunidades 60S.

En conclusión, en esta Tesis se demuestra que tanto L16 y L14 juegan un papel esencial en las etapas tempranas del ensamblaje de las subunidades 60S, más específicamente, durante el procesamiento del pre-rRNA $27SA_3$ y la formación de los precursores del pre-rRNA 27SB. El modo en que L16 lleva a cabo este papel aún no está claro. El laboratorio del Prof. Kressler ha demostrado que una variante truncada de la proteína ribosómica L14A, la cual carece de gran parte de su α-hélice C-terminal, confiere defectos en crecimiento y muestra una interacción sintético letal con distintos alelos de MAK5, que codifican para una helicasa de RNA involucrada en la biogénesis de la subunidad 60S, EBP2 y NOP16 [176, 305]. De este modo se ha sugerido que Mak5 podría requerirse para el correcto ensamblaje de L14 y sus vecinos en partículas tempranas pre-60S [176]. De igual modo, en *Escherichia coli*, se ha demostrado que la helicasa de RNA SrmB es requerida para el correcto ensamblaje de la proteína ribosómica L13, la cual es la ortóloga bacteriana de la proteína ribosómica L16 de *S. cerevisiae*, y posteriormente ensamblando otras proteínas ribosómicas [187, 306]. La realización de más experimentos deberían permitirnos esclarecer si, de forma similar a L14, el ensamblaje de L16 también es facilitado por la actividad de Mak5 y/o proteínas con las que interacciona genéticamente y cómo, si es el caso, contribuye la extensión c-terminal especifica de eucariotas a este ensamblaje.

A pesar del hecho de que L14 y L16 interaccionan íntimamente por sus extensiones C-terminales, el ensamblaje de L16 parece ser que precede al de L14 y no es estrictamente dependiente de estas extensiones. Son necesarios más estudios para entender a nivel molecular la conexión entre el ensamblaje de estas proteínas ribosómicas interdependientes, la activación de los factores A_3 y la asociación de los factores B. Recientemente, se ha demostrado que algunas proteínas ribosómicas vecinas tales como L5 y L11 [152] o S14 (uS11) y S26 (eS26) [290] son preferencialmente incorporadas a partículas pre-ribosómicas como sub-complejos asociados a factores de actuación en *trans* específicos. Si esto ocurre en el caso de L14 y alguna de las proteínas cercanas sería un tema interesante de ser explorado.

BIBLIOGRAFÍA

1. **Green R and Noller HF.** 1997. Ribosomes and translation. Annu Rev Biochem **66**:679-716.
2. **Planta RJ and Mager WH.** 1998. The list of cytoplasmic ribosomal proteins of *Saccharomyces cerevisiae*. Yeast **14**:471-477.
3. **Ramakrishnan V and White SW.** 1998. Ribosomal protein structures: insights into the architecture, machinery and evolution of the ribosome. Trends Biochem. Sci. **23**:208-212.
4. **Frank J and Agrawal RK.** 2000. A ratchet-like inter-subunit reorganization of the ribosome during translocation. Nature **406**:318-322.
5. **Spahn CM, Beckmann R, Eswar N, Penczek PA, Sali A, Blobel G and Frank J.** 2001. Structure of the 80S ribosome from *Saccharomyces cerevisiae*-tRNA-ribosome and subunit-subunit interactions. Cell **107**:373-386.
6. **Klein DJ, Moore PB and Steitz TA.** 2004. The roles of ribosomal proteins in the structure assembly, and evolution of the large ribosomal subunit. J. Mol. Biol. **340**:141-177.
7. **Armache JP, Jarasch A, Anger AM, Villa E, Becker T, Bhushan S, Jossinet F, Habeck M, Dindar G, Franckenberg S, Marquez V, Mielke T, Thomm M, Berninghausen O, Beatrix B, Soding J, Westhof E, Wilson DN and Beckmann R.** 2010. Cryo-EM structure and rRNA model of a translating eukaryotic 80S ribosome at 5.5-A resolution. Proc. Natl. Acad. Sci. USA **107**:19748-19753.
8. **Armache JP, Jarasch A, Anger AM, Villa E, Becker T, Bhushan S, Jossinet F, Habeck M, Dindar G, Franckenberg S, Marquez V, Mielke T, Thomm M, Berninghausen O, Beatrix B, Soding J, Westhof E, Wilson DN and Beckmann R.** 2010. Localization of eukaryote-specific ribosomal proteins in a 5.5-A cryo-EM map of the 80S eukaryotic ribosome. Proc. Natl. Acad. Sci. USA **107**:19754-19759.
9. **Ben-Shem A, Jenner L, Yusupova G and Yusupov M.** 2010. Crystal structure of the eukaryotic ribosome. Science **330**:1203-1209.
10. **Ben-Shem A, Garreau de Loubresse N, Melnikov S, Jenner L, Yusupova G and Yusupov M.** 2011. The structure of the eukaryotic ribosome at 3.0 Å resolution. Science **334**:1524-1529.
11. **Klinge S, Voigts-Hoffmann F, Leibundgut M, Arpagaus S and Ban N.** 2011. Crystal structure of the eukaryotic 60S ribosomal Subunit in Complex with initiation factor 6. Science **334**:941-948.
12. **Rabl J, Leibundgut M, Ataide SF, Haag A and Ban N.** 2011. Crystal structure of the eukaryotic 40S ribosomal subunit in complex with initiation factor 1. Science **331**:730-736.
13. **Anger AM, Armache JP, Berninghausen O, Habeck M, Subklewe M, Wilson DN and Beckmann R.** 2013. Structures of the human and Drosophila 80S ribosome. Nature **497**:80-85.
14. **Khatter H, Myasnikov AG, Natchiar SK and Klaholz BP.** 2015. Structure of the human 80S ribosome. Nature **520**:640-645.
15. **Schluenzen F, Tocilj A, Zarivach R, Harms J, Bashan A, Bartels H, Agmon I, Franceschi F and Yonath A.** 2000. Structure of functional activated small ribosomal subunit at 3.3 Å resolution. Cell **102**:615-623.
16. **Zurdo J, Parada P, van den Berg A, Nusspaumer G, Jiménez-Díaz A, Remacha M and Ballesta JP.** 2000. Assembly of *Saccharomyces cerevisiae* ribosomal stalk: binding of P1 proteins is required for the interaction of P2 proteins. Biochemistry **39**:8929-8934.
17. **Amunts A, Brown A, Bai XC, Llacer JL, Hussain T, Emsley P, Long F, Murshudov G, Scheres SH and Ramakrishnan V.** 2014. Structure of the yeast mitochondrial large ribosomal subunit. Science **343**:1485-1489.
18. **Kaushal PS, Sharma MR, Booth TM, Haque EM, Tung CS, Sanbonmatsu KY, Spremulli LL and Agrawal RK.** 2014. Cryo-EM structure of the small subunit of the mammalian mitochondrial ribosome. Proc Natl Acad Sci USA **111**:7284-7289.

19. **De Silva D, Tu YT, Amunts A, Fontanesi F and Barrientos A.** 2015. Mitochondrial ribosome assembly in health and disease. Cell Cycle **14**:2226-2250.
20. **Greber BJ and Ban N.** 2016. Structure and Function of the Mitochondrial Ribosome. Annu Rev Biochem **85**:103-132.
21. **Yusupov MM, Yusupova GZ, Baucom A, Lieberman K, Earnest TN, Cate JH and Noller HF.** 2001. Crystal structure of the ribosome at 5.5 A resolution. Science **292**:883-896.
22. **Melnikov S, Ben-Shem A, Garreau de Loubresse N, Jenner L, Yusupova G and Yusupov M.** 2012. One core, two shells: bacterial and eukaryotic ribosomes. Nat. Struct. Mol. Biol. **19**:560-567.
23. **Hall DB, Wade JT and Struhl K.** 2006. An HMG protein, Hmo1, associates with promoters of many ribosomal protein genes and throughout the rRNA gene locus in *Saccharomyces cerevisiae*. Mol. Cell. Biol. **26**:3672-3679.
24. **Freed EF, Bleichert F, Dutca LM and Baserga SJ.** 2010. When ribosomes go bad: diseases of ribosome biogenesis. Mol. Biosyst. **6**:481-493.
25. **Warner JR.** 1999. The economics of ribosome biosynthesis in yeast. Trends Biochem. Sci. **24**:437-440.
26. **Lestrade L and Weber MJ.** 2006. snoRNA-LBME-db, a comprehensive database of human H/ACA and C/D box snoRNAs. Nucleic Acids Res. **34**:D158-162.
27. **Piekna-Przybylska D, Decatur WA and Fournier MJ.** 2007. New bioinformatic tools for analysis of nucleotide modifications in eukaryotic rRNA. RNA **13**:305-312.
28. **Tafforeau L, Zorbas C, Langhendries JL, Mullineux ST, Stamatopoulou V, Mullier R, Wacheul L and Lafontaine DL.** 2013. The complexity of human ribosome biogenesis revealed by systematic nucleolar screening of Pre-rRNA processing factors. Mol. Cell **51**:539-551.
29. **Kressler D, Hurt E and Bassler J.** 2010. Driving ribosome assembly. Biochim. Biophys. Acta **1803**:673-683.
30. **Woolford JL, Jr. and Baserga SJ.** 2013. Ribosome biogenesis in the yeast Saccharomyces cerevisiae. Genetics **195**:643-681.
31. **Mayer C and Grummt I.** 2006. Ribosome biogenesis and cell growth: mTOR coordinates transcription by all three classes of nuclear RNA polymerases. Oncogene **25**:6384-6391.
32. **Nomura M, Nogi Y and Oakes M.** 2004. Transcription of rDNA in the yeast *Saccharomyces cerevisiae*. In: Olson MOJ (ed) Nucleolus, Landes Bioscience/Eurekah.com, Georgetown pp. 128-153.
33. **Kobayashi T.** 2011. Regulation of ribosomal RNA gene copy number and its role in modulating genome integrity and evolutionary adaptability in yeast. Cell. Mol. Life Sci. **68**:1395-1403.
34. **Ofengand J and Fournier MJ.** 1998. The pseudouridine residues of rRNA: number, location, biosynthesis, and function. In: Grosjean H and Benne R (eds) Modification and editing of RNA, ASM Press, Washington, D. C. pp. 229-253.
35. **Henras AK, Plisson-Chastang C, O'Donohue MF, Chakraborty A and Gleizes PE.** 2015. An overview of pre-ribosomal RNA processing in eukaryotes. Wiley Interdiscip Rev RNA **6**:225-242.
36. **Veldman GM, Brand RC, Klootwijk J and Planta R.** 1980. Some characteristics of processing sites in ribosomal precursor RNA of yeast. Nucleic Acids Res. **8**:2907-2920.
37. **Hughes JMX and Ares M, Jr.** 1991. Depletion of U3 small nucleolar RNA inhibits cleavage in the 5' external transcribed spacer of yeast pre-ribosomal RNA and impairs formation of 18S ribosomal RNA. EMBO J. **10**:4231-4239.
38. **Veinot-Drebot LM, Singer RA and Johnston GC.** 1988. Rapid initial cleavage of nascent pre-rRNA transcripts in yeast. J. Mol. Biol. **199**:107-113.
39. **Osheim YN, French SL, Keck KM, Champion EA, Spasov K, Dragon F, Baserga SJ and Beyer AL.** 2004. Pre-18S ribosomal RNA is structurally compacted into the SSU processome prior to being cleaved from nascent transcripts in *Saccharomyces cerevisiae*. Mol. Cell **16**:943-954.

40. **Kos M and Tollervey D.** 2010. Yeast pre-rRNA processing and modification occur cotranscriptionally. Mol. Cell **37**:809-820.
41. **Lebaron S, Schneider C, van Nues RW, Swiatkowska A, Walsh D, Bottcher B, Granneman S, Watkins NJ and Tollervey D.** 2012. Proofreading of pre-40S ribosome maturation by a translation initiation factor and 60S subunits. Nat. Struct. Mol. Biol. **19**:744-753.
42. **Chu S, Archer RH, Zengel JM and Lindahl L.** 1994. The RNA of RNase MRP is required for normal processing of ribosomal RNA. Proc. Natl. Acad. Sci. USA **91**:659-663.
43. **Henry Y, Wood H, Morrissey JP, Petfalski E, Kearsey S and Tollervey D.** 1994. The 5' end of yeast 5.8S rRNA is generated by exonucleases from an upstream cleavage site. EMBO J. **13**:2452-2463.
44. **Oeffinger M, Zenklusen D, Ferguson A, Wei KE, El Hage A, Tollervey D, Chait BT, Singer RH and Rout MP.** 2009. Rrp17p is a eukaryotic exonuclease required for 5' end processing of Pre-60S ribosomal RNA. Mol. Cell **36**:768-781.
45. **Faber AW, Vos HR, Vos JC and Raué HA.** 2006. 5'-end formation of yeast 5.8SL rRNA is an endonucleolytic event. Biochem. Biophys. Res. Commun. **345**:796-802.
46. **Veldman GM, Klootwijk J, van Heerikhuizen H and Planta RJ.** 1981. The nucleotide sequence of the intergenic region between the 5.8S and 26S rRNA genes of the yeast ribosomal RNA operon. Possible implications for the interaction between 5.8S and 26S rRNA and the processing of the primary transcript. Nucleic Acids Res. **9**:4847-4863.
47. **Kufel J, Dichtl B and Tollervey D.** 1999. Yeast Rnt1p is required for cleavage of the pre-ribosomal RNA in the 3' ETS but not the 5' ETS. RNA **5**:909-917.
48. **Fernández-Pevida A, Kressler D and de la Cruz J.** 2015. Processing of preribosomal RNA in Saccharomyces cerevisiae. Wiley Interdiscip. Rev. RNA **6**:191-209.
49. **Gasse L, Flemming D and Hurt E.** 2015. Coordinated ribosomal ITS2 RNA processing by the Las1 complex integrating endonuclease, polynucleotide kinase, and exonuclease Activities. Mol Cell **60**:808-815.
50. **Briggs MW, Burkard KTD and Butler JS.** 1998. Rrp6p, the yeast homologue of the human PM-Scl 100-kDa autoantigen, is essential for efficient 5.8S rRNA 3' end formation. J. Biol. Chem. **273**:13255-13263.
51. **Allmang C, Kufel J, Chanfreau G, Mitchell P, Petfalski E and Tollervey D.** 1999. Functions of the exosome in rRNA, snoRNA and snRNA synthesis. EMBO J. **18**:5399-5410.
52. **van Hoof A, Lennertz P and Parker R.** 2000. Three conserved members of the RNase D family have unique and overlapping functions in the processing of 5S, 5.8S, U4, U5, RNase MRP and RNase P RNAs in yeast. EMBO J. **19**:1357-1365.
53. **Faber AW, Van Dijk M, Raué HA and Vos JC.** 2002. Ngl2p is a Ccr4p-like RNA nuclease essential for the final step in 3'- end processing of 5.8S rRNA in *Saccharomyces cerevisiae*. RNA **8**:1095-1101.
54. **Thomson E and Tollervey D.** 2010. The final step in 5.8S rRNA processing is cytoplasmic in *Saccharomyces cerevisiae*. Mol. Cell. Biol. **30**:976-984.
55. **Geerlings TH, Vos JC and Raué HA.** 2000. The final step in the formation of 25S rRNA in *Saccharomyces cerevisiae* is performed by 5'-3' exonucleases. RNA **6**:1698-1703.
56. **Ciganda M and Williams N.** 2011. Eukaryotic 5S rRNA biogenesis. Wiley Interdiscip. Rev. RNA **2**:523-533.
57. **DeRisi JL, Iyer VR and Brown PO.** 1997. Exploring the metabolic and genetic control of gene expression on a genomic scale. Science **278**:680-686.
58. **Lascaris RF, Mager WH and Planta RJ.** 1999. DNA-binding requirements of the yeast protein Rap1p as selected in silico from ribosomal protein gene promoter sequences. Bioinformatics **15**:267-277.
59. **Zhao Y, McIntosh KB, Rudra D, Schawalder S, Shore D and Warner JR.** 2006. Fine-structure analysis of ribosomal protein gene transcription. Mol. Cell. Biol. **26**:4853-4862.

60. **Wade JT, Hall DB and Struhl K.** 2004. The transcription factor Ifh1 is a key regulator of yeast ribosomal protein genes. Nature **432**:1054-1058.
61. **Jorgensen P, Rupes I, Sharom JR, Schneper L, Broach JR and Tyers M.** 2004. A dynamic transcriptional network communicates growth potential to ribosome synthesis and critical cell size. Genes Dev. **18**:2491-2505.
62. **Urban J, Soulard A, Huber A, Lippman S, Mukhopadhyay D, Deloche O, Wanke V, Anrather D, Ammerer G, Riezman H, Broach JR, De Virgilio C, Hall MN and Loewith R.** 2007. Sch9 is a major target of TORC1 in Saccharomyces cerevisiae. Mol. Cell **26**:663-674.
63. **Wilson DN and Nierhaus KH.** 2005. Ribosomal proteins in the spotlight. Crit. Rev. Biochem. Mol. Biol. **40**:243-267.
64. **Xue S and Barna M.** 2012. Specialized ribosomes: a new frontier in gene regulation and organismal biology. Nat. Rev. Mol. Cell. Biol. **13**:355-369.
65. **Moore PB and Steitz TA.** 2002. The involvement of RNA in ribosome function. Nature **418**:229-235.
66. **Steitz TA and Moore PB.** 2003. RNA, the first macromolecular catalyst: the ribosome is a ribozyme. Trends Biochem Sci. **28**:411-418.
67. **Ban N, Nissen P, Hansen J, Moore PB and Steitz TA.** 2000. The complete atomic structure of the large ribosomal subunit at 2.4 Å resolution. Science **289**:905-920.
68. **Mizushima S and Nomura M.** 1970. Assembly mapping of 30S ribosomal proteins in *E. coli*. Nature **226**:1214-1218.
69. **Held WA, Mizushima S and Nomura M.** 1973. Reconstitution of *Escherichia coli* 30 S ribosomal subunits from purified molecular components. J. Biol. Chem. **248**:5720-5730.
70. **Spillmann S, Dohme F and Nierhaus KH.** 1977. Assembly in vitro of the 50 S subunit from Escherichia coli ribosomes: proteins essential for the first heat-dependent conformational change. J. Mol. Biol. **115**:513-523.
71. **Spillmann S and Nierhaus KH.** 1978. The ribosomal protein L24 of *Escherichia coli* is an assembly protein. J. Biol. Chem. **253**:7047-7050.
72. **Rohl R and Nierhaus KH.** 1982. Assembly map of the large subunit (50S) of *Escherichia coli* ribosomes. Proc. Natl. Acad. Sci. USA **79**:729-733.
73. **Herold M and Nierhaus KH.** 1987. Incorporation of six additional proteins to complete the assembly map of the 50 S subunit from *Escherichia coli* ribosomes. J. Biol. Chem. **262**:8826-8833.
74. **Nierhaus KH.** 1991. The assembly of prokaryotic ribosomes. Biochimie **73**:739-755.
75. **Léger-Silvestre I, Milkereit P, Ferreira-Cerca S, Saveanu C, Rousselle JC, Choesmel V, Guinefoleau C, Gas N and Gleizes PE.** 2004. The ribosomal protein Rps15p is required for nuclear exit of the 40S subunit precursors in yeast. EMBO J. **23**:2336-2347.
76. **Ferreira-Cerca S, Pöll G, Gleizes PE, Tschochner H and Milkereit P.** 2005. Roles of eukaryotic ribosomal proteins in maturation and transport of pre-18S rRNA and ribosome function. Mol. Cell **20**:263-275.
77. **Ferreira-Cerca S, Pöll G, Kuhn H, Neueder A, Jakob S, Tschochner H and Milkereit P.** 2007. Analysis of the *in vivo* assembly pathway of eukaryotic 40S ribosomal proteins. Mol. Cell **28**:446-457.
78. **de la Cruz J, Karbstein K and Woolford JL, Jr.** 2015. Functions of ribosomal proteins in assembly of eukaryotic ribosomes in vivo. Annu. Rev. Biochem. **84**:93-129.
79. **Ban N, Beckmann R, Cate JH, Dinman JD, Dragon F, Ellis SR, Lafontaine DL, Lindahl L, Liljas A, Lipton JM, McAlear MA, Moore PB, Noller HF, Ortega J, Panse VG, Ramakrishnan V, Spahn CM, Steitz TA, Tchorzewski M, Tollervey D, Warren AJ, Williamson JR, Wilson D, Yonath A and Yusupov M.** 2014. A new system for naming ribosomal proteins. Curr. Opin. Struct. Biol. **24**:165-169.
80. **Dragon F, Gallagher JE, Compagnone-Post PA, Mitchell BM, Porwancher KA, Wehner KA, Wormsley S, Settlage RE, Shabanowitz J, Osheim Y, Beyer AL, Hunt DF and Baserga SJ.** 2002. A large nucleolar U3 ribonucleoprotein required for 18S ribosomal RNA biogenesis. Nature **417**:967-970.

81. **Grandi P, Rybin V, Bassler J, Petfalski E, Strauss D, Marzioch M, Schäfer T, Kuster B, Tschochner H, Tollervey D, Gavin AC and Hurt E.** 2002. 90S pre-ribosomes include the 35S pre-rRNA, the U3 snoRNP, and 40S subunit processing factors but predominantly lack 60S synthesis factors. Mol. Cell **10**:105-115.
82. **Kornprobst M, Turk M, Kellner N, Cheng J, Flemming D, Kos-Braun I, Kos M, Thoms M, Berninghausen O, Beckmann R and Hurt E.** 2016. Architecture of the 90S Pre-ribosome: A Structural View on the Birth of the Eukaryotic Ribosome. Cell **166**:380-393.
83. **Chaker-Margot M, Barandun J, Hunziker M and Klinge S.** 2017. Architecture of the yeast small subunit processome. Science **355**.
84. **Amlacher S, Sarges P, Flemming D, van Noort V, Kunze R, Devos DP, Arumugam M, Bork P and Hurt E.** 2011. Insight into structure and assembly of the nuclear pore complex by utilizing the genome of a eukaryotic thermophile. Cell **146**:277-289.
85. **Pérez-Fernández J, Roman A, de Las Rivas J, Bustelo XR and Dosil M.** 2007. The 90S preribosome is a multimodular structure that is assembled through a hierarchical mechanism. Mol. Cell. Biol. **27**:5414-5429.
86. **Pérez-Fernández J, Martín-Marcos P and Dosil M.** 2011. Elucidation of the assembly events required for the recruitment of Utp20, Imp4 and Bms1 onto nascent pre-ribosomes. Nucleic Acids Res. **39**:8105-8121.
87. **Chaker-Margot M, Hunziker M, Barandun J, Dill BD and Klinge S.** 2015. Stage-specific assembly events of the 6-MDa small-subunit processome initiate eukaryotic ribosome biogenesis. Nat. Struct. Mol. Biol. **22**:920-923.
88. **Zhang L, Wu C, Cai G, Chen S and Ye K.** 2016. Stepwise and dynamic assembly of the earliest precursors of small ribosomal subunits in yeast. Genes Dev. **30**:718-732.
89. **Wells GR, Weichmann F, Colvin D, Sloan KE, Kudla G, Tollervey D, Watkins NJ and Schneider C.** 2016. The PIN domain endonuclease Utp24 cleaves pre-ribosomal RNA at two coupled sites in yeast and humans. Nucleic Acids Res **44**:5399-5409.
90. **Schäfer T, Strauss D, Petfalski E, Tollervey D and Hurt E.** 2003. The path from nucleolar 90S to cytoplasmic 40S pre-ribosomes. EMBO J. **22**:1370-1380.
91. **Gerbasi VR, Weaver CM, Hill S, Friedman DB and Link AJ.** 2004. Yeast Asc1p and mammalian RACK1 are functionally orthologous core 40S ribosomal proteins that repress gene expression. Mol. Cell. Biol. **24**:8276-8287.
92. **Milkereit P, Gadal O, Podtelejnikov A, Trumtel S, Gas N, Petfalski E, Tollervey D, Mann M, Hurt E and Tschochner H.** 2001. Maturation and intranuclear transport of pre-ribosomes requires Noc proteins. Cell **105**:499-509.
93. **Nissan TA, Bassler J, Petfalski E, Tollervey D and Hurt E.** 2002. 60S pre-ribosome formation viewed from assembly in the nucleolus until export to the cytoplasm. EMBO J. **21**:5539-5547.
94. **Fatica A, Cronshaw AD, Dlakic M and Tollervey D.** 2002. Ssf1p prevents premature processing of an early pre-60S ribosomal particle. Mol. Cell **9**:341-351.
95. **Dez C, Froment C, Noaillac-Depeyre J, Monsarrat B, Caizergues-Ferrer M and Henry Y.** 2004. Npa1p, a component of very early pre-60S ribosomal particles, associates with a subset of small nucleolar RNPs required for peptidyl transferase center modification. Mol. Cell. Biol. **24**:6324-6337.
96. **Kressler D, Roser D, Pertschy B and Hurt E.** 2008. The AAA ATPase Rix7 powers progression of ribosome biogenesis by stripping Nsa1 from pre-60S particles. J. Cell Biol. **181**:935-944.
97. **Oeffinger M, Dlakic M and Tollervey D.** 2004. A pre-ribosome-associated HEAT-repeat protein is required for export of both ribosomal subunits. Genes Dev. **18**:196-209.
98. **Schäfer T, Maco B, Petfalski E, Tollervey D, Bottcher B, Aebi U and Hurt E.** 2006. Hrr25-dependent phosphorylation state regulates organization of the pre-40S subunit. Nature **441**:651-655.

99. **Ray P, Basu U, Ray A, Majumdar R, Deng H and Maitra U.** 2008. The Saccharomyces cerevisiae 60 S ribosome biogenesis factor Tif6p is regulated by Hrr25p-mediated phosphorylation. J. Biol. Chem. **283**:9681-9691.
100. **Lebaron S, Segerstolpe A, French SL, Dudnakova T, de Lima Alves F, Granneman S, Rappsilber J, Beyer AL, Wieslander L and Tollervey D.** 2013. Rrp5 binding at multiple sites coordinates pre-rRNA processing and assembly. Mol. Cell **52**:707-719.
101. **Dunbar DA, Wormsley S, Agentis TM and Baserga SJ.** 1997. Mpp10p, a U3 small nucleolar ribonucleoprotein component required for pre-18S rRNA processing in yeast. Mol. Cell. Biol. **17**:5803-5812.
102. **Lee SJ and Baserga SJ.** 1999. Imp3p and Imp4p, two specific components of the U3 small nucleolar ribonucleoprotein that are essential for 18S rRNA processing. Mol. Cell. Biol. **19**:5441-5452.
103. **Wehner KA, Gallagher JE and Baserga SJ.** 2002. Components of an Interdependent Unit within the SSU Processome Regulate and Mediate Its Activity. Mol. Cell. Biol. **22**:7258-7267.
104. **Granneman S and Baserga SJ.** 2003. Probing the yeast proteome for RNA-processing factors. Genome Biol. **4**:229.
105. **Vos HR, Faber AW, de Gier MD, Vos JC and Raué HA.** 2004. Deletion of the three distal S1 motifs of *Saccharomyces cerevisiae* Rrp5p abolishes pre-rRNA processing at site A_2 without reducing the production of functional 40S subunits. Eukaryotic Cell **3**:1504-1512.
106. **Gerhardy S, Menet AM, Pena C, Petkowski JJ and Panse VG.** 2014. Assembly and nuclear export of pre-ribosomal particles in budding yeast. Chromosoma **123**:327-344.
107. **Fernández-Pevida A, Martín-Villanueva S, Murat G, Lacombe T, Kressler D and de la Cruz J.** 2016. The eukaryote-specific N-terminal extension of ribosomal protein S31 contributes to the assembly and function of 40S ribosomal subunits. Nucleic Acids Res. **44**:7777-7791.
108. **Dutca LM and Culver GM.** 2008. Assembly of the 5' and 3' minor domains of 16S ribosomal RNA as monitored by tethered probing from ribosomal protein S20. J. Mol. Biol. **376**:92-108.
109. **Mulder AM, Yoshioka C, Beck AH, Bunner AE, Milligan RA, Potter CS, Carragher B and Williamson JR.** 2010. Visualizing ribosome biogenesis: parallel assembly pathways for the 30S subunit. Science **330**:673-677.
110. **Karbstein K.** 2011. Inside the 40S ribosome assembly machinery. Curr. Opin. Chem. Biol. **15**:657-663.
111. **O'Donohue MF, Choesmel V, Faubladier M, Fichant G and Gleizes PE.** 2010. Functional dichotomy of ribosomal proteins during the synthesis of mammalian 40S ribosomal subunits. J. Cell. Biol. **190**:853-866.
112. **Strunk BS, Loucks CR, Su M, Vashisth H, Cheng S, Schilling J, Brooks CL, III., Karbstein K and Skiniotis G.** 2011. Ribosome assembly factors prevent premature translation initiation by 40S assembly intermediates. Science **333**:1449-1453.
113. **Ghalei H, Schaub FX, Doherty JR, Noguchi Y, Roush WR, Cleveland JL, Stroupe ME and Karbstein K.** 2015. Hrr25/CK1delta-directed release of Ltv1 from pre-40S ribosomes is necessary for ribosome assembly and cell growth. J. Cell Biol. **208**:745-759.
114. **Dunbar DA, Dragon F, Lee SJ and Baserga SJ.** 2000. A nucleolar protein related to ribosomal protein L7 is required for an early step in large ribosomal subunit biogenesis. Proc. Natl. Acad. Sci. USA **97**:13027-13032.
115. **Rodríguez-Mateos M, Abia D, García-Gómez JJ, Morreale A, de la Cruz J, Santos C, Remacha M and Ballesta JPG.** 2009. The amino terminal domain from Mrt4 protein can functionally replace the RNA binding domain of the ribosomal P0 protein. Nucleic Acids Res. **37**:3514-3521.
116. **Strunk BS, Novak MN, Young CL and Karbstein K.** 2012. A translation-like cycle is a quality control checkpoint for maturing 40S ribosome subunits. Cell **150**:111-121.

117. **Pausch P, Singh U, Ahmed YL, Pillet B, Murat G, Altegoer F, Stier G, Thoms M, Hurt E, Sinning I, Bange G and Kressler D.** 2015. Co-translational capturing of nascent ribosomal proteins by their dedicated chaperones. Nat Commun **6**:7494.
118. **Mitterer V, Murat G, Rety S, Blaud M, Delbos L, Stanborough T, Bergler H, Leulliot N, Kressler D and Pertschy B.** 2016. Sequential domain assembly of ribosomal protein S3 drives 40S subunit maturation. Nat Commun **7**:10336.
119. **Segref A, Sharma K, Doye V, Hellwig A, Huber J, Luhrmann R and Hurt E.** 1997. Mex67p, a novel factor for nuclear mRNA export, binds to both poly(A)+ RNA and nuclear pores. EMBO J. **16**:3256-3271.
120. **Santos-Rosa H, Moreno H, Simos G, Segref A, Fahrenkrog B, Pante N and Hurt E.** 1998. Nuclear mRNA export requires complex formation between Mex67p and Mtr2p at the nuclear pores. Mol. Cell. Biol. **18**:6826-6838.
121. **Schutz S, Fischer U, Altvater M, Nerurkar P, Pena C, Gerber M, Chang Y, Caesar S, Schubert OT, Schlenstedt G and Panse VG.** 2014. A RanGTP-independent mechanism allows ribosomal protein nuclear import for ribosome assembly. Elife **3**:e03473.
122. **Turowski TW, Lebaron S, Zhang E, Peil L, Dudnakova T, Petfalski E, Granneman S, Rappsilber J and Tollervey D.** 2014. Rio1 mediates ATP-dependent final maturation of 40S ribosomal subunits. Nucleic Acids Res. **42**:12189-12199.
123. **McCaughan UM, Jayachandran U, Shchepachev V, Chen ZA, Rappsilber J, Tollervey D and Cook AG.** 2016. Pre-40S ribosome biogenesis factor Tsr1 is an inactive structural mimic of translational GTPases. Nat Commun **7**:11789.
124. **Axt K, French SL, Beyer AL and Tollervey D.** 2014. Kinetic analysis demonstrates a requirement for the Rat1 exonuclease in cotranscriptional pre-rRNA cleavage. PLoS One **9**:e85703.
125. **Ohmayer U, Gamalinda M, Sauert M, Ossowski J, Pöll G, Linnemann J, Hierlmeier T, Pérez-Fernández J, Kumcuoglu B, Leger-Silvestre I, Faubladier M, Griesenbeck J, Woolford J, Tschochner H and Milkereit P.** 2013. Studies on the assembly characteristics of large subunit ribosomal proteins in *S. cerevisae*. PLoS One **8**:e68412.
126. **Rotenberg M, Moritz M and Woolford JL, Jr.** 1988. Depletion of *Saccharomyces cerevisiae* ribosomal protein L16 causes a decrease in 60S ribosomal subunits and formation of half-mer polysomes. Genes Dev. **2**:160-172.
127. **van Beekvelt CA, de Graaff-Vincent M, Faber AW, van't Riet J, Venema J and Raué HA.** 2001. All three functional domains of the large ribosomal subunit protein L25 are required for both early and late pre-rRNA processing steps in *Saccharomyces cerevisiae*. Nucleic Acids Res. **29**:5001-5008.
128. **Martín-Marcos P, Hinnebusch AG and Tamame M.** 2007. Ribosomal protein L33 is required for ribosome biogenesis, subunit joining, and repression of *GCN4* translation. Mol. Cell. Biol. **27**:5968-5985.
129. **Rosado IV, Kressler D and de la Cruz J.** 2007. Functional analysis of *Saccharomyces cerevisiae* ribosomal protein Rpl3p in ribosome synthesis. Nucleic Acids Res. **35**:4203-4213.
130. **Zhang J, Harnpicharnchai P, Jakovljevic J, Tang L, Guo Y, Oeffinger M, Rout MP, Hiley SL, Hughes T and Woolford JL, Jr.** 2007. Assembly factors Rpf2 and Rrs1 recruit 5S rRNA and ribosomal proteins rpL5 and rpL11 into nascent ribosomes. Genes Dev. **21**:2580-2592.
131. **Babiano R and de la Cruz J.** 2010. Ribosomal protein L35 is required for 27SB pre-rRNA processing in *Saccharomyces cerevisiae* Nucleic Acids Res. **38**:5177-5192.
132. **Sahasranaman A, Dembowski J, Strahler J, Andrews P, Maddock J and Woolford JL, Jr.** 2011. Assembly of *Saccharomyces cerevisiae* 60S ribosomal subunits: role of factors required for 27S pre-rRNA processing. EMBO J. **30**:4020-4032.
133. **Babiano R, Gamalinda M, Woolford JL, Jr. and de la Cruz J.** 2012. *Saccharomyces cerevisiae* ribosomal protein L26 is not essential for ribosome assembly and function. Mol. Cell. Biol. **32**:3228-3241.

134. **Fernández-Pevida A, Rodríguez-Galán O, Díaz-Quintana A, Kressler D and de la Cruz J.** 2012. Yeast ribosomal protein L40 assembles late into precursor 60S ribosomes and is required for their cytoplasmic maturation. J. Biol. Chem. **287**:38390-38407.
135. **Jakovljevic J, Ohmayer U, Gamalinda M, Talkish J, Alexander L, Linnemann J, Milkereit P and Woolford JL, Jr.** 2012. Ribosomal proteins L7 and L8 function in concert with six A_3 assembly factors to propagate assembly of domains I and II of 25S rRNA in yeast 60S ribosomal subunits. RNA **18**:1805-1822.
136. **Gamalinda M, Jakovljevic J, Babiano R, Talkish J, de la Cruz J and Woolford JL, Jr.** 2013. Yeast polypeptide exit tunnel ribosomal proteins L17, L35 and L37 are necessary to recruit late-assembling factors required for 27SB pre-rRNA processing. Nucleic Acids Res. **41**:1965-1983.
137. **Espinar-Marchena FJ, Fernández-Fernández J, Rodríguez-Galán O, Fernández-Pevida A, Babiano R and de la Cruz J.** 2016. Role of the yeast ribosomal protein L16 in ribosome biogenesis. FEBS J. **283**:2968-2985.
138. **Lebreton A, Rousselle JC, Lenormand P, Namane A, Jacquier A, Fromont-Racine M and Saveanu C.** 2008. 60S ribosomal subunit assembly dynamics defined by semi-quantitative mass spectrometry of purified complexes. Nucleic Acids Res. **36**:4988-4999.
139. **Robledo S, Idol RA, Crimmins DL, Ladenson JH, Mason PJ and Bessler M.** 2008. The role of human ribosomal proteins in the maturation of rRNA and ribosome production. RNA **14**:1918-1929.
140. **Gamalinda M, Ohmayer U, Jakovljevic J, Kumcuoglu B, Woolford J, Mbom B, Lin L and Woolford JL, Jr.** 2014. A hierarchical model for assembly of eukaryotic 60S ribosomal subunit domains. Genes Dev. **28**:198-210.
141. **Chen SS and Williamson JR.** 2013. Characterization of the ribosome biogenesis landscape in E. coli using quantitative mass spectrometry. J. Mol. Biol. **425**:767-779.
142. **Yusupova G and Yusupov M.** 2014. High-resolution structure of the eukaryotic 80S ribosome. Annu. Rev. Biochem. **83**:467-486.
143. **Rosado IV, Dez C, Lebaron S, Caizergues-Ferrer M, Henry Y and de la Cruz J.** 2007. Characterization of *Saccharomyces cerevisiae* Npa2p (Urb2p) reveals a low-molecular-mass complex containing Dbp6p, Npa1p (Urb1p), Nop8p, and Rsa3p involved in early steps of 60S ribosomal subunit biogenesis. Mol. Cell. Biol. **27**:1207-1221.
144. **de la Cruz J, Karbstein K and Woolford JL, Jr.** 2015. Functions of ribosomal proteins in assembly of eukaryotic ribosomes in vivo. Annu Rev Biochem **84**:93-129.
145. **Saveanu C, Bienvenu D, Namane A, Gleizes PE, Gas N, Jacquier A and Fromont-Racine M.** 2001. Nog2p, a putative GTPase associated with pre-60S subunits and required for late 60S maturation steps. EMBO J. **20**:6475-6484.
146. **Lebreton A, Saveanu C, Decourty L, Jacquier A and Fromont-Racine M.** 2006. Nsa2, an unstable, conserved factor required for the maturation of 27SB pre-rRNAs. J. Biol. Chem. **281**:27099-27108.
147. **Wu S, Tutuncuoglu B, Yan K, Brown H, Zhang Y, Tan D, Gamalinda M, Yuan Y, Li Z, Jakovljevic J, Ma C, Lei J, Dong MQ, Woolford JL, Jr. and Gao N.** 2016. Diverse roles of assembly factors revealed by structures of late nuclear pre-60S ribosomes. Nature **534**:133-137.
148. **Matsuo Y, Granneman S, Thoms M, Manikas RG, Tollervey D and Hurt E.** 2014. Coupled GTPase and remodelling ATPase activities form a checkpoint for ribosome export. Nature **505**:112-116.
149. **Sengupta J, Bussiere C, Pallesen J, West M, Johnson AW and Frank J.** 2010. Characterization of the nuclear export adaptor protein Nmd3 in association with the 60S ribosomal subunit. J. Cell. Biol. **189**:1079-1086.
150. **Greber BJ, Gerhardy S, Leitner A, Leibundgut M, Salem M, Boehringer D, Leulliot N, Aebersold R, Panse VG and Ban N.** 2016. Insertion of the Biogenesis Factor Rei1 Probes the Ribosomal Tunnel during 60S Maturation. Cell **164**:91-102.

151. **Thoms M, Thomson E, Bassler J, Gnadig M, Griesel S and Hurt E.** 2015. The Exosome Is Recruited to RNA Substrates through Specific Adaptor Proteins. Cell **162**:1029-1038.
152. **Kressler D, Bange G, Ogawa Y, Stjepanovic G, Bradatsch B, Pratte D, Amlacher S, Strauss D, Yoneda Y, Katahira J, Sinning I and Hurt E.** 2012. Synchronizing nuclear import of ribosomal proteins with ribosome assembly. Science **338**:666-671.
153. **Leidig C, Thoms M, Holdermann I, Bradatsch B, Berninghausen O, Bange G, Sinning I, Hurt E and Beckmann R.** 2014. 60S ribosome biogenesis requires rotation of the 5S ribonucleoprotein particle. Nat Commun **5**:3491.
154. **Bassler J, Kallas M, Pertschy B, Ulbrich C, Thoms M and Hurt E.** 2010. The AAA-ATPase Rea1 drives removal of biogenesis factors during multiple stages of 60S ribosome assembly. Mol. Cell **38**:712-721.
155. **Yao W, Roser D, Kohler A, Bradatsch B, Bassler J and Hurt E.** 2007. Nuclear export of ribosomal 60S subunits by the general mRNA export receptor Mex67-Mtr2. Mol. Cell **26**:51-62.
156. **Bange G, Murat G, Sinning I, Hurt E and Kressler D.** 2013. New twist to nuclear import: When two travel together. Commun. Integr. Biol. **6**:e24792.
157. **Eisinger DP, Dick FA and Trumpower BL.** 1997. Qsr1p, a 60S ribosomal subunit protein, is required for joining of 40S and 60S subunits. Mol. Cell. Biol. **17**:5136-5145.
158. **DeLabre ML, Kessl J, Karamanou S and Trumpower BL.** 2002. RPL29 codes for a non-essential protein of the 60S ribosomal subunit in *Saccharomyces cerevisiae* and exhibits synthetic lethality with mutations in genes for proteins required for subunit coupling. Biochim. Biophys. Acta **1574**:255-261.
159. **Kappel L, Loibl M, Zisser G, Klein I, Fruhmann G, Gruber C, Unterweger S, Rechberger G, Pertschy B and Bergler H.** 2012. Rlp24 activates the AAA-ATPase Drg1 to initiate cytoplasmic pre-60S maturation. J. Cell Biol. **199**:771-782.
160. **Saveanu C, Namane A, Gleizes PE, Lebreton A, Rousselle JC, Noaillac-Depeyre J, Gas N, Jacquier A and Fromont-Racine M.** 2003. Sequential protein association with nascent 60S ribosomal particles. Mol. Cell. Biol. **23**:4449-4460.
161. **Lo KY, Li Z, Bussiere C, Bresson S, Marcotte EM and Johnson AW.** 2010. Defining the pathway of cytoplasmic maturation of the 60S ribosomal subunit. Mol. Cell **39**:196-208.
162. **Lebreton A, Saveanu C, Decourty L, Rain JC, Jacquier A and Fromont-Racine M.** 2006. A functional network involved in the recycling of nucleocytoplasmic pre-60S factors. J. Cell Biol. **173**:349-360.
163. **Demoinet E, Jacquier A, Lutfalla G and Fromont-Racine M.** 2007. The Hsp40 chaperone Jjj1 is required for the nucleo-cytoplasmic recycling of preribosomal factors in *Saccharomyces cerevisiae*. RNA **13**:1570-1581.
164. **Kemmler S, Occhipinti L, Veisu M and Panse VG.** 2009. Yvh1 is required for a late maturation step in the 60S biogenesis pathway. J. Cell Biol. **186**:863-880.
165. **Lo KY, Li Z, Wang F, Marcotte EM and Johnson AW.** 2009. Ribosome stalk assembly requires the dual-specificity phosphatase Yvh1 for the exchange of Mrt4 with P0. J. Cell Biol. **186**:849-862.
166. **Rodríguez-Mateos M, García-Gómez JJ, Francisco-Velilla R, Remacha M, de la Cruz J and Ballesta JPG.** 2009. Role and dynamics of the ribosomal protein P0 and its related *trans*-acting factor Mrt4 during ribosome assembly in *Saccharomyces cerevisiae*. Nucleic Acids Res. **37**:7519-7532.
167. **Sarkar A, Pech M, Thoms M, Beckmann R and Hurt E.** 2016. Ribosome-stalk biogenesis is coupled with recruitment of nuclear-export factor to the nascent 60S subunit. Nat. Struct. Mol. Biol. **23**:1074-1082.
168. **Wawiorka L, Molestak E, Szajwaj M, Michalec-Wawiorka B, Boguszewska A, Borkiewicz L, Liudkovska V, Kufel J and Tchorzewski M.** 2016. Functional analysis of the uL11 protein impact on translational machinery. Cell Cycle **15**:1060-1072.

169. **Bussiere C, Hashem Y, Arora S, Frank J and Johnson AW.** 2012. Integrity of the P-site is probed during maturation of the 60S ribosomal subunit. J. Cell Biol. **197**:747-759.
170. **Lafontaine DL.** 2010. A 'garbage can' for ribosomes: how eukaryotes degrade their ribosomes. Trends Biochem. Sci. **35**:267-277.
171. **Cole SE, LaRiviere FJ, Merrikh CN and Moore MJ.** 2009. A convergence of rRNA and mRNA quality control pathways revealed by mechanistic analysis of nonfunctional rRNA decay. Mol. Cell **34**:440-450.
172. **Fujii K, Kitabatake M, Sakata T, Miyata A and Ohno M.** 2009. A role for ubiquitin in the clearance of nonfunctional rRNAs. Genes Dev. **23**:963-974.
173. **Kraft C, Deplazes A, Sohrmann M and Peter M.** 2008. Mature ribosomes are selectively degraded upon starvation by an autophagy pathway requiring the Ubp3p/Bre5p ubiquitin protease. Nat. Cell Biol. **10**:602-610.
174. **Roberts P, Moshitch-Moshkovitz S, Kvam E, O'Toole E, Winey M and Goldfarb DS.** 2003. Piecemeal microautophagy of nucleus in Saccharomyces cerevisiae. Mol. Biol. Cell **14**:129-141.
175. **Pöll G, Braun T, Jakovljevic J, Neueder A, Jakob S, Woolford JL, Jr., Tschochner H and Milkereit P.** 2009. rRNA maturation in yeast cells depleted of large ribosomal subunit proteins. PLoS One **4**:e8249.
176. **Pratte D, Singh U, Murat G and Kressler D.** 2013. Mak5 and Ebp2 act together on early pre-60S particles and their reduced functionality bypasses the requirement for the essential pre-60S factor Nsa1. PLoS One **8**:e82741.
177. **Klinge S, Voigts-Hoffmann F, Leibundgut M and Ban N.** 2012. Atomic structures of the eukaryotic ribosome. Trends Biochem Sci **37**:189-198.
178. **Henras AK, Soudet J, Gerus M, Lebaron S, Caizergues-Ferrer M, Mougin A and Henry Y.** 2008. The post-transcriptional steps of eukaryotic ribosome biogenesis. Cell. Mol. Life Sci. **65**:2334-2359.
179. **Nerurkar P, Altvater M, Gerhardy S, Schutz S, Fischer U, Weirich C and Panse VG.** 2015. Eukaryotic ribosome assembly and nuclear export. Int Rev Cell Mol Biol **319**:107-140.
180. **Turowski TW.** 2013. The impact of transcription on posttranscriptional processes in yeast. Gene **526**:23-29.
181. **Turowski TW and Tollervey D.** 2015. Cotranscriptional events in eukaryotic ribosome synthesis. Wiley Interdiscip Rev RNA **6**:129-139.
182. **de la Cruz J, Kressler D and Linder P.** 2004. Ribosomal subunit assembly. In: Olson MOJ (ed) Nucleolus, Kluwer academic. Landes Bioscience/eurekah.com, Georgetown pp. 258-285
183. **Moriggi G, Nieto B and Dosil M.** 2014. Rrp12 and the exportin Crm1 participate in late assembly events in the nucleolus during 40S ribosomal subunit biogenesis. PLoS Genet **10**:e1004836.
184. **Panse VG and Johnson AW.** 2010. Maturation of eukaryotic ribosomes: acquisition of functionality. Trends Biochem. Sci. **35**:260-266.
185. **Fromont-Racine M, Senger B, Saveanu C and Fasiolo F.** 2003. Ribosome assembly in eukaryotes. Gene **313**:17-42.
186. **Lacombe T, García-Gómez JJ, de la Cruz J, Roser D, Hurt E, Linder P and Kressler D.** 2009. Linear ubiquitin fusion to Rps31 and its subsequent cleavage are required for the efficient production and functional integrity of 40S ribosomal subunits. Mol. Microbiol. **72**:69-84.
187. **Charollais J, Pflieger D, Vinh J, Dreyfus M and Iost I.** 2003. The DEAD-box RNA helicase SrmB is involved in the assembly of 50S ribosomal subunits in Escherichia coli. Mol. Microbiol. **48**:1253-1265.
188. **Shajani Z, Sykes MT and Williamson JR.** 2011. Assembly of bacterial ribosomes. Annu. Rev. Biochem. **80**:501-526.

189. **Chaudhuri S, Vyas K, Kapasi P, Komar AA, Dinman JD, Barik S and Mazumder B.** 2007. Human ribosomal protein L13a is dispensable for canonical ribosome function but indispensable for efficient rRNA methylation. RNA **13**:2224-2237.
190. **Das P, Basu A, Biswas A, Poddar D, Andrews J, Barik S, Komar AA and Mazumder B.** 2013. Insights into the mechanism of ribosomal incorporation of mammalian L13a protein during ribosome biogenesis. Mol. Cell. Biol. **33**:2829-2842.
191. **Mazumder B, Sampath P, Seshadri V, Maitra RK, DiCorleto PE and Fox PL.** 2003. Regulated release of L13a from the 60S ribosomal subunit as a mechanism of transcript-specific translational control. Cell **115**:187-198.
192. **Ohmayer U, Gil-Hernandez A, Sauert M, Martin-Marcos P, Tamame M, Tschochner H, Griesenbeck J and Milkereit P.** 2015. Studies on the coordination of ribosomal protein assembly events involved in processing and stabilization of yeast early large ribosomal subunit precursors. PLoS One **10**:e0143768.
193. **Pettersen EF, Goddard TD, Huang CC, Couch GS, Greenblatt DM, Meng EC and Ferrin TE.** 2004. UCSF Chimera-a visualization system for exploratory research and analysis. J. Comput. Chem. **25**:1605-1612.
194. **Thomson E and Tollervey D.** 2005. Nop53p is required for late 60S ribosome subunit maturation and nuclear export in yeast. RNA **11**:1215-1224.
195. **Kruiswijk T, Planta RJ and Krop JM.** 1978. The course of the assembly of ribosomal subunits in yeast. Biochim. Biophys. Acta **517**:378-389.
196. **Wehner KA and Baserga SJ.** 2002. The sigma(70)-like motif: a eukaryotic RNA binding domain unique to a superfamily of proteins required for ribosome biogenesis. Mol. Cell **9**:329-339.
197. **Harnpicharnchai P, Jakovljevic J, Horsey E, Miles T, Roman J, Rout M, Meagher D, Imai B, Guo Y, Brame CJ, Shabanowitz J, Hunt DF and Woolford JL, Jr.** 2001. Composition and functional characterization of yeast 66S ribosome assembly intermediates. Mol. Cell **8**:505-515.
198. **Kallstrom G, Hedges J and Johnson A.** 2003. The putative GTPases Nog1p and Lsg1p are required for 60S ribosomal subunit biogenesis and are localized to the nucleus and cytoplasm, respectively. Mol. Cell. Biol. **23**:4344-4355.
199. **Santos C and Ballesta JPG.** 1994. Ribosomal protein P0, contrary to phosphoproteins P1 and P2, is required for ribosome activity and *Saccharomyces cerevisiae* viability. J. Biol. Chem. **269**:15689-15696.
200. **West M, Hedges JB, Chen A and Johnson AW.** 2005. Defining the order in which Nmd3p and Rpl10p load onto nascent 60S ribosomal subunits. Mol. Cell. Biol. **25**:3802-3813.
201. **Pillet B, Garcia-Gomez JJ, Pausch P, Falquet L, Bange G, de la Cruz J and Kressler D.** 2015. The dedicated chaperone Acl4 escorts ribosomal protein Rpl4 to its nuclear pre-60S assembly site. PLoS Genet **11**:e1005565.
202. **Gamalinda M and Woolford JL, Jr.** 2014. Deletion of L4 domains reveals insights into the importance of ribosomal protein extensions in eukaryotic ribosome assembly. RNA **20**:1725-1731.
203. **Warner JR, Mitra G, Schwindinger WF, Studeny M and Fried HM.** 1985. Saccharomyces cerevisiae coordinates accumulation of yeast ribosomal proteins by modulating mRNA splicing, translational initiation, and protein turnover. Mol. Cell. Biol. **5**:1512-1521.
204. **Finley D, Bartel B and Varshavsky A.** 1989. The tails of ubiquitin precursors are ribosomal proteins whose fusion to ubiquitin facilitates ribosome biogenesis. Nature **338**:394-401.
205. **Komili S, Farny NG, Roth FP and Silver PA.** 2007. Functional specificity among ribosomal proteins regulates gene expression. Cell **131**:557-571.
206. **Thomas BJ and Rothstein R.** 1989. Elevated recombination rates in transcriptionally active DNA. Cell **56**:619-630.
207. **Longtine MS, McKenzie A, 3rd, Demarini DJ, Shah NG, Wach A, Brachat A, Philippsen P and Pringle JR.** 1998. Additional modules for versatile and economical

PCR-based gene deletion and modification in *Saccharomyces cerevisiae*. Yeast **14**:953-961.
208. **Gietz D, St. Jean A, Woods RA and Schiestl RH.** 1992. Improved method for high efficiency transformation of intact yeast cells. Nucleic Acids Res. **20**:1425.
209. **Schmidt A, Bickle M, Beck T and Hall MN.** 1997. The yeast phosphatidylinositol kinase homolog TOR2 activates RHO1 and RHO2 via the exchange factor ROM2. Cell **88**:531-542.
210. **Ulbrich C, Diepholz M, Bassler J, Kressler D, Pertschy B, Galani K, Bottcher B and Hurt E.** 2009. Mechanochemical removal of ribosome biogenesis factors from nascent 60S ribosomal subunits. Cell **138**:911-922.
211. **Kressler D, de la Cruz J, Rojo M and Linder P.** 1997. Fal1p is an essential DEAD-box protein involved in 40S-ribosomal-subunit biogenesis in *Saccharomyces cerevisiae*. Mol. Cell. Biol. **17**:7283-7294.
212. **de la Cruz J, Kressler D, Rojo M, Tollervey D and Linder P.** 1998. Spb4p, an essential putative RNA helicase, is required for a late step in the assembly of 60S ribosomal subunits in *Saccharomyces cerevisiae*. RNA **4**:1268-1281.
213. **Gautschi M, Lilie H, Funfschilling U, Mun A, Ross S, Lithgow T, Rucknagel P and Rospert S.** 2001. RAC, a stable ribosome-associated complex in yeast formed by the DnaK-DnaJ homologs Ssz1p and zuotin. Proc. Natl. Acad. Sci. USA **98**:3762-3767.
214. **Petitjean A, Bonneaud N and Lacroute F.** 1995. The duplicated *Saccharomyces cerevisiae* gene *SSM1* encodes a eucaryotic homolog of the eubacterial and archeabacterial L1 ribsomal protein. Mol. Cell. Biol. **15**:5071-5081.
215. **Emery B, de la Cruz J, Rocak S, Deloche O and Linder P.** 2004. Has1p, a member of the DEAD-box family, is required for 40S ribosomal subunit biogenesis in *Saccharomyces cerevisiae*. Mol. Microbiol. **52**:141-158.
216. **Zanelli CF, Maragno AL, Gregio AP, Komili S, Pandolfi JR, Mestriner CA, Lustri WR and Valentini SR.** 2006. eIF5A binds to translational machinery components and affects translation in yeast. Biochem. Biophys. Res. Commun. **348**:1358-1366.
217. **Tron T, Yang M, Dick FA, Schmitt ME and Trumpower BL.** 1995. *QSR1*, an essential yeast gene with a genetic relationship to a subunit of the mitochondrial cytochrome bc_1 complex, is homologous to a gene implicated in eukaryotic cell differentiation. J. Biol. Chem. **270**:9961-9970.
218. **Venema J, Planta RJ and Raué HA.** 1998. *In vivo* mutational analysis of ribosomal RNA in *Saccharomyces cerevisiae*. In: Martin R (ed) Protein synthesis: Methods and protocols, Humana Press, Totowa, N. J. pp. 257-270.
219. **Kressler D, de la Cruz J, Rojo M and Linder P.** 1998. Dbp6p is an essential putative ATP-dependent RNA helicase required for 60S-ribosomal-subunit assembly in *Saccharomyces cerevisiae*. Mol. Cell. Biol. **18**:1855-1865.
220. **García-Gómez JJ, Lebaron S, Froment C, Monsarrat B, Henry Y and de la Cruz J.** 2011. Dynamics of the putative RNA helicase Spb4 during ribosome assembly in *Saccharomyces cerevisiae*. Mol. Cell. Biol. **31**:4156-4164.
221. **Lafontaine DL and Tollervey D.** 2001. The function and synthesis of ribosomes. Nature Rev. Mol. Cell Biol. **2**:514-520.
222. **Wilson DN and Doudna Cate JH.** 2012. The structure and function of the eukaryotic ribosome. Cold Spring Harb Perspect Biol **4**.
223. **Ramagopal S.** 1992. Are eukaryotic ribosomes heterogeneous? Affirmations on the horizon. Biochem. Cell Biol. **70**:269-272.
224. **Slavov N, Semrau S, Airoldi E, Budnik B and van Oudenaarden A.** 2015. Differential Stoichiometry among Core Ribosomal Proteins. Cell Rep **13**:865-73.
225. **Mauro VP and Edelman GM.** 2002. The ribosome filter hypothesis. Proc. Natl. Acad. Sci. USA **99**:12031-12036.
226. **Sloan KE, Warda AS, Sharma S, Entian KD, Lafontaine DL and Bohnsack MT.** 2016. Tuning the ribosome: The influence of rRNA modification on eukaryotic ribosome biogenesis and function. RNA Biol **2**:1-16.

227. **Sauert M, Temmel H and Moll I.** 2015. Heterogeneity of the translational machinery: Variations on a common theme. Biochimie **114**:39-47.
228. **Armache JP, Anger AM, Marquez V, Franckenberg S, Frohlich T, Villa E, Berninghausen O, Thomm M, Arnold GJ, Beckmann R and Wilson DN.** 2013. Promiscuous behaviour of archaeal ribosomal proteins: implications for eukaryotic ribosome evolution. Nucleic Acids Res. **41**:1284-1293.
229. **Boisvert FM, van Koningsbruggen S, Navascues J and Lamond AI.** 2007. The multifunctional nucleolus. Nat. Rev. Mol. Cell. Biol. **8**:574-585.
230. **Thomson E, Ferreira-Cerca S and Hurt E.** 2013. Eukaryotic ribosome biogenesis at a glance. J Cell Sci **126**:4815-4821.
231. **Udem SA and Warner JR.** 1973. The cytoplasmic maturation of a ribosomal precursor ribonucleic acid in yeast. J. Biol. Chem. **248**:1412-1416.
232. **Trapman J, Retèl J and Planta RJ.** 1975. Ribosomal precursor particles from yeast. Exp. Cell Res. **90**:95-104.
233. **Warner JR and Soeiro R.** 1967. Nascent ribosomes from HeLa cells. Proc. Natl. Acad. Sci. USA **58**:1984-1990.
234. **Karbstein K.** 2013. Quality control mechanisms during ribosome maturation. Trends Cell Biol **23**:242-250.
235. **Hector RD, Burlacu E, Aitken S, Le Bihan T, Tuijtel M, Zaplatina A, Cook AG and Granneman S.** 2014. Snapshots of pre-rRNA structural flexibility reveal eukaryotic 40S assembly dynamics at nucleotide resolution. Nucleic Acids Res **42**:12138-12154.
236. **Davis JH, Tan YZ, Carragher B, Potter CS, Lyumkis D and Williamson JR.** 2016. Modular Assembly of the Bacterial Large Ribosomal Subunit. Cell **167**:1610-1622.
237. **Davis JH and Williamson JR.** 2017. Structure and dynamics of bacterial ribosome biogenesis. Philos Trans R Soc Lond B Biol Sci **372**.
238. **Warner JR.** 1971. The assembly of ribosomes in yeast. J. Biol. Chem. **246**:447-454.
239. **Auger-Buendia MA, Longuet M and Tavitian A.** 1979. Kinetic studies on ribosomal proteins assembly in preribosomal particles and ribosomal subunits of mammalian cells. Biochim Biophys Acta **563**:113-128.
240. **Lastick SM.** 1980. The assembly of ribosomes in HeLa cell nucleoli. Eur. J. Biochem. **113**:175-182.
241. **Bassler J, Grandi P, Gadal O, Lessmann T, Petfalski E, Tollervey D, Lechner J and Hurt E.** 2001. Identification of a 60S preribosomal particle that is closely linked to nuclear export. Mol. Cell **8**:517-529.
242. **Gavin AC, Bosche M, Krause R, Grandi P, Marzioch M, Bauer A, Schultz J, Rick JM, Michon AM, Cruciat CM, Remor M, Hofert C, Schelder M, Brajenovic M, Ruffner H, Merino A, Klein K, Hudak M, Dickson D, Rudi T, Gnau V, Bauch A, Bastuck S, Huhse B, Leutwein C, Heurtier MA, Copley RR, Edelmann A, Querfurth E, Rybin V, Drewes G, Raida M, Bouwmeester T, Bork P, Séraphin B, Kuster B, Neubauer G and Superti-Furga G.** 2002. Functional organization of the yeast proteome by systematic analysis of protein complexes. Nature **415**:141-147.
243. **Krogan NJ, Cagney G, Yu H, Zhong G, Guo X, Ignatchenko A, Li J, Pu S, Datta N, Tikuisis AP, Punna T, Peregrin-Alvarez JM, Shales M, Zhang X, Davey M, Robinson MD, Paccanaro A, Bray JE, Sheung A, Beattie B, Richards DP, Canadien V, Lalev A, Mena F, Wong P, Starostine A, Canete MM, Vlasblom J, Wu S, Orsi C, Collins SR, Chandran S, Haw R, Rilstone JJ, Gandi K, Thompson NJ, Musso G, St Onge P, Ghanny S, Lam MH, Butland G, Altaf-Ul AM, Kanaya S, Shilatifard A, O'Shea E, Weissman JS, Ingles CJ, Hughes TR, Parkinson J, Gerstein M, Wodak SJ, Emili A and Greenblatt JF.** 2006. Global landscape of protein complexes in the yeast *Saccharomyces cerevisiae*. Nature **440**:637-643.
244. **Altvater M, Chang Y, Melnik A, Occhipinti L, Schutz S, Rothenbusch U, Picotti P and Panse VG.** 2012. Targeted proteomics reveals compositional dynamics of 60S pre-ribosomes after nuclear export. Mol Syst Biol **8**:628.

245. **Ford CL, Randal-Whitis L and Ellis SR.** 1999. Yeast proteins related to the p40/laminin receptor precursor are required for 20S ribosomal RNA processing and the maturation of 40S ribosomal subunits. Cancer Res. **59**:704-710.
246. **Léger-Silvestre I, Caffrey JM, Dawaliby R, Alvarez-Arias DA, Gas N, Bertolone SJ, Gleizes PE and Ellis SR.** 2005. Specific role for yeast homologs of the Diamond Blackfan Anemia-associated Rps19 protein in ribosome synthesis. J. Biol. Chem. **280**:38177-38185.
247. **Bradatsch B, Leidig C, Granneman S, Gnadig M, Tollervey D, Bottcher B, Beckmann R and Hurt E.** 2012. Structure of the pre-60S ribosomal subunit with nuclear export factor Arx1 bound at the exit tunnel. Nature Struct. Mol. Biol. **19**:1234-1241.
248. **Weis F, Giudice E, Churcher M, Jin L, Hilcenko C, Wong CC, Traynor D, Kay RR and Warren AJ.** 2015. Mechanism of eIF6 release from the nascent 60S ribosomal subunit. Nat Struct Mol Biol **22**:914-919.
249. **Ma C, Wu S, Li N, Chen Y, Yan K, Li Z, Zheng L, Lei J, Woolford JL, Jr. and Gao N.** 2017. Structural snapshot of cytoplasmic pre-60S ribosomal particles bound by Nmd3, Lsg1, Tif6 and Reh1. Nat Struct Mol Biol **24**:214-220.
250. **Johnson MC, Ghalei H, Doxtader KA, Karbstein K and Stroupe ME.** 2017. Structural Heterogeneity in Pre-40S Ribosomes. Structure **25**:329-340.
251. **Greber BJ.** 2016. Mechanistic insight into eukaryotic 60S ribosomal subunit biogenesis by cryo-electron microscopy. RNA **22**:1643-1662.
252. **Biedka S, Wu S, LaPeruta AJ, Gao N and Woolford JL, Jr.** 2017. Insights into remodeling events during eukaryotic large ribosomal subunit assembly provided by high resolution cryo-EM structures. RNA Biol **7**:1-8.
253. **Calvino FR, Kharde S, Ori A, Hendricks A, Wild K, Kressler D, Bange G, Hurt E, Beck M and Sinning I.** 2015. Symportin 1 chaperones 5S RNP assembly during ribosome biogenesis by occupying an essential rRNA-binding site. Nat Commun **6**:6510.
254. **Huber FM and Hoelz A.** 2017. Molecular basis for protection of ribosomal protein L4 from cellular degradation. Nat Commun **8**:14354.
255. **Madru C, Lebaron S, Blaud M, Delbos L, Pipoli J, Pasmant E, Rety S and Leulliot N.** 2015. Chaperoning 5S RNA assembly. Genes Dev **29**:1432-1446.
256. **Sun Q, Zhu X, Qi J, An W, Lan P, Tan D, Chen R, Wang B, Zheng S, Zhang C, Chen X, Zhang W, Chen J, Dong MQ and Ye K.** 2017. Molecular architecture of the 90S small subunit pre-ribosome. Elife **6**.
257. **Konikkat S and Woolford JL, Jr.** 2017. Principles of 60S ribosomal subunit assembly emerging from recent studies in yeast. Biochem J **474**:195-214.
258. **Nicolas E, Parisot P, Pinto-Monteiro C, de Walque R, De Vleeschouwer C and Lafontaine DL.** 2016. Involvement of human ribosomal proteins in nucleolar structure and p53-dependent nucleolar stress. Nat Commun **7**:11390.
259. **Lecompte O, Ripp R, Thierry JC, Moras D and Poch O.** 2002. Comparative analysis of ribosomal proteins in complete genomes: an example of reductive evolution at the domain scale. Nucleic Acids Res. **30**:5382-5390.
260. **Kosugi S, Hasebe M, Tomita M and Yanagawa H.** 2009. Systematic identification of cell cycle-dependent yeast nucleocytoplasmic shuttling proteins by prediction of composite motifs. Proc. Natl. Acad. Sci. USA **106**:10171-10176.
261. **Brameier M, Krings A and MacCallum RM.** 2007. NucPred--predicting nuclear localization of proteins. Bioinformatics **23**:1159-1160.
262. **Wu B, Lukin J, Yee A, Lemak A, Semesi A, Ramelot TA, Kennedy MA and Arrowsmith CH.** 2008. Solution structure of ribosomal protein L40E, a unique C4 zinc finger protein encoded by archaeon *Sulfolobus solfataricus*. Protein Sci. **17**:589-596.
263. **Barrio-Garcia C, Thoms M, Flemming D, Kater L, Berninghausen O, Bassler J, Beckmann R and Hurt E.** 2016. Architecture of the Rix1-Rea1 checkpoint machinery during pre-60S-ribosome remodeling. Nat Struct Mol Biol **23**:37-44.

264. **Ho JH-N, Kallstrom G and Johnson AW.** 2000. Nmd3p is a Crm1p-dependent adapter protein for nuclear export of the large ribosomal subunit. J. Cell. Biol. **151**:1057-1066.
265. **Poirot O and Timsit Y.** 2016. Neuron-Like Networks Between Ribosomal Proteins Within the Ribosome. Sci Rep **6**:26485.
266. **Steffen KK, McCormick MA, Pham KM, Mackay VL, Delaney JR, Murakami CJ, Kaeberlein M and Kennedy BK.** 2012. Ribosome deficiency protects against ER stress in *Saccharomyces cerevisiae*. Genetics **191**:107-118.
267. **Zaman S, Lippman SI, Zhao X and Broach JR.** 2008. How Saccharomyces responds to nutrients. Annu Rev Genet **42**:27-81.
268. **de la Cruz J, Sanz-Martínez E and Remacha M.** 2005. The essential WD-repeat protein Rsa4p is required for rRNA processing and intra-nuclear transport of 60S ribosomal subunits. Nucleic Acids Res. **33**:5728-5739.
269. **Hurt E, Hannus S, Schmelzl B, Lau D, Tollervey D and Simos G.** 1999. A novel *in vivo* assay reveals inhibition of ribosomal nuclear export in Ran-cycle and nucleoporin mutants. J. Cell Biol. **144**:389-401.
270. **Hierlmeier T, Merl J, Sauert M, Perez-Fernandez J, Schultz P, Bruckmann A, Hamperl S, Ohmayer U, Rachel R, Jacob A, Hergert K, Deutzmann R, Griesenbeck J, Hurt E, Milkereit P, Bassler J and Tschochner H.** 2012. Rrp5p, Noc1p and Noc2p form a protein module which is part of early large ribosomal subunit precursors in S. cerevisiae. Nucleic Acids Res. **41**:1191-1210.
271. **Wan K, Yabuki Y and Mizuta K.** 2015. Roles of Ebp2 and ribosomal protein L36 in ribosome biogenesis in Saccharomyces cerevisiae. Curr. Genet. **61**:31-41.
272. **Talkish J, Zhang J, Jakovljevic J, Horsey EW and Woolford JL, Jr.** 2012. Hierarchical recruitment into nascent ribosomes of assembly factors required for 27SB pre-rRNA processing in *Saccharomyces cerevisiae*. Nucleic Acids Res. **40**:8646-8661.
273. **Kressler D, Rojo M, Linder P and de la Cruz J.** 1999. Spb1p is a putative methyltransferase required for 60S ribosomal subunit biogenesis in *Saccharomyces cerevisiae*. Nucleic Acids Res. **27**:4598-4608.
274. **Burger F, Daugeron M-C and Linder P.** 2000. Dbp10p, a putative RNA helicase from *Saccharomyces cerevisiae* required for ribosome biogenesis. Nucleic Acids Res. **28**:2315-2323.
275. **Hong B, Brockenbrough JS, Wu P and Aris JP.** 1997. Nop2p is required for pre-rRNA processing and 60S ribosome subunit synthesis in yeast. Mol. Cell. Biol. **17**:378-388.
276. **Zanchin NIT, Roberts P, DeSilva A, Sherman F and Goldfarb DS.** 1997. *Saccharomyces cerevisiae* Nip7p is required for efficient 60S ribosome subunit biogenesis. Mol. Cell. Biol. **17**:5001-5015.
277. **Basu U, Si K, Warner JR and Maitra U.** 2001. The *Saccharomyces cerevisiae TIF6* gene encoding translation initiation factor 6 is required for 60S ribosomal subunit biogenesis. Mol. Cell. Biol. **75**:1453-1462.
278. **Manikas RG, Thomson E, Thoms M and Hurt E.** 2016. The K(+)-dependent GTPase Nug1 is implicated in the association of the helicase Dbp10 to the immature peptidyl transferase centre during ribosome maturation. Nucleic Acids Res **44**:1800-1812.
279. **Bassler J, Kallas M and Hurt E.** 2006. The NUG1 GTPase reveals and N-terminal RNA-binding domain that is essential for association with 60 S pre-ribosomal particles. J. Biol. Chem. **281**:24737-24744.
280. **Yamada H, Horigome C, Okada T, Shirai C and Mizuta K.** 2007. Yeast Rrp14p is a nucleolar protein involved in both ribosome biogenesis and cell polarity. RNA **13**:1977-1987.
281. **Miles TD, Jakovljevic J, Horsey EW, Harnpicharnchai P, Tang L and Woolford JL, Jr.** 2005. Ytm1, Nop7, and Erb1 form a complex necessary for maturation of yeast 66S preribosomes. Mol. Cell. Biol. **25**:10419-10432.

282. **Merl J, Jakob S, Ridinger K, Hierlmeier T, Deutzmann R, Milkereit P and Tschochner H.** 2010. Analysis of ribosome biogenesis factor-modules in yeast cells depleted from pre-ribosomes. Nucleic Acids Res. **38**:3068-3080.
283. **Dembowski JA, Kuo B and Woolford JL, Jr.** 2013. Has1 regulates consecutive maturation and processing steps for assembly of 60S ribosomal subunits. Nucleic Acids Res. **41**:7889-7904.
284. **Puig O, Caspary F, Rigaut G, Rutz B, Bouveret E, Bragado-Nilsson E, Wilm M and Séraphin B.** 2001. The tandem affinity purification (TAP) method: a general procedure of protein complex purification. Methods **24**:218-229.
285. **Belk JP, He F and Jacobson A.** 1999. Overexpression of truncated Nmd3p inhibits protein synthesis in yeast. RNA **5**:1055-1070.
286. **Ausubel FM, Brent R, Kingston RE, Moore DD, Seidman JG, Smith JA and Struhl K.** 1994. *Saccharomyces cerevisiae*. Current Protocols in Molecular Biology, John Wiley & Sons, Inc., New York, N. Y. pp. 13.0.1-13.14.17
287. **Dieci G, Bottarelli L and Ottonello S.** 2005. A general procedure for the production of antibody reagents against eukaryotic ribosomal proteins. Protein Pept. Lett. **12**:555-560.
288. **Jakob S, Ohmayer U, Neueder A, Hierlmeier T, Perez-Fernandez J, Hochmuth E, Deutzmann R, Griesenbeck J, Tschochner H and Milkereit P.** 2012. Interrelationships between yeast ribosomal protein assembly events and transient ribosome biogenesis factors interactions in early pre-ribosomes. PLoS One **7**:e32552.
289. **Gietz RD and Sugino A.** 1988. New yeast-*Escherichia coli* shuttle vectors constructed with in vitro mutagenized yeast genes lacking six-base pair restriction sites. Gene **74**:527-534.
290. **Pena C, Schutz S, Fischer U, Chang Y and Panse VG.** 2016. Prefabrication of a ribosomal protein subcomplex essential for eukaryotic ribosome formation. Elife **5**.
291. **Talkish J, Biedka S, Jakovljevic J, Zhang J, Tang L, Strahler JR, Andrews PC, Maddock JR and Woolford JL, Jr.** 2016. Disruption of ribosome assembly in yeast blocks cotranscriptional pre-rRNA processing and affects the global hierarchy of ribosome biogenesis. RNA **22**:852-866.
292. **Adams CC, Jakovljevic J, Roman J, Harnpicharnchai P and Woolford JL, Jr.** 2002. *Saccharomyces cerevisiae* nucleolar protein Nop7p is necessary for biogenesis of 60S ribosomal subunits. RNA **8**:150-165.
293. **Fatica A, Oeffinger M, Tollervey D and Bozzoni I.** 2003. Cic1p/Nsa3p is required for synthesis and nuclear export of 60S ribosomal subunits. RNA **9**:1431-1436.
294. **Gadal O, Strauss D, Petfalski E, Gleizes PE, Gas N, Tollervey D and Hurt E.** 2002. Rlp7p is associated with 60S preribosomes, restricted to the granular component of the nucleolus, and required for pre-rRNA processing. J. Cell Biol. **157**:941-951.
295. **Granneman S, Petfalski E and Tollervey D.** 2011. A cluster of ribosome synthesis factors regulate pre-rRNA folding and 5.8S rRNA maturation by the Rat1 exonuclease. EMBO J. **30**:4006-4019.
296. **Konikkat S, Biedka S and Woolford JL, Jr.** 2017. The assembly factor Erb1 functions in multiple remodeling events during 60S ribosomal subunit assembly in S. cerevisiae. Nucleic Acids Res **45**:4853-4865.
297. **Oeffinger M, Leung A, Lamond A, Tollervey D and Lueng A.** 2002. Yeast Pescadillo is required for multiple activities during 60S ribosomal subunit synthesis. RNA **8**:626-636.
298. **Oeffinger M and Tollervey D.** 2003. Yeast Nop15p is an RNA-binding protein required for pre-rRNA processing and cytokinesis. EMBO J. **22**:6573-6583.
299. **Pestov DG, Stockelman MG, Strezoska Z and Lau LF.** 2001. *ERB1*, the yeast homolog of mammalian *Bop1*, is an essential gene required for maturation of the 25S and 5.8S ribosomal RNAs. Nucleic Acids Res. **29**:3621-3630.
300. **Shimoji K, Jakovljevic J, Tsuchihashi K, Umeki Y, Wan K, Kawasaki S, Talkish J, Woolford JL, Jr. and Mizuta K.** 2012. Ebp2 and Brx1 function cooperatively in 60S

ribosomal subunit assembly in Saccharomyces cerevisiae. Nucleic Acids Res. **40**:4574-4588.
301. **Talkish J, Campbell IW, Sahasranaman A, Jakovljevic J and Woolford JL, Jr.** 2014. Ribosome assembly factors Pwp1 and Nop12 are important for folding of 5.8S rRNA during ribosome biogenesis in Saccharomyces cerevisiae. Mol. Cell. Biol. **34**:1863-1877.
302. **Tang L, Sahasranaman A, Jakovljevic J, Schleifman E and Woolford JL, Jr.** 2008. Interactions among Ytm1, Erb1, and Nop7 required for assembly of the Nop7-subcomplex in yeast preribosomes. Mol. Biol. Cell **19**:2844-2856.
303. **Esakova O, Perederina A, Quan C, Berezin I and Krasilnikov AS.** 2011. Substrate recognition by ribonucleoprotein ribonuclease MRP. RNA **17**:356-64.
304. **Lygerou Z, Allmang C, Tollervey D and Séraphin B.** 1996. Accurate processing of a eukaryotic precursor ribosomal RNA by ribonuclease MRP in vitro. Science **272**:268-270.
305. **Zagulski M, Kressler D, Bécam AM, Rytka J and Herbert CJ.** 2003. Mak5p, which is required for the maintenance of the M1 dsRNA virus, is encoded by the yeast ORF YBR142w and is involved in the biogenesis of the 60S subunit of the ribosome. Mol. Genet. Genomics **270**:216-224.
306. **Proux F, Dreyfus M and Iost I.** 2011. Identification of the sites of action of SrmB, a DEAD-box RNA helicase involved in *Escherichia coli* ribosome assembly. Mol. Microbiol. **82**:300-311.